Technische Universität Berlin

SPATIAL SAMPLING OF A DRIVER'S VISUAL FIELD: CHARACTERISING PERIPHERAL ADAPTATION

PhD Thesis Jan Winter

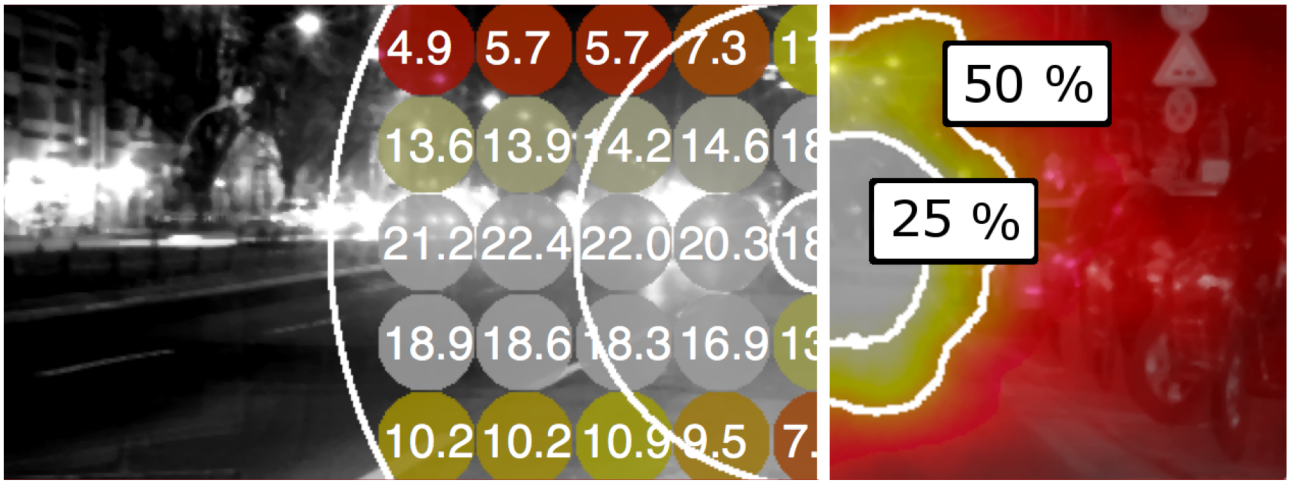

SPATIAL SAMPLING OF A DRIVER'S VISUAL FIELD: CHARACTERISING PERIPHERAL ADAPTATION

vorgelegt von
Dipl.-Ing. Jan-Christoph Winter
geb. in Stuttgart

von der Fakultät IV - Elektrotechnik und Informatik
der Technischen Universität Berlin
zur Erlangung des akademischen Grades

Doktor der Ingenieurwissenschaften
- Dr.-Ing. -

genehmigte Dissertation

Promotionsausschuss:

Vorsitzender:	Prof. Dr. Marc Alexa
Gutachter:	Prof. Dr.-Ing. Stephan Völker
Gutachter:	Prof. Steve Fotios, PhD (University of Sheffield, UK)
Gutachter:	Prof. Dr. Christoph Schierz (TU Ilmenau)

Tag der wissenschaftlichen Aussprache: 29.05.2018

Berlin, 2018

DR. CRANE

We are looking at too many
possibilities!

DR. CAMPBELL

Isn't what science is all about?
Eliminating possibilities?

— Lorraine Bracco and Sean Connery
in the kitschy movie "Medicine Man"

ABSTRACT

For the application of the recommended system of mesopic photometry of the Commission Internationale d'Eclairage (CIE) in road lighting design it is necessary to estimate the peripheral state of adaptation of a driver in an urban environment after dark.

Estimating the state of adaptation of a driver in the natural setting is not straightforward, because the visual scene is likely complex and inhomogeneous, having a range of luminances, and because of the dynamic nature of eye movements and travel along a road. As a result, different parts of the visual field stimulate different parts of the retina, and this puts the retina into a state of continuous transient adaptation.

Spatial sampling of a driver's visual field was introduced to characterise the heterogeneity of the state of adaptation of the peripheral retina. Estimates with assumptions of dynamic and static gaze were compared to the recently proposed method of the joint technical committee 1 of the CIE, i. e. the average luminance of the design area.

The static assumption represents the line of thought that during a fixation mechanisms of adaptation reach a steady state and, therefore, the luminance of a task area determines the state of adaptation. In contrast to that the basis for the dynamic assumption draws upon eye movement, where it is assumed that a crude estimate of adaptation depends on where and how long gaze was directed to within the scene, this representing an overall state of adaptation based on an eye movement probability map.

It was found that the average luminance of the design area can be assumed to represent a reasonable estimate of the state of adaptation.

Background luminances were significantly higher when estimated using the dynamic assumption than compared to the static assumption and the mean luminance of the road. The recurring sequence of fixations and saccades put the eye into a continuous change between transient and steady states of adaptation, where the former being more likely represented by the results of the dynamic assumption, whereas the latter is a likely scenario during a fixation when a particular part of the peripheral retina is exposed to the road surface. As both states cannot be neglected the implication of underestimation for the various use cases of the recommended system of mesopic photometry needs to be considered when using the design area as an estimate of adaptation.

ZUSAMMENFASSUNG

Um das von der Commission Internationale d'Eclairage (CIE) empfohlene System der mesopischen Photometrie anwenden zu können ist eine Schätzung des Adaptationszustandes der Retina eines Kraftfahrers im nächtlichen innerstädtischen Straßenverkehr notwendig.

Dies ist jedoch nicht trivial, da nächtliche Straßenverkehrsszenen komplexe, inhomogene, sich über weite Leuchtdichtenbereiche erstreckende Szenerien darstellen. Durch die ständigen Blickbewegungsänderungen und die Fortbewegung entlang der Straße ergibt sich, dass ständig verschiedene Bereiche des Gesichtsfeldes Teile der Retina stimulieren und das führt dazu, dass sich die Retina in einem ständig veränderlichen Adaptationszustand befindet.

Mittels der Methode des "Spatial Samplings" des Gesichtsfeldes wurde der heterogene Adaptationszustand der peripheren Retina charakterisiert. Dazu wurden Annahmen zu statischen und dynamischen Blickbewegungsszenarien mit den kürzlich verabschiedeten vorübergehenden Empfehlungen des technischen Verbundkomitees 1 der CIE verglichen: die mittlere Leuchtdichte der Straßendeckschicht.

Die statische Annahme basiert auf dem Gedanken, dass während einer Blickfixation die Adaptationsmechanismen einen stabilen Zustand erreichen und somit die Leuchtdichte der Straßendeckschicht das Adaptationsniveau bestimmt.

Im Gegensatz dazu repräsentiert die dynamische Annahme einen auf der Wahrscheinlichkeitsverteilung der Blickbewegungspunkte basierenden Schätzwert.

Die Ergebnisse deuten darauf hin, dass die mittlere Leuchtdichte der Straßendeckschicht einen plausiblen Schätzwert des Adaptationszustandes darstellen.

Die mittels der dynamischer Methode berechneten Hintergrundleuchtdichten waren signifikant höher als die der mittels statischer Methode berechneten auch als die der Straßendeckschicht. Die kontinuierliche Folge von Fixationen und Saccaden versetzen die Retina in eine Abfolge von transienten und stabilen Zuständen der Adaptation, wobei der erstere Zustand eher durch die dynamische Methode gekennzeichnet ist und der zweitere Zustand ein wahrscheinliches Szenario darstellt, wenn ein bestimmter Teil der peripheren Retina während einer Fixation der Straßendeckschicht ausgesetzt ist. Da beide Zustände ihre Daseinsberechtigung besitzen, müssen auch beide Beachtung finden und die daraus resultierenden Folgen einer Unterschätzung des Adaptationszustandes muss für die einzelnen Anwendungsfälle der mesopischen Photometrie kritisch geprüft werden, wenn der Adaptationszustand über die mittlere Leuchtdichte der Straßendeckschicht geschätzt wird.

PUBLICATIONS

This thesis is based on the following peer-reviewed articles:

I Winter, J., Fotios, S. & Völker, S. (2018). The effects of glare and inhomogeneous visual fields on contrast detection in the context of driving. *Lighting Research and Technology*, *50*(4), 537–551. doi:10.1177/1477153516672719. Accepted version, originally published with SAGE Publications. *This work is licensed under a Creative Commons Attribution 3.0 Unported License*.

II Winter, J., Fotios, S. & Völker, S. (2017a). Gaze direction when driving after dark on main and residential roads: Where is the dominant location? *Lighting Research and Technology*, *49*(5), 574–585. doi:10.1177/1477153516632867. Accepted version, copyright © 2018 SAGE Publications. *Reprinted by permission of SAGE Publications*.

III Winter, J., Fotios, S. & Völker, S. (2017b). The effect of assuming static or dynamic gaze behaviour on the estimated background luminance of drivers. *Lighting Research and Technology*, Epub ahead of print 17 December 2017. doi:10.1177/1477153518757594. Accepted version, copyright © 2018 SAGE Publications. *Reprinted by permission of SAGE Publications*.

Other non peer-reviewed articles arising from the work on this thesis:

IV Winter, J., Fotios, S. & Völker, S. (2016). Gaze behaviour when driving after dark on main and residential roads. In *CIE 2016 conference: Lighting quality and energy efficiency* (pp. 395–401). Melbourne, Australia

V Winter, J., Buschmann, S., Franke, R. & Völker, S. (2013). Influence of inhomogeneous adaptation fields and glare sources on visual performance. In *Proceedings of the 11th lux junior* (pp. 112–113). Dörnfeld, Germany

VI Winter, J. & Völker, S. (2013). Typical eye fixation areas of car drivers in inner-city environments at night. In *Proceedings of the 12th lux europa* (pp. 317–322). Krakow, Poland

ACKNOWLEDGMENTS

First of all I want to thank Prof. Stephan Völker for pointing out the scientific relevance of the subject, identifying the crucial cornerstones of the matter, envisioning the innovative infrastructure necessary to address the object of research and last but not least in believing in me to be the right person to investigate the topic.

In particular I would like to express my appreciation and thankfulness to my ambitious and visionary mentor Prof. Steve Fotios, who supported me in getting to the core aspects. He opened my eyes for meticulously rethinking and streamlining the scientific issues over and over again. Therefore he helped me to optimise the object of investigation gradually and moreover, made this thesis become my personal calling.

Furthermore I want to thank Dr. Marianne Maertens for hands-on support with R and Dr. Michael Böhm for continuously answering statistical questions and discussing experimental designs.

Finally I'm grateful to have my beloved partner Nina Slawik by my side, who ensured that I do not loose track, discussed the topic with me over and over again from her interdisciplinary view as a sociologist and political scientist, and helped proofreading the manuscript.

GLOSSARY

ADAPTATION Process by which the state of the visual system is modified by previous and present exposure to stimuli that may have various luminance values, spectral distributions and angular subtenses (Commission Internationale de l'Eclairage, CIE S 017 [CIE S 017], 2011).

ADAPTATION LUMINANCE Comprises of two components: background luminance L_b, i. e. the luminance around a task point, and veiling luminance L_v, i. e. the luminance within the eye due to the scattering caused by a glare source: $L_a = L_b + L_v$.

CONTRAST Refers in this thesis to Weber contrast: $C = (L_t - L_b)/L_b$.

DYNAMIC ASSUMPTION Refers to the assumption that a crude estimate of the state of adaptation depends on where and for how long the gaze rested within a scene, i. e. a weighted mean luminance based on eye movement data.

EYE MOVEMENT Comprises of two parts: saccades and fixations. A fixation is that period of time where the gaze rests at a particular point within the observed scene. A saccade is the rapid eye movement to move the visual axis towards a new point of interest.

FOVEAL VISION Central part of the retina, thin and depressed, which contains almost exclusively cones and forming the site of most distinct vision (CIE S 017, 2011).

GLARE Condition of vision in which there is discomfort or a reduction in the ability to see details or objects, caused by an unsuitable distribution or range of luminance, or by extreme contrasts (CIE S 017, 2011). In this thesis the term refers to disability glare, i. e. the influence of glare impairing visual performance.

MESOPIC VISION Vision by the normal eye intermediate between photopic and scotopic vision. In mesopic vision, both the cones and the rods are active (CIE S 017, 2011).

PERIPHERAL VISION Refers in this thesis to the 10° off-axis region of the retina, although the extent of the whole retina is broader.

STATIC ASSUMPTION Refers to the assumption that the fast mechanisms of adaptation reach a steady state within the duration of a fixation, e. g. after a change in gaze direction and the related change in luminance.

SPATIAL SAMPLING Structured process of selecting a limited number of observations in a two dimensional scene in order to measure and describe quantities of the whole scene.

VEILING LUMINANCE Luminance that superimposes on the retinal image and reduces the contrast by stray light in the eye (CIE S 017, 2011)

VISUAL FIELD Extent of space in which objects are visible to an eye in a given position (CIE S 017, 2011).

VISUAL PERFORMANCE Quality of performance of the visual system of an observer related to central and peripheral vision (CIE S 017, 2011)

ABBREVIATIONS AND SYMBOLS

ABBREVIATIONS

ANOVA Analysis of variance

ANSI American National Standards Institute

ARMarker Augmented reality marker

C Contrast

CCT Correlated colour temperature

CI Confidence interval

CIE Commission Internationale d'Eclairage

D55 Standard illuminant with a CCT of 5500 K

D65 Standard illuminant with a CCT of 6500 K

EA Eschenallee

FN False negative

FOV Field of view

FP False positive

fpr False positive rate

HS High pressure sodium

IESNA Illuminating engineering society of North America

JTC Joint technical committee

LED Light emitting diode

LS Low pressure sodium

LIDC Luminous intensity distribution curve

MH Metal halide

n.s. Not significant result

OS Otto Suhr Allee

RN Real negative

ROC Receiver operating characteristic

RP Real position

SD Standard deviation

SDT Signal detection theory

S/P Scotopic to photopic ratio

SPD Spectral power distribution

TC Technical committee

TI Threshold increment

TN True negative

TP True positive

tpr True positive rate

TS Treskowstr

$\overline{C}$ Mean contrast

EM(x,y) Eye movement data map

η^2_G Generalized η squared

E_v Vertical illuminance in lx

F_{mes} Mesopic enhancement factor

λ Wavelength in nm

L(x,y) Luminance data map

L_a Adaptation luminance in $\mathrm{cd/m^2}$

$L_{a,p}$ Photopic adaptation luminance in $\mathrm{cd/m^2}$

$L_{a,s}$ Scotopic adaptation luminance in $\mathrm{cd/m^2}$

L_b Background luminance in $\mathrm{cd/m^2}$

$\overline{L}_i$ Mean luminance e. g. within a 10° circle of image i in $\mathrm{cd/m^2}$

$\overline{L}_{i,k}$ Mean luminance of image i and sub-area k in $\mathrm{cd/m^2}$

L_{mes} Mesopic luminance in $\mathrm{cd/m^2}$

L_t Target luminance in $\mathrm{cd/m^2}$

L_v Veiling luminance in $\mathrm{cd/m^2}$

m Mesopic adaptation coefficient

N Number of observations

p Probability value

$V(\lambda)$ Photopic spectral luminous efficiency function

$V'(\lambda)$ Scotopic spectral luminous efficiency function

$V(\lambda)_{mes}$ Mesopic spectral luminous efficiency function

x Horizontal coordinate

y Vertical coordinate

Z Test statistic of Wilcoxon rank-sum test / signed rank test

* Significant result

CONTENTS

Part I

BACKGROUND

1 INTRODUCTION

1.1 RELEVANCE

The European Union has requested their member states to reduce the emission of greenhouse gas in order to mitigate climate change (The European Parliament and the Council of the European Union, 2012). That means governments, industries and individuals have to either migrate to renewable energies or find ways to reduce their footprint on fossil energy resources. To achieve the proposed emission reduction of 20 % by 2020 (compared to the emission levels of 1990) possible approaches need to be identified and implemented.

The illumination of roads is defined in national standards and mandatory for public safety (Fotios & Gibbons, 2018). The electrical energy required for road lighting depends on the chosen light level of the lighting design and the luminous efficiency of the light source. The latter is characterising the quantity of visible light emitted by a particular light source in lm per W of electrical power. A good road lighting design has to fulfil various requirements: e. g. render potential obstacles highly visible for foveal vision and if applicable for peripheral vision (Adrian, 1993; Bacelar, Cariou & Hamard, 1999; Rea, Bullough & Zhou, 2010; Fotios & Goodman, 2012), contribute to the perceived safety of pedestrians (Boomsma & Steg, 2012), aid facial recognition (Lin & Fotios, 2015), lead to an appropriate brightness level (Fotios, Atli, Cheal, Houser & Logadóttir, 2015; Fotios & Cheal, 2011; Vidovszky-Németh & Schanda, 2012) and result in acceptability by the targeted users (Viikari, Puolakka, Halonen & Rantakallio, 2012).

In road lighting design potential approaches to increase the efficiency are: optimising luminous intensity distribution curves (LIDCs) (Pachamanov & Pachamanova, 2008), choosing efficient light sources based on the $\mathrm{lm\,W^{-1}}$ ratio (Ylinen, Tähkämö, Puolakka & Halonen, 2011) or reducing light levels without harming the requirements defined above (Fotios, 2013; Fotios & Goodman, 2012; Boyce, Fotios & Richards, 2009).

1.2 RECOMMENDED SYSTEM OF MESOPIC PHOTOMETRY

The recommended system for mesopic photometry is a system for characterising the spectral efficiency of peripheral visual performance at low levels of light according to relative contributions of cone and rod photoreceptors (Commission Internationale de l'Eclairage, CIE Publication 191 [CIE 191], 2010). Mesopic vision is the process

of the visual system switching from photopic vision dominated by cone activity to scotopic vision dominated by rod activity. In the recommended system mesopic vision is defined in the range from $5 \times 10^{-3}\,\mathrm{cd/m^2}$ to $5 \times 10^{0}\,\mathrm{cd/m^2}$, luminance ranges typically found in road lighting installations (see Figure 5 of Chapter 2). If not specified further, luminances are photopic luminances, i. e. spectral radiances weighted with the photopic luminous efficiency function $V(\lambda)$. For $V(\lambda)$ see Figure 1. Although the mesopic luminances of the recommended system characterise peripheral visual performance in said region, foveal visual performance in said region is still represented by photopic luminances, i. e. characterised by $V(\lambda)$.

Equation (1) defines the iterative approach to calculate the mesopic adaptation coefficient m and mesopic luminance L_{mes} for a given photopic and scotopic adaptation luminance, starting with an initial value of $m_0 = 0.5$ and repeating the second and third line until the value of m and L_{mes} converges. For more details see CIE 191, 2010.

$$\begin{aligned} m_0 &= 0.5, \\ L_{mes,n} &= \frac{m_{(n-1)} L_{a,p} + (1 - m_{(n-1)}) L_{a,s} V'(\lambda_0)}{m_{(n-1)} + (1 - m_{(n-1)}) V'(\lambda_0)}, \\ m_n &= a + b \ \log_{10}(L_{mes,n}) \quad \text{for } 0 \leq m_n \leq 1 \end{aligned} \tag{1}$$

where:

m_0	is the initial start value for the adaptation coefficient m
$L_{mes,n}$	is the mesopic luminance of the current iteration
n	is the iteration index
m_{n-1}	is the adaptation coefficient of the previous iteration
$L_{a,p}$	is the photopic adaptation luminance, from Chapter 2 onwards referred to as L_a
$L_{a,s}$	is the scotopic adaptation luminance
$V'(\lambda_0)$	is the value of the scotopic spectral luminous efficiency function at λ_0, i. e. 683/1699
λ_0	is 555 nm
m_n	is the adaptation coefficient of the current iteration
a	is 0.7670
b	is 0.3334

Whereas $L_{a,p}$ would be either measured in a real scene or simulated during lighting design, L_s typically is not being measured but calculated via the Scotopic / Photopic ratio (S/P ratio), which commonly is part of the technical documentation of the light source: $L_{a,s} = L_{a,p}/(\text{S/P ratio})$. Hence, the two parameters required for calculating m and L_{mes} are $L_{a,p}$ and the S/P ratio.

Equation (2) defines how to calculate the spectral luminous efficiency function $V_{mes}(\lambda)$ for a given $L_{a,p}$ and S/P ratio (incorporated in m as calculated via Equation (1)). That allows for calculating L_{mes} from spectral radiances as defined Equation (3). An example for that can be seen in Figure 1.

$$M(m)V_{mes}(\lambda) = mV(\lambda) + (1-m)V'(\lambda) \quad \text{for } 0 \leq m \leq 1 \tag{2}$$

where:

$M(m)$	is a normalization factor such that $V_{mes}(\lambda)$ attains a maximum value of 1
$V_{mes}(\lambda)$	is the spectral luminous efficiency function for a given adaptation condition m
λ	is the wavelength in nm
m	is the adaptation coefficient
$V(\lambda)$	is the spectral luminous efficiency function for photopic vision
$V'(\lambda)$	is the spectral luminous efficiency function for scotopic vision

$$L_{mes} = \frac{683}{V_{mes}(\lambda_0)} \int V_{mes}(\lambda) L_e(\lambda) d\lambda \tag{3}$$

where:

$V_{mes}(\lambda_0)$	is the value of $V_{mes}(\lambda)$ at $\lambda_0 = 555\,\text{nm}$
λ	is the wavelength in nm
$V_{mes}(\lambda)$	is a given spectral luminous efficiency function
$L_e(\lambda)$	is the spectral radiance in $\text{W}/(\text{m}^2\,\text{sr}\,\text{nm})$

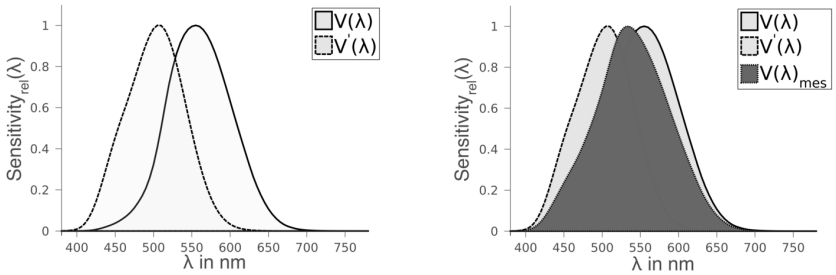

(a) (b)

Figure 1: Spectral luminous efficiency function for scotopic and photopic vision (left) and the spectral luminous efficiency function for a particular adaptation luminance and S/P ratio for mesopic vision (right, S/P = 1.71, $L_{a,p} = 0.3\,\text{cd}/\text{m}^2$).

Possible use cases of the recommended mesopic system in road lighting are:

1. Choose the SPD in order to enhance peripheral visual performance in residential areas (Fotios, 2013; Fotios & Goodman, 2012; Boyce et al., 2009)

2. Choose the most energy efficient light source based on $\mathrm{lm\,W^{-1}}$ ratio (Commission Internationale de l'Eclairage, TN 007 [CIE TN 007], 2017)

3. Reduce the light level if SPD fulfils certain requirements (Fotios, 2013; Fotios & Goodman, 2012; Boyce et al., 2009)

Mesopic luminances calculated with the recommended system represent, therefore, the predicted performance for a certain SPD and light level (i. e. adaptation luminance $L_{a,p}$) compared to the current applied photopic luminance. The predicted outcome might result in enhanced or diminished peripheral visual performance. That means a particular SPD will lead to a better visual performance than another, typically SPDs with increased blue will lead to better results (e. g. cold white light with high S/P ratios is more performant than still often used yellow light of high pressure sodium (HS) with a low S/P ratio).

Figure 2 depicts the predicted increase / decrease of visual performance (i. e. the mesopic enhancement factor $F_{mes} = L_{mes}/L_{a,p}$) for two exemplary SPDs: a white light emitting diode (LED) with a high S/P ratio of 1.6 and a high pressure sodium SPD with a low S/P ratio of 0.56 for the specified luminance levels of the lighting classes of Commission Internationale de l'Eclairage, CIE Publication 115 [CIE 115], 2010 (ME6 = $0.3\,\mathrm{cd/m^2}$ to ME1 = $2.0\,\mathrm{cd/m^2}$). It is obvious that the predicted change in peripheral visual performance between the two SPDs increases with decreasing luminance. With lower luminances peripheral visual performance improves for the LED whereas for HS peripheral visual performance deteriorates. Assuming one would upgrade an existing lighting installation from HS to that particular LED one could reduce the light level by 22 % for a ME6 lighting class or by 18 % for a ME5 without having a negative impact on peripheral visual performance (at least compared to the level of visual performance that was present before the reduction). As the chosen luminance level correlates with the consumed electrical energy that would be close to the requested reduction by The European Parliament and the Council of the European Union, 2012.

One of the required parameters for calculating a mesopic luminance via Equation (1) is part of the technical documentation of the light source or can be measured quite easily with a spectroradiometer in the field: the S/P ratio. For the second parameter, the peripheral adaptation luminance, it is currently not defined how to perform an

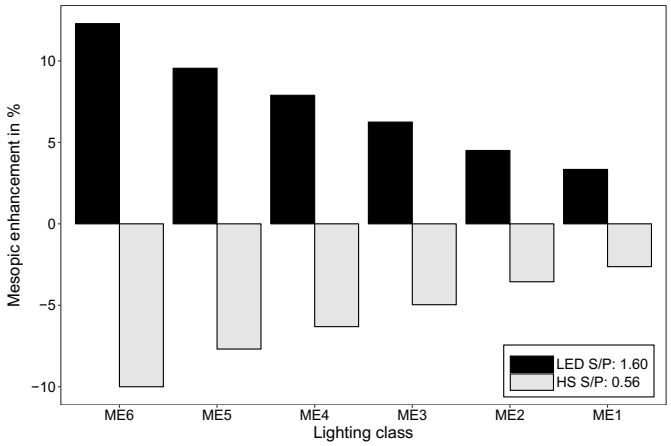

Figure 2: Predicted increase / decrease of peripheral visual performance (i. e. mesopic enhancement factor F_{mes} of CIE TN 007, 2017) compared to when using photopic luminances for two exemplary SPDs and assumed adaptation luminances as defined in the lighting classes of CIE 115, 2010. Note: HS = high pressure sodium.

estimation in a real road scene at night. The underlying research for the recommended system of mesopic photometry was undertaken mostly in the laboratory with homogeneous adaptation conditions (Walkey et al., 2007; Viikari et al., 2012; Várady et al., 2007). Real road scenes are complex with a wide range of luminances (Figure 5), contain glare sources and due to the dynamic nature of driving and eye movement of the driver joint technical committee 1 (JTC-1) of the Commission Internationale d'Eclairage (CIE) has requested proposals for estimating the state of adaptation, so that the recommended system of mesopic photometry can be applied into lighting design guidance e. g. into new versions of CIE 115, 2010 (Puolakka, Cengiz, Luo & Halonen, 2012). However, the JTC-1 just recently published an interim recommendation for practical application of the system of mesopic photometry (CIE TN 007, 2017), which recommends the design area, i. e. the mean luminance of the road surface as a reasonable estimate for adaptation luminance. That proposed recommendation shall be scrutinised.

1.3 ESTIMATING THE STATE OF ADAPTATION

Figure 3 depicts sketches of various approaches for estimating adaptation. Current standards such as Commission Internationale de l'Eclairage, CIE Publication 140 [CIE 140], 2000 propose a static assumption, where a foveal target is assumed to be observed under a static geometry (Figure 3 upper left). Here the estimated adaptation luminance might be represented by the mean luminance within a 2° circle at an assumed task point. Typically this is the mean luminance of the road surface (CIE 140, 2000). Other approaches follow a

dynamic approach based on where and for how long the gaze rested within the scene (Figure 3 upper right, Boyce, 2014). With that approach the estimated adaptation luminance might consist of the weighted mean luminance within the 2° circles based on eye movement data. Both approaches consider foveal adaptation. Based on the thoughts of Wördenweber, Wallaschek, Boyce and Hoffman, 2007 I propose a new method for estimating peripheral adaptation: the spatial sampling of a driver's visual field, which can be applied both to the static assumption (Figure 3 lower left) and the dynamic assumption (Figure 3 lower right). More details on the definition of adaptation and the mentioned assumptions are in Chapter 2 and Part iv.

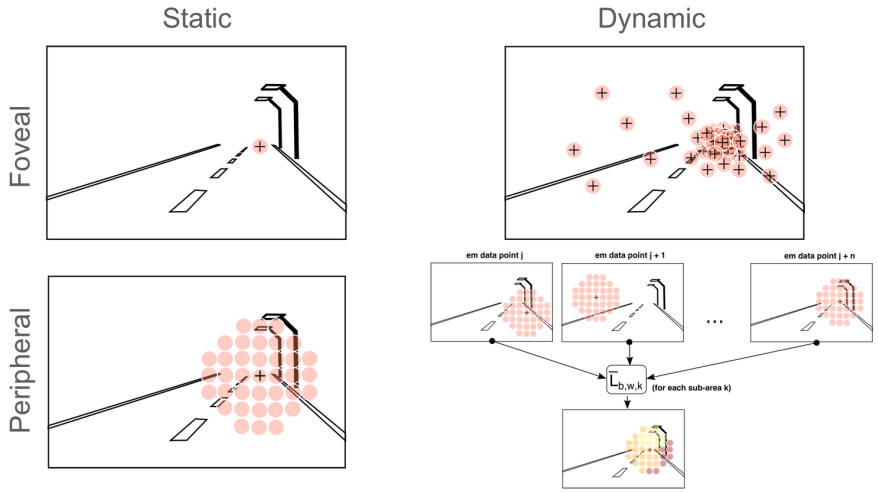

Figure 3: Sketch of various approaches for estimating adaptation in urban road scenes after dark. The static approach (left) assumes that readaptation in between fixations of eye movement converges and can be characterised by a defined task area. The dynamic approach (right) assumes that adaptation depends on where and for how long gaze was directed to. The fovea is assumed to be mainly influenced by the region of a single 2° circle, the periphery is represented by the spatial sampling pattern consisting of 68 circular 2° sub-regions.

1.4 AIM OF RESEARCH

The aim of this PhD thesis is to help solving practical problems of JTC-1 of the CIE which hinder the application of the recommended system of mesopic photometry by providing supporting data and answers to open questions.

Figure 4 depicts the context of the publications this thesis is based on. In order for JTC-1 to propose guidelines for applying the recommended system of mesopic photometry in road lighting design it is necessary to estimate the peripheral adaptation luminance of a driver

in a complex and dynamic environment. Chapter 2 gives an overview of the related work in this field.

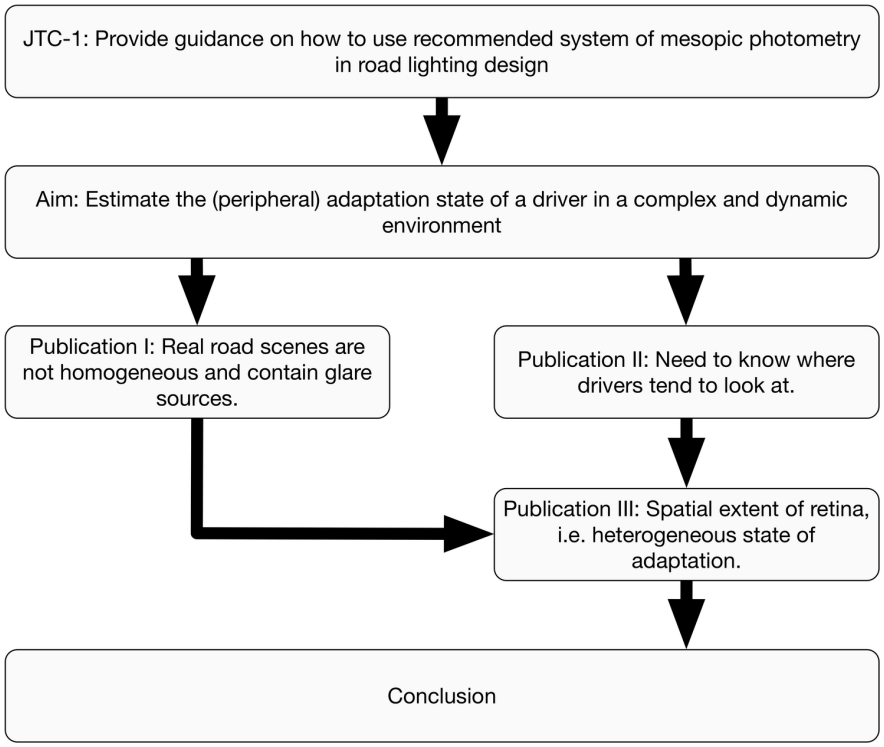

Figure 4: Context of the publications of this thesis.

Publication *I* (Winter et al., 2018, Chapter 7) addressed the issue that real road scenes are not homogeneous and contain glare sources. Questions to be answered were:

- How is adaptation affected by inhomogeneity and glare?
- Which mechanism (global or local) prevails?

Publication *II* (Winter et al., 2017a, Part iii) identified typical eye movement behaviour of car drivers and its change along a road. Questions to be answered were:

- Where do most of the drivers tend to look at most of the time?
- Which primitive shape approximates viewing behaviour best?

Publication *III* (Winter et al., 2017b, Part iv) introduced my new proposed method of the spatial sampling of a driver's visual field to deal with the the complexity of real road scenes and the spatial extent of the retina: meaning there is no such thing as a single adaptation luminance, because the complexity of the scene will result in a heterogeneous state of adaptation of the retina. Questions to be answered were:

- How to estimate peripheral adaptation?

- Which difference does it make when assuming a static or a dynamic approach?
- What does it mean if a simplified method (mean luminance of road) is used to estimate peripheral adaptation, but other methods might be more accurate?

Part v provides a summary and general discussion of the three publications and puts the findings into context to the recently published interim recommendation of JTC-1, which recommends using the average luminance of the design area, i. e. the road surface, as an estimate of adaptation.

The scope is set on quantifying the range of luminances the retina or more precise specific parts of it are exposed to in urban traffic scenes after dark. That with the here proposed method of the spatial sampling of a driver's visual field by focusing mainly on characterising luminances of typical scenes rather than modelling optics of the eye or synaptic interactions in the retina.

2 ESTIMATING THE STATE OF ADAPTATION

2.1 DEFINITION OF ADAPTATION IN GENERAL

Moon and Spencer, 1943 defined adaptation as the process of the retina of adjusting to the quantity and quality of light: if the eye is exposed for a sufficient time to a uniform condition every part of retina reaches an equilibrium state and the eye can be said to be adapted to that level of light. CIE S 017, 2011 adds some details specifying the extent of said uniform condition regarding adaptation as the process by which the state of the visual system is modified by previous and present exposure to stimuli that may have various luminance values, spectral distributions and angular subtenses. Such a definition might suffice in laboratory conditions where observers are exposed to a controlled environment, typically homogeneous in nature.

2.2 URBAN ROAD SCENES AFTER DARK

Figure 5 shows an example of the range of luminances encountered when driving in main and residential roads after dark. Although the total range of luminances is quite wide ($10^{-3}\,cd/m^2$ to $10^{4}\,cd/m^2$, 99% of the luminances are within ±1 log, that being from 10^{-2} to 10^{0} on a main road and from 10^{-3} to 10^{-1} on a residential street and a simulated street based on the data of Winter et al., 2017b. Thus most of the time neural adaptation will be capable to adjust to changes between fixations (for the theoretical background see Section 2.4). That data, however, represents the range of luminances within the whole scene and does not consider that particular parts of the periphery might be exposed to the 1% that are outside the ±1 log range, nor does it reflect the proportion of time various of said parts are exposed to. The very high luminances of the glare sources influence the state of adaptation via the veiling luminance and via the direct exposure of the photoreceptors to the glare source itself and are likely to take vision for a brief period of time when appearing suddenly, such as with an approaching vehicle.

2.3 ADAPTATION IN THE CONTEXT OF DRIVING

The distribution of luminances within a driver's visual field in urban scenes after dark is unlikely to be homogeneous. For a given design luminance as of CIE 115, 2010 there is some variation in luminance at different points according to the permitted uniformity, although this

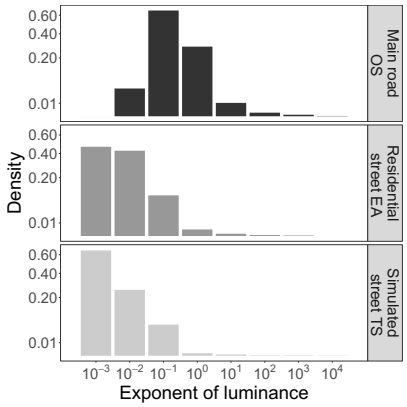

Figure 5: Histogram of luminances in the field of view (63° x 45°) in urban road scenes after dark for a main road, residential street and a simulated street. The scenes are based on the data of Winter, Fotios and Völker, 2017b and depict the distribution of luminances within 10 luminance images.

may be of relatively low importance in complex scenes. The visual field may contain discrete sources of high luminance such as the headlamps of approaching vehicles, the road lighting installation, shop lighting and advertisements. The visual field is further complicated by the headlamps of one's own vehicle and that this field is dynamic because of the vehicle travel and the gaze continuously scanning for potential hazards and controlling direction of travel. In a typical field of view, when driving along an urban route, the road surface may lie in the range of 0.3 cd/m^2 to 2.0 cd/m^2 (CIE 115, 2010), the extent of luminances found in typical urban scenes after dark, however, is quite more distinct spanning multiple log units (Figure 5).

Estimating the state of adaptation in complex road scenes is not a new task in itself, with guidance already available for tunnel lighting (Commission Internationale de l'Eclairage, CIE Publication 88 [CIE 88], 2004) for assessing the influence of glare via the threshold increment (TI) (Commission Internationale de l'Eclairage, CIE Publication 31 [CIE 31], 1976; CIE 115, 2010; CIE 140, 2000) and for calculating the visibility level of a small target (Illuminating Engineering Society of North America, RP-8-14 [ANSI IESNA RP-8-14], 2014). In these, adaptation luminance L_a is assumed to be the sum of the background luminance L_b around a task and the veiling luminance L_v:

$$L_a = L_b + L_v \tag{4}$$

This approach takes into account the scattered light due to glare within the visual field expressed via L_v (Stiles, 1929b). The aim of estimating adaptation in these purposes is, however, to consider the visibility of a target as seen by the fovea statically against its background. That is the static assumption. In contrast, determination of adaptation luminance for the mesopic photometry requires that the

overall state of adaptation of the peripheral retina is of interest, which might comprise of a more dynamic assumption of probabilities certain areas of the retina are exposed to within a road scene based on eye movement (Uchida et al., 2016).

Therefore, different parts of the retina will be differently adapted depending on where and for how long the eye has fixated (Wördenweber et al., 2007). That is the dynamic assumption. One way to gain a crude estimate for the overall adaptation luminance would therefore be to look at the pattern of fixation points and the time spent at each (Boyce, 2014): Uchida et al., 2016 proposed a method for calculating adaptation luminance that takes eye movement into account. A simpler, but less accurate, approach would be to use the average luminance of a region of the observed scene, for example a circular field with an angular diameter of 10 to 20 degrees (Narisada, 1992).

2.3.1 *Influence of glare in the context of driving*

The influence of glare on foveal adaptation has been investigated by Holladay, 1926; Stiles, 1929a and led to the scattering theory (Stiles, 1929b). This theory states that bright light sources within the visual field introduce a veiling within the eye of the observer, increasing the state of adaptation within the eye and leaving it under-adjusted for the actually lower luminances of the observed scene. The effect decreases visual performance (Holladay, 1926) and to estimate the effect an equivalent veiling luminance can be calculated (Commission Internationale de l'Eclairage, CIE Publication 31 CIE 31, 1976; Commission Internationale de l'Eclairage, CIE Publication 146 [CIE 146], 2002). This is a theoretical luminance superimposed on the actual scene used to estimate the increase of adaptation within the eye of an observer, that causes the same decrease in visual performance as a glare source. This decreases the actual contrast of an object (see Equations (5) and (6)), which results in poorer visual performance. Stiles and Crawford, 1937 augmented this formula for peripheral vision, which has recently been confirmed by Uchida and Ohno, 2014b and slightly updated (Uchida & Ohno, 2017).

$$C = \frac{L_t - L_b}{L_b} \text{ (without glare)} \tag{5}$$

$$C = \frac{(L_t + L_v) - (L_b + L_v)}{L_b + L_v} \text{ (with glare)} => C = \frac{L_t - L_b}{L_b + L_v} \tag{6}$$

2.3.2 *Current application of estimating adaptation for tunnel lighting*

Tunnel lighting should provide enough light to render visible those obstacles in the threshold zone (the entrance zone of the tunnel) as seen when approaching the tunnel from outside at a distance equal to the stopping distance. CIE 88, 2004 proposes two methods for estimating the state of adaptation of a driver approaching the entrance of a tunnel at daytime and at a given speed, the veiling luminance method and the L20 method.

The veiling luminance method calculates the luminance in the threshold zone based on the visibility of a target, i. e. by a defined minimum contrast. It takes into account the veiling luminance of the area surrounding the tunnel entrance. This is done by dividing the surrounding area into a 2° to 56.8° circular field of multiple areal glare sources, which are assumed to result in scattered light within the eye and, therefore, reduce the contrast of that target. Additionally the transmissivity of the windshield, the veiling of the atmosphere and the veiling of the windshield are taken into account.

The L20 method restricts to between 1/10 and 1/20 (depending on travel speed) the ratio of two luminances; (*i*) the luminance within a 20° circle around the tunnel entrance; and (*ii*) the luminance in the threshold zone. Thus this approach is an attempt to limit the drop-off in luminance from outside to inside the tunnel.

2.3.3 *Current application of estimating adaptation for glare assessment*

Road lighting design criteria include limits on disability glare caused to drivers by a proposed road lighting installation (CIE 115, 2010). This limit is defined by the Threshold Increment (TI) value. Consider an object for which the target to background contrast renders it just visible: this is the threshold contrast. Specifically this is the smallest contrast, produced at the eye of an observer by a given object, which renders the object perceptible against a given background (CIE S 017, 2011). TI is the percentage increase in contrast required for the same object to be just visible when visibility is impaired by glare (CIE S 017, 2011). Increasing adaptation luminances reduces the negative influence of glare. For this the adaptation luminance is assumed to be the average luminance of the road surface, as calculated (or simulated) according to (CIE 140, 2000), and is the mean luminance within a measurement field 60 m ahead of an assumed observer between two successive luminaires. This static approach does not take into account any influence on adaptation of a driver's dynamic gaze about a visual scene.

2.3.4 *Current application of estimating adaptation for visibility assessment*

In IESNA road lighting guidance (ANSI IESNA RP-8-14, 2014) the visibility of a target can be used as a design criterion for road lighting, where the adaptation luminance is considered to be the mean luminance of a point on the road slightly above and below a target of a given size and additionally the veiling luminance caused by the glare of road lighting installation.

2.4 ADAPTATION MECHANISMS

Figure 6 depicts the anatomy of the eye and the distribution of rods and cones within the retina. The light of a scene is projected onto the retina through the lens which is covered by the iris acting as an aperture. Contraction or expansion of the iris changes the diameter of the pupil, which reduces or increases the amount of light falling onto the retina (Reece et al., 2011), thus a mechanism influencing the whole retina when reacting to brightness changes. The retina itself consists of rods and cones, where the distribution of cones is prevalent in the fovea (i. e. the region within the central 2°) and the distribution of rods towards the 20° off-axis periphery (Wandell, 1995).

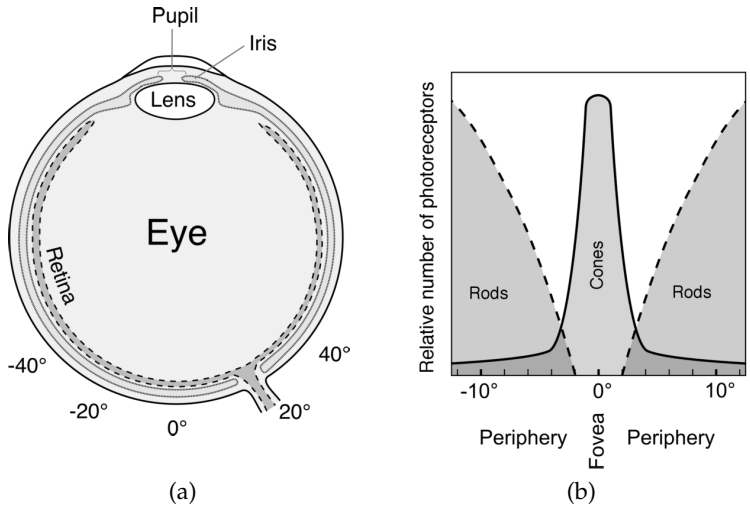

Figure 6: The eye and the distribution of rods and cones within the retina / eye (left Figure after Reece et al., 2011, right Figure after Wandell, 1995). Note that the right Figure is zoomed into the area of interest of CIE 191, 2010 (i. e. ±10° off-axis).

Three mechanisms are responsible for adaptation on retina-level: neural adaptation (i. e. change in sensitivity produced by synaptic interactions within the retina), photochemical adaptation within the photoreceptors, and the change from cone to rod vision (Boyce, 2014; Hofer & Williams, 2002).

The mechanisms are able to account for different degrees of change and do so with different response times. Change in pupil size can cover a luminance range of approximately 1 log within 0.3 s to 1.5 s. Neural adaptation is rather fast (< 200 ms) and covers 2 to 3 log. Photochemical adaptation is rather slow, taking minutes to tens of minutes, longer periods of time required for adaptation to darker surroundings, e. g. moonlight.

The change in pupil size influences adaptation globally, i. e. the amount of light falling onto the whole retina, whereas the other mechanisms control adaptation at a local level.

The change from cone to rod vision (and vice versa) can be seen as the signal of one photoreceptor becoming stronger than the other with decreasing (increasing) luminances within the scene. Stockman and Sharpe, 2006 described what a precise mesopic system should incorporate, however some of the reviewed literature is less relevant to the mesopic system of CIE 191, 2010, which focuses on visual performance, not flicker. Although it was discovered, that within the retina of monkeys the signal of the cones excited by a stimulus mostly perceivable by cones was faster than that of a rod signal excited by a stimulus mostly perceivable by rods (Gouras & Link, 1966; Gouras, 1967), it hasn't been revealed, yet, how the signals would behave when excited with signals perceivable by both photoreceptors as typical in the mesopic region. What the current mesopic system of CIE 191, 2010 represents might be a simplified approach, but it is well based on experiments (Freiding et al., 2007; Várady et al., 2007; Walkey et al., 2007), which, therefore, can be assumed to represent the change from cone to rod vision not most precise but good enough in a practical manner such as required in road lighting design.

With decreasing luminance levels the dominance of photoreceptors changes from cone to rod vision, with the rods being far more sensitive to lower luminance levels than cones (Boyce, 2014). The distribution of rods and cones being dependent on the region of the retina, where cones have their highest density in the fovea, the region where rods are absent, and rods at 20° off-axis (Wandell, 1995) (Figure 6b). Of interest to the mesopic system is that region of the retina where the distribution of rods and cones changes from one type to the other, which is in the region of 2° to 10° off-axis, 10° off-axis being the focus of the underlying research of CIE 191, 2010 (Freiding et al., 2007; Várady et al., 2007; Walkey et al., 2007).

Age has an influence on the adaptation processes. For example, the pupil diameter reduces with age (Winn, Whitaker, Elliott & Phillips, 1994) and the speed of photochemical adaptation becomes slower with increased age (Owsley, 2011). As it is assumed, that most of the heavy lifting while driving along a road will be performed by neural adaptation age is not a factor that is considered in the following analysis.

2.5 EYE MOVEMENT AND TRANSIENT ADAPTATION

Estimating the state of adaptation of a driver in the natural setting is not straightforward, because the visual scene is likely complex and inhomogeneous, having a range of luminances, and because of the dynamic nature of eye movements and travel along a road. As a result, different parts of the visual field stimulate different parts of the retina, and this puts the retina into a state of continuous transient adaptation (Adrian, 1987).

2.5.1 *Eye movement*

The gaze direction of a driver is dynamic, constantly moving to different regions of the visual field, in part determined by experience and distractions (Winter et al., 2016; Cengiz, Kotkanen et al., 2014; Kountouriotis, Spyridakos, Carsten & Merat, 2016; Crundall, Chapman, Phelps & Underwood, 2003). Eye movements comprise two parts, saccades and fixations. There are a couple of other types and sub-types of eye movement (e. g. smooth pursuit movements when tracing an object, Purves et al., 2001), but in this thesis I do not further distinguish. Fixations are periods of time, where the gaze rests at a particular position, e. g. when assessing a traffic scene regarding action needs to be undertaken. Saccades are the rapid movements of the eye between fixations. Eye movements are used in a feed-forward role to the motor system, to locate the information needed for the execution of an act (Land, 2006). A task during driving mainly fulfilled by peripheral vision seems to be maintaining the lane position (Summala, Nieminen & Punto, 1996). Note, however, that fixation on an object or area does not imply for certain where the observers attention is focused - gaze location does not uniquely specify the information being extracted (Rothkopf, Ballard & Hayhoe, 2007). However, when exposing the retina or more precise particular parts of it to a light scene the mechanisms of adaptation are triggered regardless whether attention is gathered or not. Of course the longer a gaze rests at a particular part of the road lured by attention, the more likely will the transient re-adaptation process be to converge, i. e. to complete the process as defined by Moon and Spencer, 1943.

Vision selectively suppressed during saccade.

During a saccade it was found that vision is impaired during the fast movement of the eye (Volkmann, 1962; Judge, Wurtz & Rochmond, 1980) which leads to a lack of perception during the actual movement. Uchikawa and Sato, 1995 identified, that this effect is greater for achromatic than for chromatic targets, where Ross, Burr and Morrone, 1996 extended this theory with the finding that the magnocellular pathway is selectively suppressed (i. e. the fast pathway to the visual cortex responsible for perception of movement and depth), while the parvocellular pathway seems to be unimpaired (i. e.

the slower pathway responsible for the perception of colour and fine details Boyce, 2014). According to Schütz, Braun and Gegenfurtner, 2009 post-saccadic visual performance rose for 150 ms to 200 ms to reach a steady state.

Main types of saccades are either reaction to a stimulus, i. e. reflexive, or voluntary, such as when requested to look towards a particular direction (Rayner & Castelhano, 2007). Where the next saccade will be headed depends on the information acquired within the current fixation (Findlay & Walker, 2012). New visual information can influence the target of the next saccade only if occurring 70 ms before start (Quaia, Lefèvre & Optican, 1999).

Even during a fixation small-scale motion keeps the eye continuously moving, which seems to be to prevent the fading of the visual scene (Martinez-Conde, Macknik & Hubel, 2004).

The fixation duration of drivers has been investigated by asking test participants to watch videos as if they were driving. In these fixation durations ranged from 0.35 s to 0.8 s (Chapman & Underwood, 1998; Underwood, Chapman, Bowden & Crundall, 2002). Within this range, there is likely to be a difference between daytime and after dark, with after dark fixations being about 10% longer (Crundall et al., 2003). However, eye movements whilst watching videos may not match those captured when the same event is experienced live (Foulsham, Walker & Kingstone, 2011). In simpler non-driving related laboratory experiments fixation duration depends on the task and results in shorter durations: 260 ms to 330 ms for scene perception and 180 ms to 275 ms for visual search (Rayner & Castelhano, 2007). The duration of a saccade depends on the magnitude of the location change ranging from 20 ms to 100 ms (Findlay & Walker, 2012). Figure 7 depicts an example of a potential sequence of fixations and saccades.

Typical duration of saccades and fixations.

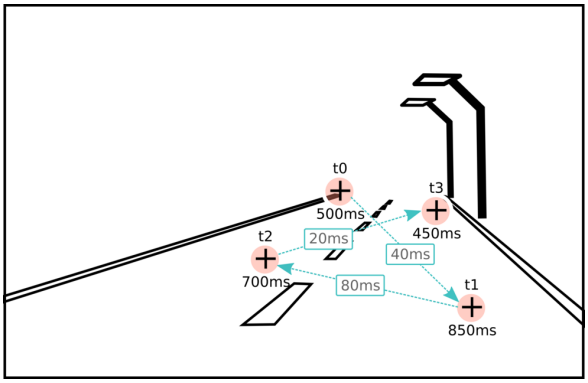

Figure 7: Example of a potential sequence of fixations and saccades at various points in time t_i putting the retina into a continuous state of transient adaptation. The given durations for fixation and saccade are examples based on theory of related work.

2.5.2 *Transient adaptation*

Boyce, 2014 defines transient adaptation as the state of changing adaptation if the visual system is not completely adapted to the prevailing illumination, such as when entering a tunnel or switching from instruments to exterior. Adrian, 1987 extends this to driving and eye movements as gaze fixation is normally changing and sequentially directed to different parts of the visual field, which effects a transition of the adaptation. Rinalducci and Beare, 1975 refine further: some of these changes in sensivity are accomplished in a few hundred milliseconds, but others take several minutes to an hour. The research on transient adaptation is concerned with the faster changes, which are thought to be primarily neural in nature. Based on Jahn Adrian, 1989 assumes that if the eyes sweep over very different luminances adaptation undergoes transition and if within ±2 log units transition is happening very fast and approaches steady-state within 0.2 s.

In the context of driving from daylight into tunnels Bourdy, Chiron, Cottin and Monot, 1987 tested a decrease of background luminance of 3 log and found that process to take up to 30 s concluding that photochemical adaptation is likely to be involved. Schreuder, 1975 found changes of that magnitude when entering a tunnel in from daylight to last 15 s. It could be the case, however, that when driving from bright daylight into a lit tunnel with a brightness change of that magnitude has a different effect on the slower mechanisms of adaptation (i. e. change in pupil size and photochemical adaptation) than when moving the gaze within an urban scene at night where small local areas might experience brightness changes of that magnitude.

Boynton and Miller, 1963 found that the adaptation effect caused by a change of brightness level depends primarily upon the ratio of change and is relative independent of absolute levels. They tested in the range from 0.127 cd/m^2 to 127 cd/m^2. Influence on visual performance were similar for both upward and downward changes reaching a steady-state within 0.3 s. In the experiment of Rinalducci, Lassiter and Mitchell, 1990 it was found that a drop of brightness level has a bigger influence than a rise. Changes within 1 log were not significant compared to the baseline visual performance, drops / rises within 2 log had significant differences. They tested in the range from 0.34 cd/m^2 to 34 cd/m^2. Both studies tested in luminance ranges where targets probably are in the range of Weber's law where threshold contrasts remain constant i. e. independent of background luminance. In lower luminance ranges Ricco's law prevails, where threshold contrasts increase with decreasing luminances (Adrian, 1989). However, there is no theoretical reason to assume neural adaptation would be slower when adapting to changes in the latter region just because the threshold contrast behaviour is different, but should be kept in mind.

2.5.3 *Practical implication for estimating the state of adaptation*

Narisada, 1992 proposed for the estimation of a driver's adaptation before entering a tunnel that when an observer is looking at an object against an area for instance, in the non-uniform field, the observer's fovea is initially adapted to a time average of the luminances of parts of the non-uniform field over which the observer is scanning his or her major visual attention for a span of time. He points out that eye movement should be known to estimate a precise state of adaptation, but doubts that no driver would repeat the same eye movements again and, therefore, knowing eye movement data of a single subject would be of no use and alternatively proposes to use an average luminance in an arbitrary chosen circular field of an angular diameter of 10° to 20° around the object as a first approximation. That area within the visual field that influences adaptation is defined as the visual adaptation field by JTC-1, but its size is yet to be defined.

Although Narisada, 1992 proposed that knowing the eye movement data of a single subject would be of no use, it has to be known where most of the drivers look at most of the time in order to a.) identify areas within road scenes that gain most of the attention and as a consequence mostly influence adaptation and b.) to analyse which simplified geometric shape approximates the viewing behaviour best in order to ease later application in road lighting design. Adaptation is influenced by the pattern of surrounding luminances, and that influence is apparently stronger for the luminance of the local surroundings (i. e. luminances of the area within the visual field that immediately surrounds a task point) than for the luminances further away (Moon & Spencer, 1943; Uchida & Ohno, 2014a). This is the local luminance hypothesis.

Consider a driver who is driving along a particular type of road with a particular class of road lighting installation (e. g. a main road or a residential street). It can be assumed that neural adaptation and change in pupil size will be the mechanisms responsible for re-adaptation when gaze location moves around the scene. These two mechanisms can respond to changes in luminance of up to 3 log within 0.2 s or up to 4 log within 1.2 s (but less for the elderly because of the more limited ability of change in pupil size). If, however, the change in luminance is greater than about 4 log units, then adaptation is likely to take longer, in the region of several minutes (Plainis, Murray & Charman, 2005). Following others (Adrian, 1989) I here consider the range of fast re-adaptation to be limited to ±2 log.

Given that a typical fixation duration lies in the range of 0.35 s to 0.8 s, and that photochemical adaptation has a much longer time course, it is unlikely photochemical adaptation plays a significant part. In the following analysis neural adaptation and change in pu-

pil size dominate the adaptation response and that the role of photochemical adaptation is negligible.

2.6 ESTIMATING PERIPHERAL ADAPTATION

With the JTC-1 calling for research investigating potential methods for estimating peripheral adaptation several approaches were recently published.

Cengiz, Kotkanen et al., 2014 analysed the combined eye-movement and luminance measurements along a road, with estimates of the peripheral adaptation calculated as the mean luminances of circular fields of various sizes (1° to 20° in diameter) centred around the fixations of drivers. Other studies suggest that only the local luminance (i. e. the luminance at and around a task point) influences visual performance, which is an estimate for adaptation (Moon & Spencer, 1943; Uchida & Ohno, 2014a; Cengiz, Puolakka & Halonen, 2014; Cengiz, Maksimainen, Puolakka & Halonen, 2016; Winter et al., 2018). That assumption would make field sizes larger than 2° around an assumed static task point irrelevant. As Narisada, 1992 pointed out knowing the variation to which particular drivers were exposed to is not helpful as it is unlikely that the same changes were to happen again. Therefore, it is necessary to describe a pattern which reassembles where most of the drivers tend to look at most of the time rather than analysing individual drivers.

Maksimainen, Puolakka, Tetri and Halonen, 2017 examined mean luminances within various elliptical and circular fields of size 1° to 90°, centred 1° below the horizon / at the horizon at the centre of the lane and compared these to the mean luminance on the road surface. Additionally to that the influence of glare was assessed by calculating L_v with various approaches, which resulted in the finding that for the calculation of the mesopic adaptation coefficient m it did not make a difference whether L_v was included or not indicating that L_b is the more relevant parameter when calculating m. It is still an open question which of the various field sizes would describe peripheral adaptation.

Uchida et al., 2016 used a numerical simulation method for estimating the state of peripheral adaptation. Their simulation takes input from luminance distribution, eye movement, surrounding luminance (veiling luminance) and an assumed measurement field. It was found that for scenes with glare sources the simulated adaptation luminance was higher than the mean luminance of the road. Although the method looks very promising incorporating all relevant parameters into one simulated result it is hard to follow for the reader to assess the influence of the various parameters. Therefore, it would be helpful to provide analyses for the sub-steps to evaluate the influence of the various parameters independently.

2.7 SUMMARY

Various approaches for estimating the state of adaptation of a driver are either applied in existing standards or reported in research commonly being the sum of the background luminance around a task point and the veiling luminance caused by the scene. The nature of the wide range of luminances within typical scenes comprising of areas of dark sky to parts with very bright sources of glare, the movement of the eyes, the travel along the road, the extent of the retina and the fact, that the actual state of adaptation cannot be measured as a ground truth reference makes proposals for estimating adaptation solely based on theories and assumptions backed with findings of laboratory or field experiments measuring proxies of adaptation such as visual performance. Methods range from the mean luminance of a task area (road surface) to mean luminances within simplified geometries assuming to approximate typical viewing behaviour for estimates of foveal adaptation. Other proposals analyse viewing behaviour and the connected change of exposure to various parts of the scene on a per-driver basis or proposed a method of taking all parameters, eye movement, veiling luminance, periphery and the area of measurement into account.

However, these studies and standards neglect the fact that the recommended system of mesopic photometry requires a proposal for estimating the peripheral state of adaptation, which I assume is a less trivial task than calculating the mean luminance within a simplified geometry such as a 10° circle or similar. Based on the thoughts of Wördenweber et al., 2007 I propose to analyse various parts of the periphery independently, which I do in Part iv with my new proposed method of the spatial sampling of the visual field for both the static and the dynamic assumption. Chapter 7 and Part iii provides the basis for doing that and Section 19.4 puts the findings into the context for the task of JTC-1.

Part II

CONTRAST DETECTION IN THE CONTEXT OF DRIVING

This part is the accepted version of an article that has been published as:

Winter, J., Fotios, S. & Völker, S. (2018). The effects of glare and inhomogeneous visual fields on contrast detection in the context of driving. *Lighting Research and Technology*, *50*(4), 537–551. doi:10.1177/1477153516672719 Originally published with SAGE Publications.

I designed the study, oversaw the data collection, visualised and analysed the data and wrote the manuscript. S. Fotios provided supervision, discussed the interpretation of the results and revised the manuscript. S. Völker gave general advice and helpful comments and proofread the manuscript.

3 INTRODUCTION

For the application of mesopic luminances according to the CIE recommended system for mesopic photometry (CIE 191, 2010) Joint Technical Committee 1 of the Commission Internationale de l'Eclairage (CIE JTC-1) has requested proposals on how to estimate the adaptation state of a typical observer depending on the task. For this paper, the task is driving a motor vehicle. Adaptation is the process of adjusting to the quantity and quality of light: if the eye is exposed for a sufficient time to a uniform condition every part of retina reaches an equilibrium state and the eye can be said to be adapted to that level of light (Moon & Spencer, 1943). In laboratory settings the luminance of a homogeneous background is used to control the adaptation luminance of the retina. Many of the experiments which provided the basic research for CIE recommended system (CIE 191, 2010) were carried out in laboratories with a homogeneous background (Freiding et al., 2007; Walkey et al., 2007; Várady et al., 2007), although some data were gathered in field studies (Akashi, Rea & Bullough, 2007).

Foveal eye movements for a car driver after dark tend to fall within a 10° circle centred either on the lane ahead or slightly to the near side, depending on the type of road and hence anticipated hazards (Winter et al., 2017a). The typical field of view for a city motorist therefore comprises the road surface, which may be considered as near-homogeneous (assuming the light distribution meets the minimum uniformity of CIE 115, 2010), but also inhomogeneous parts such as areas illuminated by the car head lamps, shop lighting and advertisements on the near side and glare sources such as the lamps of approaching vehicles or the luminaires of the fixed road lighting installation. Estimating the adaptation state under such circumstances is less straightforward. It is possible to predict the influence of glare with a homogeneous background (Stiles & Crawford, 1937; Uchida & Ohno, 2014b, 2017), and the influence of luminance on adaptation under a homogeneous background (Adrian, 1989). Moon and Spencer, 1943 found that under a homogeneous background the size of an extraneous light source has only a small effect and concluded that adaptation is mostly influenced by local luminance surrounding the target position. It is, however, unknown how all three findings work together under non-homogeneous circumstances such as those of a real traffic scene with simultaneous inhomogeneities and glare.

The influence of glare on foveal adaptation has been investigated (Holladay, 1926; Stiles, 1929a) and has led to the scattering theory (Stiles, 1929b). This theory states that disability glare introduces scat-

tered light within the eye of the observer, which causes a homogeneous overlay of a veiling luminance throughout the retina, thereby increasing the adaptation state within the eye and leaving it underadjusted for the actually lower luminances of the observed scene. This effect depends on the angle between the glare source and the task position, decreasing with an increase between the two. This effect decreases visual performance (Holladay, 1926) and to estimate the effect an equivalent veiling luminance can be calculated (Commission Internationale de l'Eclairage, CIE Publication 31 CIE 31, 1976; CIE 146, 2002). This is a theoretical luminance superimposed on the actual scene used to estimate the increase of adaptation within the eye of an observer that causes the same decrease in visual performance as a glare source. Stiles (Stiles & Crawford, 1937) augmented this formula for peripheral vision, which has recently been confirmed (Uchida & Ohno, 2014b) and slightly updated (Uchida & Ohno, 2017).

Adaptation is influenced by the pattern of surrounding luminances, and that influence is apparently stronger for the luminance of the local surroundings (i. e. luminances of the area within the visual field that immediately surrounds a task point) than for the luminances of points further away (Moon & Spencer, 1943; Völker, 2006; Uchida & Ohno, 2014a). This is the local luminance hypothesis. Indeed, road lighting design standards (e. g. ANSI IESNA RP-8-14, 2014) determine adaptation using a local background luminance along with a veiling luminance to account for glare. This is a foveal approach. Mesopic luminances, however, represent non-foveal visual performance, for which the adaptation state needs to be calculated for one or several peripheral task point(s). This paper reports a laboratory experiment in which contrast threshold was measured for the detection of foveal and peripheral targets for a background of constant luminance but with glare and extraneous light sources at foveal and peripheral locations.

4 METHOD

An experiment was carried out in the context of the driver of a motor vehicle and their need to see approaching objects. As a driver approaches an object it becomes visually larger (subtends an increased visual size): after dark, and when headlamps are being used, its luminance is also likely to increase (due to the headlamps of the vehicle). This experiment considers variations in target luminance but not size, measuring contrast threshold using the method of ascending limits as used in recent studies (Freiding et al., 2007; Kent, Altomonte, Tregenza & Wilson, 2014; Cengiz et al., 2016). The independent variables were target position, position of an extraneous light source and glare; the dependent variable was contrast threshold.

4.1 APPARATUS

The experiment was carried out using a homogeneous hemisphere (radius = 0.31 m; white plastic interior surface) and four light sources (Figure 8). Test participants sat at the front of the sphere, facing the centre of the hemisphere, with their position stabilized using a chin rest. The characteristics of the four light sources are shown in Table 1. One source illuminated the sphere from above through a translucent diffuser, this providing the background (adapting) luminance. The adaptation luminance used was 1.0 cd/m^2, this being the road surface luminance defined by the ME3 lighting class (CIE 115, 2010). A second source provided the targets and this was delivered via a Texas Instruments LightCrafter pico-projector.

The target was a 1° square which was projected to either a foveal (on-axis) or peripheral (off-axis) location, this being 10° to the right of the fixation point. The background and target light sources were Optronics OL-490 spectrally programmable light sources, having xenon lamps, which permit replication of a wide range of spectra in the range from 380 nm to 780 nm. To provide extraneous light patches in the visual field, i. e. inhomogeneity in the visual field, a third light source (a light-emitting diode (LED)) projected a 5° circular patch of 5 cd/m^2 at one of three possible positions, either superimposed on the foveal target, or located 10 degrees to either the left or right hand side of the foveal position. This increased the background luminance of the sphere surface by approximately 1.6 %.

A single spectral power distribution (SPD) was used for the target, background and extraneous light sources, this being a white light (S/P ratio = 1.71, CCT = 4322 K). The SPDs were measured directly

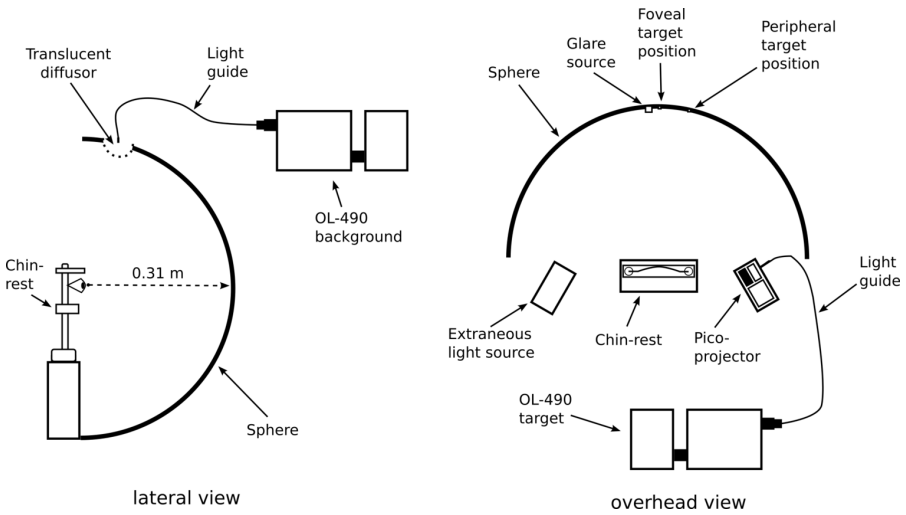

Figure 8: Vertical section (left) and plan section (right) of the apparatus.

Table 1: Characteristics of the four light sources used in this experiment.

Light source	Setting	E_v	Type of source
1. Background	1 cd/m^2	3.3 lx	Spectrally programmable light source: S/P ratio = 1.71, CCT = 4322 K
2. Target	Ascending luminance upon detection	-	Spectrally programmable light source: S/P ratio = 1.71, CCT = 4322 K
3. Extraneous light	5 cd/m^2	0.2 lx	Single white LED: S/P ratio = 1.71, CCT = 4322 K
4. Glare	1.0 lx at the observers' eyes	1.0 lx	Two LEDs (S/P = 2.7, CCT = 13.665 K) located 2.88° and 4.87° left of foveal target location, each contributing 0.5 lx

Note: E_v = vertical illuminance at the observer's eye.

using a Konica-Minolta CS-2000 spectroradiometer placed at the observer's position, and this was measured after each test session to ensure it was consistent. The luminous flux of the xenon lamps (background and target light source) deteriorated by approximately 0.5 % per hour during use, and to monitor and correct for this a correction was applied daily. The final light source was used to simulate the discomfort glare caused by an oncoming vehicle at 50 m distance. This was set to produce a vertical illuminance of 1 lx at the observer's eye, close to the maximum value used by Theeuwes, Alferdinck and Perel, 2002. The glare source comprised two white LEDs (S/P=2.7, CCT=13.665 K) located at 2.88° and 4.87° to the left of the foveal fixation point. The left-hand and right-hand LEDs had luminances of 70 kcd/m^2 and 40 kcd/m^2 respectively, each contributing 0.5 lx of the

illuminance at the observer's eye. This provided estimated veiling luminances of $0.81\,cd/m^2$ and $0.10\,cd/m^2$ for targets at the foveal and peripheral positions, respectively, as calculated according to the methods described in Commission Internationale de l'Eclairage, CIE Publication 31 CIE 31, 1976; Uchida and Ohno, 2014b. In trials, the glare source was switched on 2 s before the target was presented and remained on until the test participant pressed the button to indicate detection of the target. Results from Boynton and Miller, 1963 suggest that visual performance becomes stable after approximately 300 ms adaptation when background luminance changes from a lower to a higher value. Figure 9 shows the locations of the target, glare and extraneous light sources within the field of view and Figure 10 shows their SPDs.

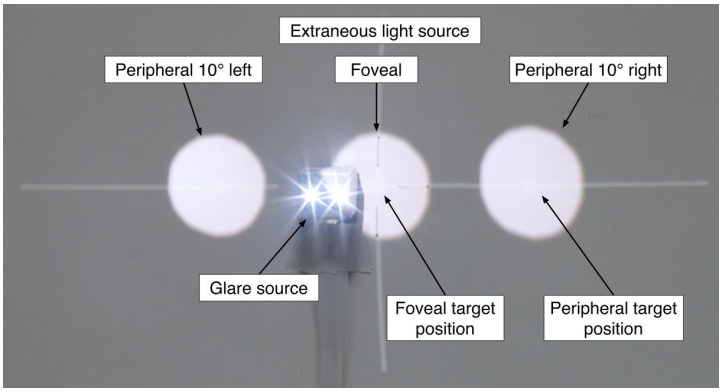

Figure 9: Photograph of the field of view for observers with all light sources presented simultaneously (i. e. background, target, glare and extraneous).

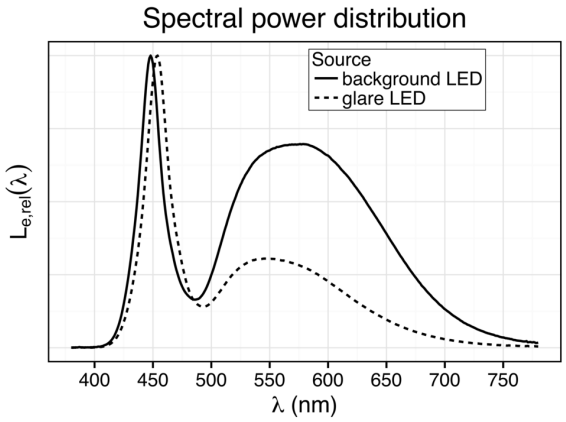

Figure 10: Spectral power distributions (SPDs) of the light sources used. Note: the SPDs of the target and extraneous light source are the same as the background.

Table 2: Combinations of glare, extraneous light and target location used in trials as independent variables.

Combination	Glare	Extraneous light	Target
1	Off	None	On axis
2		None	Peripheral (10° right)
3		Foveal	On axis
4		Foveal	Peripheral (10° right)
5		10° right	On axis
6		10° right	Peripheral (10° right)
7		10° left	On axis
8		10° left	Peripheral (10° right)
9	On	None	On axis
10		None	Peripheral (10° right)
11		Foveal	On axis
12		Foveal	Peripheral (10° right)
13		10° right	On axis
14		10° right	Peripheral (10° right)
15		10° left	On axis
16		10° left	Peripheral (10° right)

4.2 PROCEDURE

Contrast threshold was measured as the dependent variable using the method of ascending limits. The target luminance was initially low, at which level it could not be detected, and was gradually increased under automatic control until it was detected by the test participant. Observers used binocular vision during trials and indicated target detection by pressing a button.

There were 16 combinations of target location, extraneous light sources and glare (Table 2) and these were used in a semi-random order. Trials were carried out in two blocks, glare or no-glare, with the block order being chosen at random. Within each block, the four extraneous light conditions (off, foveal, 10° right, 10° left) were used in random order.

With a target expected to appear in a known location there is a risk that test participants may look in that direction, specifically, they may look towards the direction of a target expected to appear in the periphery rather than towards a fixation mark. Hence the target was presented to the on-axis or peripheral locations in a random order. In essence, light source combinations 1 and 2 (and 3 and 4, ... 15 and 16) were run in pairs.

The effectiveness of this order randomization would be somewhat limited if there were only one target presentation at each location, as

Table 3: Range of target luminances used within each local luminance.

Light source	Local luminance (cd/m^2)	Limits of target luminance (cd/m^2) Lower limit ($C = 0.005$)	Upper limit ($C = 0.6$)
Background only	1.0	1.005	1.60
Background and extraneous source	6.0	6.03	9.60

Note: contrast calculated as $C = (L_t - L_b)/L_b$ where L_b = local background luminance and L_t = target luminance.

after having seen the on-axis target then it would be known that the next stimulus was at the peripheral location. To overcome this, the target was presented at each location for either two, three or four trials, this number being a part of the randomization process. Repeated trials give rise to potential practice effects, such as practice or adaptation. Hence it was planned that analyses would be carried out using the second trial for each light source combination, as suggested by Collie, Maruff, Darby and McStephen, 2003 and Poulton, 1989. Practice effects in these data are discussed below.

While the background luminance remained constant ($1.0\,cd/m^2$) throughout all trials, the local luminance at the target increased to $6.0\,cd/m^2$ for those trials where the extraneous light source was superimposed onto this background at the target location. The ranges of target luminances were therefore chosen to maintain a similar range of target to background contrasts ($C = 0.005$ to $C = 0.6$) for both local adaptation luminances (Table 3). These ranges were divided into 150 linear steps. The light source was programmed to give a gradual increase in luminance at the rate of 0.15 seconds per step, and hence it would have taken 22.5 seconds to increase from the lowest to highest luminance in the range.

At the start of a test session, 10 minutes was allowed for adaption to the background luminance of $1.0\,cd/m^2$. After switching on the extraneous light source, a further 30 s period was allowed for readaptation. The test participant was instructed to focus on the fixation point (a dark cross mark) and to press the response button when a target was detected either at the foveal or the peripheral 10° off-axis target location. To check for guessing they were also required to say whether the target appeared in the foveal or peripheral position. The wrong location was reported in less than 1% of trials and when this occurred the results were omitted and the trial repeated.

4.3 PARTICIPANTS

There were 24 test participants, and they received a remuneration for their participation. This sample comprised six females and 18 males

and they were aged between 20 and 36 years (mean = 27 years, SD = 4 years). Participants' vision was tested prior to trials with an Oculus Binoptometer 4P. All test participants were found to have at least normal visual acuity (i. e. $\geq 6/6$), which was tested using a Landolt ring chart at photopic ($300\,\mathrm{cd/m^2}$) and mesopic ($0.032\,\mathrm{cd/m^2}$) luminances under standard illuminant D65, and normal colour vision, which was tested using the Ishihara test charts under a D55 light source. None of the subjects required visual aids.

5 RESULTS

5.1 PRACTICE EFFECT

There were two, three or four trials per light source combination, this being done to reduce cues as to expected target location, but these repeats may give rise to a practice effect. Figure 11 shows the mean contrast threshold for each trial averaged across all stimulus combinations and shows a slight reduction in contrast for the second, third and fourth trials compared with the first. The Pearson product-moment correlation between trials was positive ($r \geq 0.67, p < 0.001$) suggesting a tendency to give a similar response on successive trials. A two-way analysis of variance (ANOVA) for repeated measures was carried out for repetitions 1 and 2 (as described above, trials 3 and 4 were not used in all cases, according to the randomised presentation, and were omitted here to permit a balanced ANOVA design). This indicated a significant difference between repetitions ($p = 0.016, \eta^2_G = 0.01$, negligible effect size), a significant difference between conditions ($p < 0.001, \eta^2_G = 0.18$, medium effect size) and a near-significant interaction ($p = 0.06, \eta^2_G = 0.01$, negligible effect size). Although the effect size of factor repetition is negligible it is consistent with Collie et al., 2003 who found that results from first trials tend to be poorer than from subsequent trials but there was little impact of practice on subsequent trials. As planned, analyses of the results below were carried out using results from the second trial only.

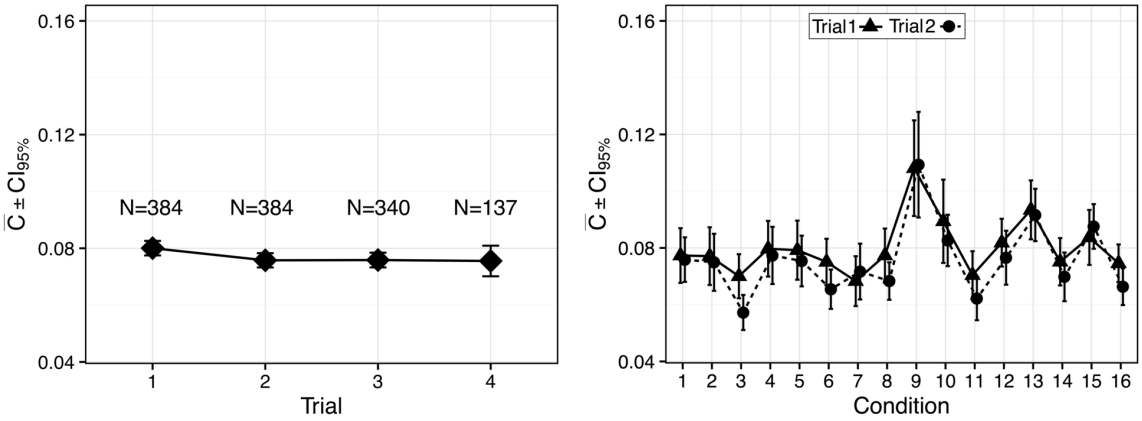

Figure 11: Contrast threshold determined for the trial repetitions. The left-hand graph shows all conditions merged, with the number of data for each repetition. The right-hand graph shows the repetitions by condition, referenced via numbers as in Table 2. Error bars show ±95% confidence interval.

5.2 THRESHOLD CONTRASTS

The results presented here are the mean threshold contrasts ($\overline{C}$), i. e. the contrast required to detect the target as derived from the target luminance recorded during trials. Figure 12 shows the mean threshold contrasts for each light source condition and target position averaged across the 24 observers.

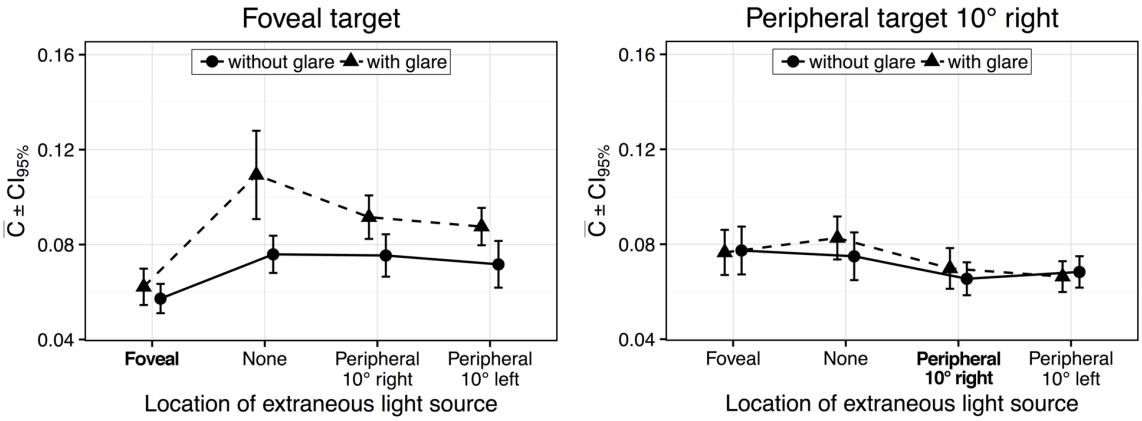

Figure 12: Results measured as local contrast at the foveal (left) and 10° off-axis peripheral (right) target positions for $N = 24$ test participants. Error bars show ±95% confidence interval (CI). Note: the x-axis label marked in bold font indicates the location of the extraneous light source that overlaps the target position, the connecting lines were added for clarity, to aid recognition of the glare and no-glare trials.

The reference condition for this analysis is those trials carried out without glare and without an extraneous light source. First, consider trials when the target was presented at the foveal location. It can be seen that without glare, extraneous light at the peripheral locations results in a similar threshold contrast to that obtained in the reference condition. Superimposing extraneous light onto the target in the foveal location reduces the threshold contrast, which is consistent with the local luminance hypothesis (Uchida & Ohno, 2014a). When the glare source was added the threshold contrast increased; this increase is larger for trials with no extraneous light, and smaller for trials when extraneous light was superimposed onto the target.

The confidence interval for one condition (foveal target, with glare, without extraneous light) is larger than for other conditions. In that condition the response gained from one observer was extreme compared with the responses from other observers (i. e. their result was greater than 2 standard deviations from the mean). Removing the results of that particular observer did not, however, significantly change the confidence interval: the variability in this condition is generally high so this observer's responses were retained in all analyses.

Consider next the trials when the target was presented at the peripheral location. These results do not indicate a strong effect of glare or extraneous light on contrast threshold for target detection.

The foveal target results are consistent with the local luminance hypothesis as found by others (Moon & Spencer, 1943; Völker, 2006; Uchida & Ohno, 2014a; Cengiz et al., 2016), when no glare is present. The negative influence of glare seems to be reduced by the distribution of the surrounding luminances, i. e. the extraneous light source presented at non-target locations.

Levene's test confirms the assumption of equality of variance at both the foveal and peripheral target positions ($p \geq 0.19$). Distribution normality was examined using a Shapiro-Wilk test and this suggested data from 11 of the 16 light source combination were drawn from a normally distributed population. The cases not suggested to be normally distributed were four with the foveal target position (with glare no extraneous light source, with glare peripheral 10° right, without glare peripheral 10° left and without glare peripheral 10° right) and one case for the peripheral target (with glare foveal offset). Type I error rate of the F test is, however, suggested to be robust to violation of normality (Harwell, Rubinstein, Hayes & Olds, 1992) and hence a two-way ANOVA for repeated measurements was used for inferential statistics. Reported effect sizes are generalized eta squares (η^2_G) as suggested for repeated measurement designs (Bakeman, 2005).

For the foveal target position a two way ANOVA for repeated measurements with within factors showed that both glare (η^2_G=0.12, small effect size, as defined by Bakeman, 2005) and the extraneous light source ($\eta^2_G = 0.19$, medium effect size), as well as their interaction ($\eta^2_G = 0.06$, small effect size) had a significant influence ($p < 0.01$). At the peripheral target position only the extraneous light source ($p < 0.001, \eta^2_G = 0.07$, small effect size) had an effect; the effect of glare was not suggested to be significant ($p = 0.26, \eta^2_G = 0.00$, negligible effect size) and the interaction was also not significant ($p = 0.27, \eta^2_G = 0.01$, negligible effect size).

5.3 FOVEAL TARGET POSITION

Because the ANOVA was significant on both factors and their interaction a series of pairwise paired t-tests were carried out to investigate the significant interaction between glare and the extraneous light source for the foveal target position. Reported effect sizes for these comparisons are Cohen's d for independent means (Sullivan & Feinn, 2012; Cohen, 1992). As suggested (Perneger, 1998; Rothman, 1990) these results are not corrected for multiple comparisons but conclusions drawn instead by considering the overall pattern of findings.

Comparisons were made between the reference condition (no glare, no extraneous light source) and the seven combinations of glare and/or extraneous light. In the absence of glare, extraneous light sources at the non-target positions did not have a significant effect (peripheral 10° right, $p = 0.92$, negligible effect; peripheral 10° left, $p = 0.37$, negligible effect). Moon and Spencer, 1943 also found that contrast threshold was mainly influenced by the local luminances around of the task point and therefore the current results support their local luminance theory. Glare led to a significant increase in contrast threshold when extraneous light was absent ($p < 0.001$, large effect size) or if extraneous light was located at non-target positions (peripheral 10° right $p < 0.001$, large effect size; peripheral 10° left $p = 0.003$, medium effect size). Extraneous light located at the target location led to a significant decrease in the mean contrast, both with glare ($p = 0.001$, medium effect size) and without glare ($p < 0.001$, large effect size). This confirms the above assumed agreement with the local luminance hypothesis for the foveal target position. However, when glare is within the visual field the distribution of the surrounding luminances matters, i. e. it makes a difference whether or not the luminance of the surrounding visual field is homogeneous.

Glare was found to be a significant effect, but reduced in size (decreasing the required contrasts) when the extraneous light source was presented at non-target positions (peripheral 10° left $p = 0.026$, medium effect size; peripheral 10° right, near significant $p = 0.057$, medium effect size). Glare was not suggested to be significant when the extraneous light source was presented at the target location ($p = 0.11$, small effect size). These results are visualized in Figure 13.

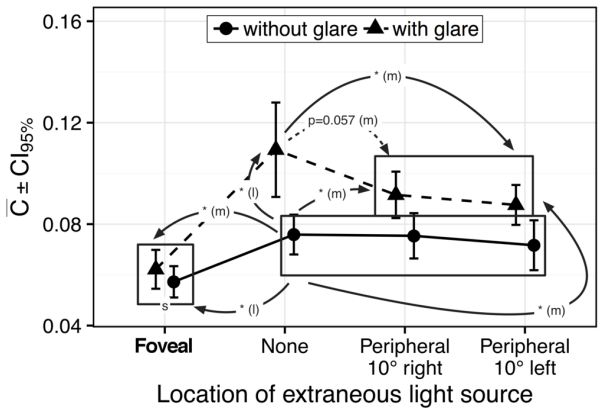

Figure 13: Results of trials with the foveal target illustrating significant differences ($p < 0.05$) in threshold contrast between different conditions. Solid line = significant differences; dashed line = differences which are close to significant; effect size indicated as l (large), m (medium) or s (small). Note: the x-axis label marked in bold font indicates the location of the extraneous light source that overlaps the target position, the connecting lines were added for clarity, to aid recognition of the glare and no-glare trials.

5.4 PERIPHERAL TARGET POSITION

For trials where the target was presented at the peripheral position, the ANOVA showed a significant effect of extraneous light source position but did not suggest that glare was significant. It would, therefore, have been possible to continue with the post-hoc test with results from both glare conditions merged. However, since glare has an influence on visual performance (Stiles & Crawford, 1937; Uchida & Ohno, 2014b, 2017), even if not found to be significant under these conditions, the further analyses of extraneous light source location were carried out using paired t-tests and this was done for the with and without-glare trials separately.

Without glare it was found that, compared to the reference condition with no extraneous light source, illuminating the target location improves visual performance significantly ($p = 0.037$, small effect size), illuminating the visual field with additional $5\,\mathrm{cd/m^2}$ 10° left of the peripheral target position (the foveal position) has no significant influence ($p = 0.58$, negligible effect size), both findings supporting the local luminance hypothesis. However, illuminating the visual field 20° left of the peripheral target position (peripheral 10° left) reduces contrast threshold to an extent that is close to significant ($p < 0.052$, small effect size). Comparing the two positions of the extraneous light source within the visual field but not at the target position, the left peripheral position of the extraneous light source has a lower contrast than the foveal position ($p = 0.031$, small effect size). Peripheral 10° left and peripheral 10° right show no difference in means ($p = 0.4$, negligible effect size). Presence of glare affirmed these findings, increasing the effect sizes, as visualized in Figure 14.

The findings for the peripheral target position partially support the local luminance theory: the distribution of the surrounding luminances does not matter for peripheral visual performance if altered in the region of the fovea, but matters if the inhomogeneity occurs in the periphery. That effect is increased under the presence of glare.

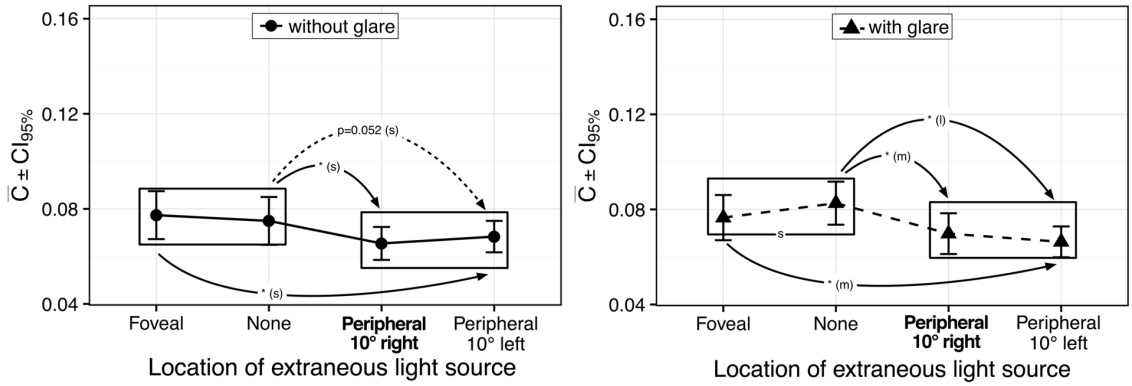

Figure 14: Illustration of significant differences ($p < 0.05$) in threshold contrast between different conditions with the peripheral target. Solid line = significant differences; dashed line = differences which are close to significant; effect size indicated as l (large), m (medium) or s (small). Note: the x-axis label marked in bold font indicates the location of the extraneous light source that overlaps the target position, the connecting lines were added for clarity, to aid recognition of the glare and no-glare trials.

6 DISCUSSION

This experiment shows that the effect of glare on contrast needed to detect a foveal or peripheral target is affected by the presence of extraneous light sources. The uniform fields typically used in glare evaluations (Commission Internationale de l'Eclairage, CIE Publication 31 CIE 31, 1976; CIE 146, 2002) may therefore give an incomplete picture of the impact of glare.

6.1 METHOD OF ASCENDING LIMITS

Following previous work (Freiding et al., 2007; Kent et al., 2014; Cengiz et al., 2016) the procedure used here was ascending limits. This means that the target luminance was gradually increased until the required task could be carried out, i. e. the target could be detected (Freiding et al., 2007; Cengiz et al., 2016) or a specified level of perceived intensity was reached (Kent et al., 2014). It is known that the starting point for such an experiment forms an anchor to the response and that if different starting points are used, different results may be obtained (Logadóttir, Christoffersen & Fotios, 2011; Logadóttir et al., 2013). If, instead, the luminance had been gradually decreased (i. e. descending limits), and observers instructed to state when the target was no longer visible, this is likely to have resulted in a different estimate of threshold luminance.

Two errors are anticipated - habituation and/or expectation (Gescheider, 1985). The error of habituation is a tendency to repeat the same response on subsequent trials, leading to higher thresholds; the error of expectation is a tendency to falsely anticipate the arrival of a stimulus at threshold and may lead to deceptively low thresholds on ascending trials. The magnitudes of habituation and expectation are unlikely to be equal, and the stronger error will lead the direction of bias. One approach to countering this anticipated bias is to use both ascending and descending variations in luminance on separate trials and use the mean of the two responses as an estimate of threshold luminance (Gescheider, 1985). If an absolute threshold is required, the method of ascending limits alone may be insufficient. Assuming that the effect of bias is consistent across conditions, then ascending limits are sufficient to investigate relative effects across conditions, which is the focus of the current work.

6.2 PRACTICE EFFECT

This experiment employed repeated trials (up to four) with the same condition and planned to analyse results of the second trial to overcome a possible practise effect. Analysis above (Section 5.1) suggests that the difference between the first and second trials was significant, but the effect size was negligible. Omitting the first trial would not have been required based on the statistics, but still can be considered good practice as proposed by Collie et al., 2003.

Previous studies have used alternative approaches. Cengiz et al., 2016; Cengiz, Puolakka and Halonen, 2014 discarded exceptionally low results (i. e. less than the mean minus two standard deviations) to eliminate those trials where the test participants may have been anticipating the results. Similarly, Walkey et al., 2007 discarded unusually long or short reaction times (mean ±2 SD) to eliminate anticipatory and delayed responses. Freiding et al., 2007 monitored performance by repeating trials with a standard stimulus throughout a test. Kent et al., 2014 investigated whether time of day affected glare evaluations. Since responses at the four times of day were always recorded in the same order, this confounds suggestion that the gradual increase in tolerance it was associated with time of day and may have instead been a gradual adaptation to glare regardless of absolute time of day.

6.3 COMPARISON TO EXISTING MODELS

The influence of changes in adaptation on contrast threshold can be predicted with Adrian's contrast formula (Adrian, 1989) in the updated version to be found in ANSI IESNA RP-8-14, 2014. Table 4 shows relative comparisons of the findings of this paper to the predicted decrease of contrast threshold by Adrian's model. At the foveal target positions the finding and the model match well, while at the peripheral target position the finding is less distinct than the predicted effect. Note that the Adrian's formula was not meant to predict peripheral visual performance.

Based on the veiling luminance introduced by the glare source it is possible to predict the negative influence of glare with the threshold increment (TI) value (CIE 31, 1976). At the foveal target position for both adaptation states the finding and the prediction match rather well. At the peripheral target position the TI value underestimates the negative influence of glare, note that the TI model was also not meant to predict the decrease of peripheral visual performance.

Table 4: Comparison of some of the results to predictions of existing models.

	Finding	Prediction	Model	Parameters
FOVEAL COMPARISONS				
Extraneous light source: Foveal vs None, without glare	−25%	−25%	ANSI IESNA RP-8-14, 2014; Adrian, 1989	L_{b1} = 1.0 cd/m^2, L_{b2} = 6.0 cd/m^2, age=27, t=0.2, $alpha$=60′, k=2.7
With glare vs without glare: No extraneous light source	+44%	+53%	CIE 31, 1976: L_v, TI	L_b = 1.0 cd/m^2, L_v = 0.81 cd/m^2, α_1=2.88°, E_{v1}=0.5 lx, α_2=4.87°, E_{v2}=0.5 lx
With glare vs without glare: Extraneous light source at foveal position	+9%	+13%	CIE 31, 1976: L_v, TI	L_b = 6.0 cd/m^2, L_v = 0.81 cd/m^2, α_1=2.88°, E_{v1}=0.5 lx, α_2=4.87°, E_{v2}=0.5 lx
PERIPHERAL COMPARISONS				
Extraneous light source: Peripheral 10° right vs None; without glare	−13%	−25%	ANSI IESNA RP-8-14, 2014; Adrian, 1989	L_{b1} = 1.0 cd/m^2, L_{b2} = 6.0 cd/m^2, age=27, t=0.2, $alpha$=60′, k=2.7
With glare vs without glare: No extraneous light source	+10%	+7%	Uchida and Ohno, 2017: L_v, CIE 31, 1976: TI	L_b = 1.0 cd/m^2, L_v = 0.10 cd/m^2, α_1=12.88°, E_{v1}=0.5 lx, α_2=14.87°, E_{v2}=0.5 lx
With glare vs without glare: Extraneous light source at peripheral 10° right position	+7%	+2%	Uchida and Ohno, 2017: L_v, CIE 31, 1976: TI	L_b = 6.0 cd/m^2, L_v = 0.10 cd/m^2, α_1=12.88°, E_{v1}=0.5 lx, α_2=14.87°, E_{v2}=0.5 lx

Note: ANSI IESNA RP-8-14, 2014, Adrian, 1989 is not meant to calculate peripheral contrast thresholds, nor the TI value of CIE 31, 1976.

7 CONCLUSION

The influences of glare and extraneous light sources within the visual field were investigated by comparing contrast detection threshold for targets presented at foveal and off-axis (peripheral 10° right) locations.

The local luminance hypothesis as suggested by others (Moon & Spencer, 1943; Uchida & Ohno, 2014a; Cengiz et al., 2016) was again found to be applicable for the foveal target position, i. e. visual performance is influenced mostly by the luminances directly surrounding the target position and it is assumed, that this is applicable to adaptation as well. However this was found to be valid for conditions without glare. Under the presence of glare visual performance was better if an extraneous light source provided additional illumination within the periphery of the visual field, which indicates a global influence of the surrounding luminances.

At the peripheral target position the local luminance hypothesis was only valid if the additional illumination of the extraneous light source was centred around the fovea. Under both the presence and absence of glare, visual performance was better if an extraneous light source provided additional illumination within the periphery of the visual field. The effect size increased under the presence of glare, where illuminating the fovea slightly improved visual performance.

This paper reveals a global influence of the surrounding luminance. One interesting result is that, for the peripheral target (10° right) the extraneous light at 10° left reduced the contrast threshold while the foveal extraneous light, which is closer to the task point than the 10° left, did not.

As current equations for assessing glare tend to be more conservative than is potentially required in a less homogeneous surrounding such as an illuminated street at night, these equations favour safety, rather than exact predictions. For the calculation for the mesopic luminances based on estimation of the adaptation state Maksimainen et al., 2017 found that the influence of glare on adaptation and therefore on the calculated mesopic luminance is rather low and the bias introduced by neglecting the influence of glare is trivial. However as the glare of approaching cars increases rapidly temporal adaptation changes might create more extreme values than have been reviewed in this experiment or that were considered by Maksimainen et al., 2017.

Part III

EYE MOVEMENT WHEN DRIVING AFTER DARK

This part is the accepted version of an article that has been published as:

Winter, J., Fotios, S. & Völker, S. (2017a). Gaze direction when driving after dark on main and residential roads: Where is the dominant location? *Lighting Research and Technology*, *49*(5), 574–585. doi:10.1177/1477153516632867.

I designed the study, oversaw the data curation, visualised and analysed the data and wrote the manuscript. S. Fotios provided supervision, discussed the interpretation of the results and revised the manuscript. S. Völker gave general advice and helpful comments and proofread the manuscript.

8

INTRODUCTION

The aim of CIE Joint Technical Committee JTC-1 is to investigate implementation of the CIE recommended system for mesopic photometry defined by CIE 191, 2010. This article responds to the JTC-1 request for data regarding the shape and size of the part of the visual field into which a driver's visual gaze tends to fall, these data being used to characterise the visual adaptation of drivers.

Gaze behaviour analysis has been used to investigate where car drivers look (Mourant & Rockwell, 1970; Stahl, 2004), for example to determine gaze behaviour when steering (Land & Lee, 1994). The JTC-1 proposal is to use the visual field capturing the majority of eye movements as the field for estimating adaptation luminance. This discussion includes questions of whether the suitable field of view relevant to the adaptation state of a driver is circular or elliptical in shape, whether the size is close to that of the fovea (2°) or whether additional areas of peripheral vision should be taken into account, perhaps field sizes of 10° or 20°, or whether areas such as the road surface or the vehicle windscreen area lead toward a better estimate of adaptation.

In one study (Heynderickx, Ciociou & Zhu, 2013) this was done by first video recording the driver's field of view when driving along an urban road after dark and then recording eye tracking whilst test participants watched a video on a monitor in a laboratory. A limitation of this approach is that, for pedestrians at least, eye movement when walking in a natural setting does not match those found when watching a video of the same setting (Foulsham et al., 2011). Cengiz, Kotkanen et al., 2014 did record eye tracking whilst driving in order to investigate the effect of size of a circular field (subtending 1°, 5°, 10°, 15° and 20° at the eye) on adaptation luminance but did not consider visual fields of shape other than circular.

Uchida et al., 2016 used a numerical simulation method for estimating the state of peripheral adaptation as required for calculating mesopic luminances (CIE 191, 2010). His simulation takes input from luminance distribution, eye movement, surrounding luminance (veiling luminance) and an assumed measurement field. For scenes with few potential glare sources, it was found that the road surface luminance provided a good approximation of a driver's adaptation, with an average error of only 2.6% between road surface luminance and simulated adaptation luminance. However, for scenes with a larger number of bright sources, potential glare sources (the 'urban' scenes),

there was a large degree of error, increasing rapidly with an increase in the distribution (standard deviation) of eye movements.

In this article, drivers gaze behaviour in inner-city environments after dark was investigated using eye tracking. This was done through secondary analysis of the data captured by others (Böhm, 2013) in which test participants were asked to drive a motor car along a predefined route without any specific task other than safely driving towards a goal whilst their eye movement was captured using eye tracking. The analysis used all available gaze direction data, both fixations and saccades, collectively referred to below as eye movement data.

9 METHOD

Described here is the apparatus and procedure used by Böhm, 2013. Drivers' eye movements were recorded using a head-mounted eye tracking system (Ergoneers Dikablis). This apparatus has two cameras, one facing the driver's field of view and one facing the driver's eye as shown in Figure 15. Before each trial the eye tracking system was calibrated by instructing fixation onto distinctive objects within the visual field whilst the vehicle was stationary in a parking lot. The manufacturer states an angular resolution accuracy of $< 0.5°$ when the eye tracking device is calibrated at the start of each trial by fixation on three fixed positions, the standard procedure for eye tracking. This procedure was followed by Böhm, 2013, with an additional secondary check of this calibration with each test participant. The apparatus recorded with a frequency of 25 Hz resulting in 1.8 recorded eye movement data points per meter when driving at $50\,\mathrm{km\,h^{-1}}$ or 3 recorded data points per meter when driving $30\,\mathrm{km\,h^{-1}}$.

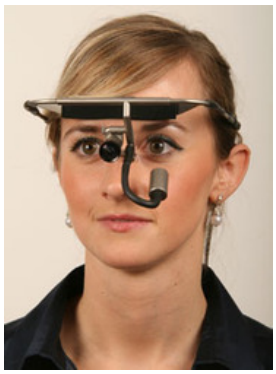

Figure 15: The Ergoneers Dikablis head-mounted eye tracking apparatus.

The head-mounted eye tracking apparatus used here leads to a head-centred coordinate system because the origin of the coordinate system moves in conjunction with head movement (Pinker, 1984). For JTC-1 an environment-centred system of coordinates is needed, e. g. vehicle-centred or road-centred. Road-centred means that gaze locations are represented in world frame coordinates. When the car is on a straight road (as is the case for the current study), the car-centred system and the road-centred system are similar. Therefore a third camera (TechnoTeam LMK 98-4) was mounted behind the driver's seat (Figure 16) to enable conversion from the head-centred system to the car/road-centred system. This translation was undertaken using the Augmented Reality Marker (ARMarker) fitted to the vehicle dashboard on the left-hand side of the steering wheel following the

method of Kato and Billinghurst, 1999. This third camera was static and aimed to capture the scene observable through the front windscreen. Following previous work, we considered only eye movement toward the road ahead. Eye movements toward the dashboard may also affect the state of adaptation and the significance of this will be examined in further work.

Figure 16: Photograph of the interior of the test vehicle to illustrate the location of the fixed camera (mounted behind the driver's seat) and the augmented reality markers (ARMarkers), here located on the left-hand and right-hand sides of the steering wheel.

Eye movements were monitored whilst driving along two sections of road in Berlin as described in Table 5. All test participants followed the same route and the test was carried out in Summer, starting after sunset (i. e. at 2230 CEST). One section of road was a main traffic route (Otto Suhr Allee - OS) having four lanes, separated carriageways, some parked vehicles on the right-hand side of the road and in-between the two carriageways, and intersections with traffic lights. The total length for which eye movement was recorded was 1460 m, this being 650 m and 810 m in the forward and reverse directions respectively. The second section of road was a residential street (Eschenallee - EA) having two lanes without markings, with cars parked on both sides and intersections where the right-of-way is to the right. The total length for which eye movements were recorded was 1140 m, this being 570 m in both the forward and reverse directions. Eye movements were collated for travel in both directions.

The data were collected from 23 test participants, comprising 14 females and 9 males aged between 22 and 73 years (mean = 37 years, SD = 16). Six were relatively inexperienced drivers, having reported less than 10 000 km total driving experience. The test participants were informed that they were participating in a scientific experiment but were naïve as to the research objectives and were remunerated.

Table 5: Description of the two roads in which eye tracking was recorded.

Name of road	Type of road	Carriageway	Length of road section (km)	Light source[a]	Speed limit ($km\,h^{-1}$)
Otto Suhr Allee (OS)	Main traffic route	Dual	1.46	HM	50
Eschenallee (EA)	Residential area	Single	1.14	Gas	30

[a]HM: High pressure Mercury; Gas: gas lighting.

10

VISUALISATION OF EYE MOVEMENT DISTRIBUTION

The aim of this work is to identify whether the distribution of drivers eye movement can be categorised by a simple geometric shape. The first approach to analysis employed heat maps to reveal the spread of distributions and suggest possible geometries for subsequent evaluation with quantitative methods.

The data recorded were the locations of drivers' eye movements. Following past work (Heynderickx et al., 2013; Cengiz, Kotkanen et al., 2014) these data are presented as heat maps (Holmqvist et al., 2011) essentially being a 2D-histogram using colour to denote relative magnitude rather than the height of a bar. To draw these it was necessary to extract the raw data (eye movement coordinates) from the eye tracking software and place these within the field of view using the ARMarker i. e. the eye movement data point locations in image coordinates within the head mounted eye tracking videos were transformed into image coordinates of the fixed- forward perspective of the single image from camera 3 located behind the driver's seat (Figure 17)

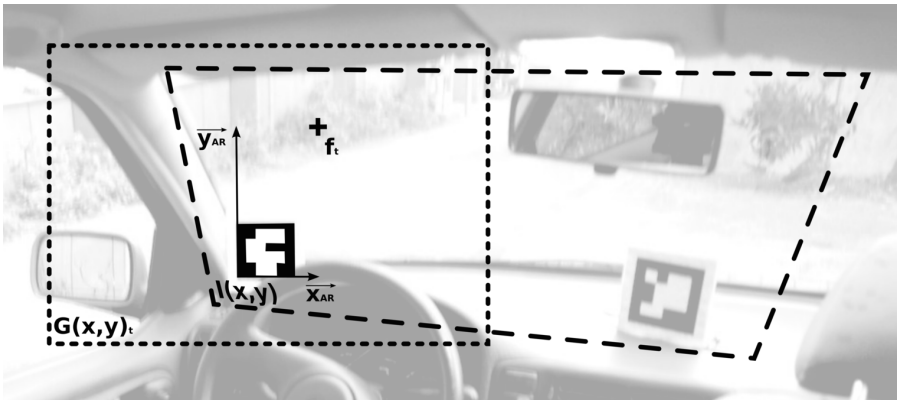

Figure 17: Sketch of the coordinate transformation of an eye movement data point from the eye tracking image $G(x,y)_t$ to the image taken of the fixed-forward perspective $I(x,y)$. Image $G(x,y)_t$ contains an eye movement data point f_t at time t – note that this field of view is dynamic and varies with head movement. The image coordinate of the data point ft is being transformed into the ARMarker's vector space with the origin O in one corner and the standard basis defined by the edges of the ARMarker: $\vec{O}f_t = \vec{x}_{AR} + \vec{y}_{AR}$. Finally each data point is cumulated by being inverse transformed from the ARMarker's vector space into image coordinates of the static fixed-forward perspective image $I(x,y)$.

The eye movement heatmaps for both roads are shown in Figure 18. These illustrate that for the main road (OS) the contour capturing 95% of eye movement is roughly elliptical, but the area of greatest eye movement density (50% and 25% contours) tends toward circular, aiming straight ahead from the driver. For the residential road (EA) the distribution of eye movement is approximately elliptical. Drivers gaze behaviour appears to follow different patterns on these two types of road. The eye movement heatmaps reported by Cengiz, Kotkanen et al., 2014 also suggest ellipses rather than circles but they did not focus on that issue.

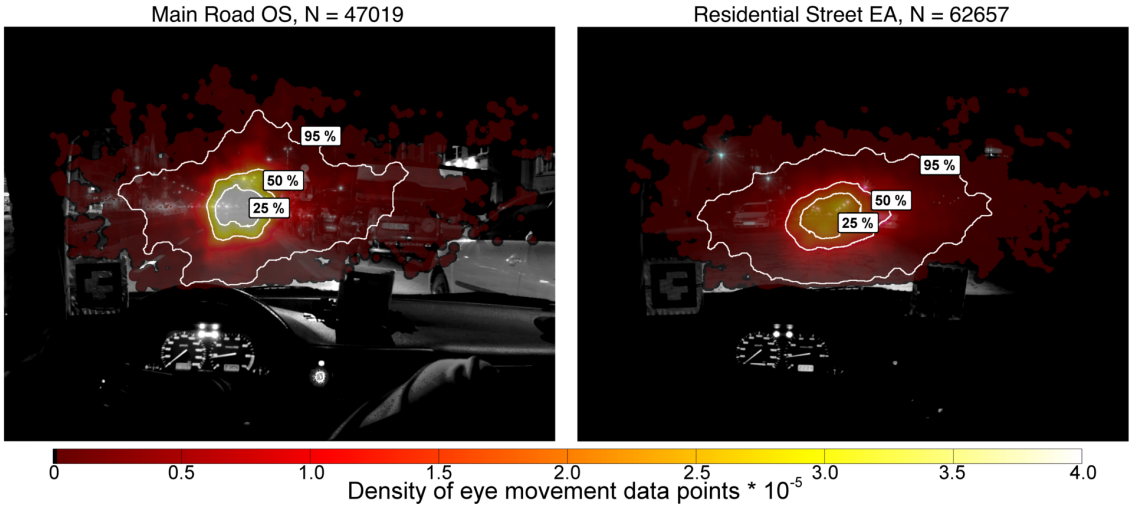

Figure 18: Density Distribution of eye movement data points for main road OS (left) and residential street EA (right) for the 23 subjects. Contours show the 25%, 50% and 95% percentiles. Note: The background image shows for context one particular part of the specific section, although the data shown in the overlain heat map was accumulated along the complete track.

Figure 19 illustrates the distribution of these eye movements for two roads along the horizontal and vertical dimensions. In the vertical dimension the difference is small. However, for the horizontal dimension, eye movement in the residential road is more widely distributed than on the main road. In particular, for the main road the focus of attention is the centre of the road ahead, while in the residential road there is a tendency to look also at the near side, the location of potential pedestrians and of junctions where priority is given to those entering the road.

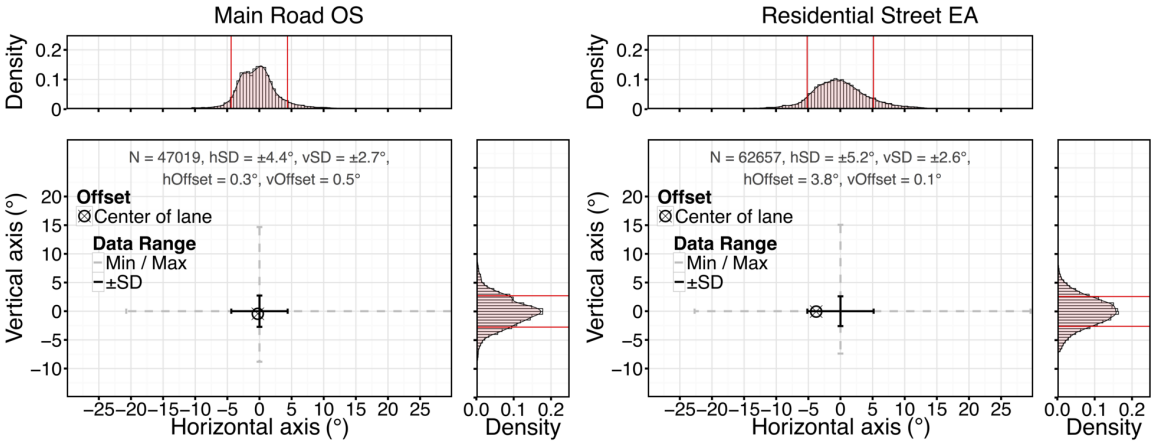

Figure 19: Descriptive statistics for main road OS and residential street EA for the 23 subjects, centred at the horizontal / vertical mean value. Offset represents the vertical / horizontal shift from the centre of the lane at the horizon. Note: the circle shows the centre of the lane ahead.

Pairwise t-tests comparing the two types of road for the 23 drivers suggest a significant difference in the standard deviation of horizontal eye movement distribution ($p < 0.001$) and a significant difference in offset from the centre line of the road ahead ($p < 0.001$). In the vertical dimension the t-test does not suggest a significant difference in distributions ($p = 0.44$) or in offset from centre ($p = 0.25$) between the two roads. This confirms the differences observed in Figure 18. EA is more elliptical and OS is more circular (or even rectangular) and also EA is shifted to the right (as indicated by the circle in Figure 19 which represents the centre of the lane ahead).

Given that there is an apparent difference in eye movement behaviour between roads EA and OS, a post-hoc analysis was carried out to investigate whether there were significant differences between different sections of the same type of road. Four discrete sections of each

Table 6: Horizontal offset of the eye movements for subsections of the main road OS for 13 subjects.

Subsection	Mean (standard deviation)
OS1	+1.71 (1.9)
OS2	−0.19 (2.4)
OS3	−0.50 (1.8)
OS4	−1.45 (2.1)

road type were established (OS1-OS4 and EA1-EA4), these defined as the distance between two successive lamp posts, and were distances of 28 m and 40 m for OS and EA respectively. This analysis was carried out using the eye tracking data for only 13 of the 23 drivers on account of the requirement for a high amount of manual labelling: comparing using ANOVA the eye movement for this subset of 13 drivers with those of all 23 drivers did not suggest significant differences ($p \geq 0.59$) in any case of horizontal or vertical distribution or offset from centre and thus it was assumed to be a reasonably representative sample.

Analysis of these discrete sections using ANOVA, for the two road types separately, did not suggest differences in the distribution of eye movement nor the offset from centre to be significant ($p \geq 0.13$) except for one case: on road OS there was a significant difference in offset from the centre line of the road ahead in the horizontal dimension ($p = 0.003$). Pairwise comparisons using the Tukey HSD test suggest that the differences in offset for OS are that OS1 lead to a different offset than OS3 ($p = 0.04$) and OS4 ($p = 0.002$) (Table 6). The difference between OS1 and OS2 is close to significant ($p = 0.10$) but differences between OS2, OS3 and OS4 are far from significant ($p \geq 0.42$). Thus in section OS1 drivers were tending to look to the nearside but in OS2, OS3 and OS4 they were looking slightly to the left of centre. Reasons for looking to the right-hand side in OS1 are that there were locations for potential hazards, e. g. approaching a traffic light controlled intersection, a road junction, and cars parked on the side of the road. In OS3 and OS4 there were potential hazards (parked cars) on the left hand side, between the two carriageways.

These analyses suggest that different types of road (i. e. a main road and a residential road) led to different patterns of eye movement. Figure 18 suggests that these may be circular on the main road (OS) and elliptical on the residential road (EA). Past studies (Land & Lee, 1994) suggest that drivers tend to look towards locations necessary in order to prevent accidents. This behaviour can be seen in the current data, as they follow expectation of likely hazards for which the driver is searching. On the main road (OS) they are tending to look straight ahead, approximately to the centre of the lane (or the rear of the vehicle in front), but may look towards a specific location for expec-

ted hazards, hence towards the right-hand side in OS1 and towards the left-hand side in OS2-OS4 (cars parked between the two traffic lanes). In the residential street (EA) they are tending to look toward the nearside of the road. The next section analyses the effectiveness of circular and elliptical visual fields at capturing eye movement on the two types of road (the location of pedestrians and to prevent accidents with vehicles coming from the right hand side, which have the right of way).

12 APPROXIMATION BY BASIC GEOMETRIC SHAPES

In order to assess how well eye movement behaviour can be described by a simple shape, some common shapes were considered for estimating the adaptation state (Table 7). These consist of shapes often used in lighting technology (2° and 10° circles), hypotheses proposed in meetings of CIE JTC-1 (Minutes of the 4th Meeting of CIE JTC-1) (2°/10° and 10°/20° ellipses, whole windscreen area, and road surface). These tentative ellipse sizes may be somewhat arbitrary; to better match the recorded eye movement distributions, alternative ellipses were examined with axes dimensions of size one and two standard deviations of eye movement (1 SD and 2 SD respectively). For analyses of circles and ellipses, these are assumed centred on the lane ahead and at the horizon, this being done to simplify later application in measurement software, although the actual centres of the eye movement data had a horizontal and vertical offset from that point, as shown in Figure 19.

Signal detection theory (SDT) was used to assess the effectiveness of these shapes on a per pixel basis of the forward looking image by classifying each eye movement data point and pixel. All data points were counted as real positives (RP) and all pixels containing no eye movement data as real negatives (RN). The discrete binary classification marked each eye movement data point as true positive (TP) if the pixel containing the data point fell within the shape, as false negative (FN) if the pixel containing the data point fell outside the shape, false positive (FP) if a pixel within the shape did not contain a data point and true negative (TN) for pixels outside the shape without data points (Figure 20).

Two quantities were determined from these data, the false positive rate (fpr) and the true positive rate (tpr) (Equations (7) and (8)) (McNicol, 1972). Tpr considers the number of eye movement data points which fell within the shape and is the ratio of the number of data points within the shape to the total number of data points (i. e. within and outside of the shape): a tpr approaching unity means the shape encapsulates the majority of eye movement data points. Fpr considers those pixels which were not the subject of a visual gaze, and is the ratio of non-fixated pixels within the shape to the total number of non-fixated pixels: a fpr approaching zero means that the shape had few non-fixated pixels as these tended to fall outside of the shape. Note that for TN and FP the empty (non-viewed) pixels were each scored as one, whereas for TP and FN these viewed pixels were scored as the number of eye movement data points on that par-

Table 7: Definition of eye movement areas considered in this analysis. The circles / ellipses were positioned at the centre of the lane on the horizon.

Name	Description	Source
2° Circle	Circle of diameter 2°	2° standard observer
10° Circle	Circle of diameter 10°	10° standard observer
2° / 10° Ellipse	Ellipse of axes 2° vertical and 10° horizontal	JTC-1, CIE 2012 conference, Hangzhou
10° / 20° Ellipse	Ellipse of axes 10° vertical and 20° horizontal	JTC-1, CIE 2012 conference, Hangzhou
1 SD Ellipse	Ellipse of axes 1 SD in vertical and horizontal directions. · OS: 5.4° vertical / 8.8° horizontal · EA: 5.2° vertical / 10.4° horizontal	Quantitative values of Chapter 11
2 SD Ellipse	Ellipse of axes 2 SD in vertical and horizontal directions. · OS: 10.8° vertical / 17.6° horizontal · EA: 10.4° vertical / 20.8° horizontal	Quantitative values of Chapter 11
Road Surface	Whole road surface of the lane ahead of vehicle to horizon	Uchida, 2015 JTC-1, CIE 2012 conference, Hangzhou
Window Area	Area of windscreen	JTC-1, CIE 2012 conference, Hangzhou

Note: (i) SD = standard deviation. (ii) Several proposals for adaptation field size were raised at the 2012 meeting of JTC-1 but were not officially recorded.

ticular pixel. The receiver operating characteristic (ROC) space was used to assess whether the shapes of Table 7 provide a satisfactory fit to the distribution of eye movements according to fpr and tpr. ROC is a common tool to assess the outcome of binary classifiers (Fawcett, 2006), showing fpr on the x axis and tpr on the y axis.

$$\text{fpr} = \text{FP}/(\text{FP} + \text{TN}) \tag{7}$$

$$\text{tpr} = \text{TP}/(\text{TP} + \text{FN}) \tag{8}$$

The shape best encapsulating drivers' gaze behaviour has tpr approaching unity and fpr approaching zero and would thus lie in the upper left region. However, that approach does not penalise false negatives and false positives within one value (if not taken into account the result would show the bigger the assumed visual field, the better the tpr, only slightly worsening the fpr, because of the relatively large number of RN, ending up with still small Euclidean distances to the upper left). Real negative eye movement data points do not exist, therefore the number of pixels within the luminance image (1031 x 1371) minus the number of pixels with data points were used to calculate TN and fpr. That means TN depends on the actual size of the

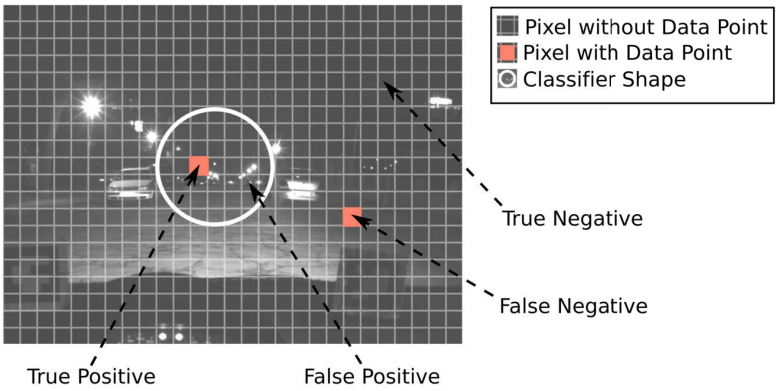

Figure 20: Illustration of per pixel classification. Each eye movement data point on a pixel within the shape was counted as a true positive (TP); data points on a pixel outside of the shape were counted as false negatives (FN); pixels within the shape upon which there were no data points were counted as false positive (FP) and pixels without data points outside the shape were true negatives (TN).

image and is mainly influenced by the focal length of the utilized lens (Figure 21). A common measure to quantify the results of classification where TN is undefined is the f1-score (Hripcsak & Rothschild, 2005).

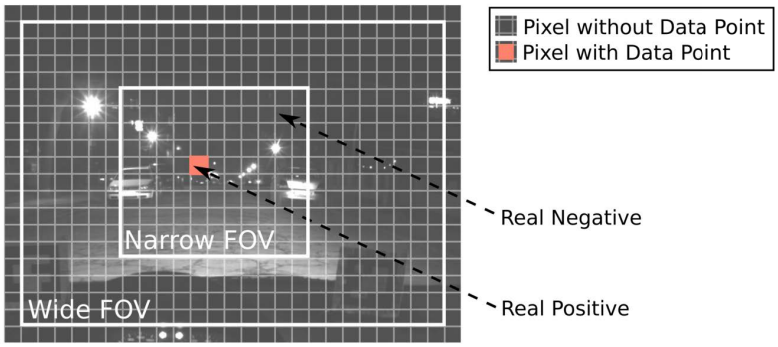

Figure 21: The number of real negatives (RN) depends on the number of pixels of the whole image minus the number of pixels with eye movement data points. The wider the field of view (FOV) of the lens, the higher the number of RNs.

The f1-score (Equation (9)) was therefore used as a second assessment parameter, this having the advantage that it does not require TN as an input value. Equation (9) is based on Van Rijsbergen's effectiveness measure (van Rijsbergen, 1979). F1-scores range from 0 to 1; a score of 1 indicates the shape is a perfect classifier, with all eye movement data points captured by the shape, no data points outside the shape boundary, and all available data points within the shape being used; a score of zero indicates the shape give a poor definition of the eye movement data point distribution. If only tpr were used

as the assessment parameter the outcome would favour the largest shape - it would incorporate the most data points with no penalty for false positives. Using only fpr would favour the smallest shape because it would incorporate the fewest false positives.

$$\text{f1-score} = 2 * \text{TP} / ((2 * \text{TP}) + \text{FN} + \text{FP}) \tag{9}$$

Figure 22 shows the ROC space for the two road types and the location within these for the eye movement shapes listed in Table 7. For both the main road and the residential street the 10° / 20° ellipse, the 2 SD ellipse and the window area were those located closest to the ideal upper-left location of the graph: for the main road, the 10° circle was also in this location. Considering the f1-score, this was lower for the window than for the other three shapes, these shapes having a similar f1-score.

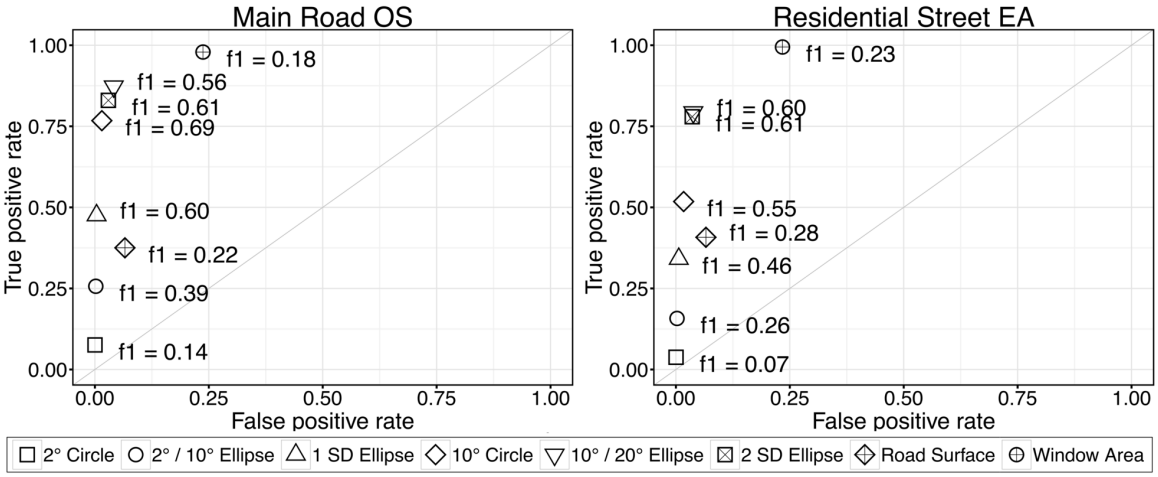

Figure 22: Receiver operating characteristic (ROC) plot for the tentative visual field shapes. These data are for the main road OS (left) and the residential street EA (right) for all 23 test participants. Each tentative eye movement field is centred at the horizon of the lane ahead.

For the residential street (EA) the ellipse of size either 10° / 20° or 2 SD performed approximately equally well at capturing eye movement data points. For simplicity of application, the 10° / 20° ellipse may be preferable to that defined by 2 SD. For the main road (OS) drivers eye movement data points were captured by an ellipse of size 10° / 20°, an ellipse of size 2 SD or by a 10° circle. The 10° circle is proposed here, with the assumption that the f1-score takes priority over the ROC location, meaning that the circle is a better measure than the ellipse. However, having a common field shape for both road types may simplify application and therefore further evaluation should consider whether assumption of an elliptical field introduces significant error.

Table 8: Results of signal detection comparing the primitive shape centred at the horizon of the lane ahead to centred at the data for the residential road EA.

Shape	Centred at / on	fpr	tpr	f1-score
10° / 20° Ellipse	horizon of lane centre	0.04	0.79	0.60
	centre of recorded gaze locations	0.04	0.85	0.64
10° Circle	horizon of lane centre	0.02	0.52	0.55
	centre of recorded gaze locations	0.01	0.66	0.67

For Figure 22, the tentative shapes were centred at the horizon of the lane ahead. Analysis of the gaze location distributions show that fixations were slightly offset from this position, a shift of 0.5° vertical, 0.3° horizontal on the main road, and 0.1° vertical, 3.8° horizontal on the residential street. If the tentative shapes are instead centred on these offset locations, the results for the main road (OS) remain in the same order, this offset being relatively small. On the residential street (EA) the order based on the f1-score would change, favouring the 10° circle over the 10° / 20° ellipse (see Table 8). What this does is show a driver's desire on a residential road to look towards the near-side, e. g. toward the kerb, pedestrians on the footpath, or an approaching side road junction.

These conclusions suggest that different types of road have different eye movement patterns and thus JTC-1 needs to consider different adaptation field shapes. A field size analysis such as that of Cengiz, Kotkanen et al., 2014 should consider an elliptical field in addition to a circular distribution. One caveat is that the primitive shapes do not represent the actual Gaussian distribution of the data, because they are flat, equally weighting the area within.

13 AGE AND EXPERIENCE

Age and experience are likely to affect eye movement because of the deterioration of vision with age (Maltz & Shinar, 1999) and the assumption that experience feeds the anticipatory probabilistic model of the world of a driver (Maltz & Shinar, 1999). In the current article we used the data from Böhm, 2013 which included 23 drivers of a wide age range (22 to 73 years) and both experienced and inexperienced drivers. Of these, only four might be considered elderly (aged, 59 years, 66 years, 70 years and 73 years) with the remainder being aged less than 50 and having a mean age of 31 years. The mix of age and experience in this sample were intended to represent approximately the gaze behaviour of the population of drivers.

Table 9 shows past studies of eye tracking and driving. Where age and experience are reported these samples have tended to represent younger drivers, and there is a mix of experienced and novice drivers. Experience brings familiarity with a given environment and an expectation of where significant hazards are found, and thus we would expect the distribution of gaze behaviour to be more compact for experienced drivers than for novice drivers. This can be seen in the results of two studies (Mourant & Rockwell, 1970, 1972). For example, Mourant and Rockwell, 1972 found that the central gaze direction of their novice drivers was lower and farther to the right (i. e. towards the kerb) than for experienced drivers, suggesting this was due to sampling of the curb in order to verify or estimate vehicle lane alignment. In contrast, Falkmer and Gregersen, 2005 found that at intersections experienced drivers tended to spread their fixations over a much wider horizontal distribution than did inexperienced drivers. Maltz and Shinar, 1999 identified that older drivers tend to need longer visual search times than younger drivers in order to extract the same amount of information of a traffic scene. They also found that the attention of the younger was distributed more evenly across the scene, whereas the older drivers focused on a smaller subset of areas within the presented image – a suggestion of experience (with age) leading a more compact field of view. If both older and younger, and novice and experienced, drivers are expected to use a road, and since these distinctions may affect gaze behaviour, then all groups should be included in the sample included in an experiment.

Table 9: Short summary of previous eye-tracking studies analysing the eye movement of drivers.

Study	Method	Test participants	
		Number	Age (years) and reported experience
Mourant and Rockwell, 1970	Eye-tracking while driving in daylight	8	21-31 y experience not reported
Mourant and Rockwell, 1972	Eye-tracking while driving in daylight	10	6 novice (16-17 y), 4 experienced (21-43 y)
Land and Lee, 1994	Eye-tracking while driving in daylight	3	
Maltz and Shinar, 1999	Eye-tracking while observing four photographs of road scenes	10	all experienced (no age given)
Falkmer and Gregersen, 2005	Eye-tracking while driving in daylight	40	5 younger (20-30 y) 5 older (62-80 y) experience not reported
Cengiz, Kotkanen et al., 2014	Eye-tracking while driving in daylight and after dark	3	22 - 27 y; one experienced (driving > 100 000 km) and two less experienced (driving < 30 000 km)

14

SUMMARY

The aim of this work is to analyse driver's eye movement on main roads and residential streets after dark. Heat maps were used to reveal the spread of distributions and statistical analysis to compare viewing behaviour between the two types of road. With a novel shape classification approach we identified the most suitable field shape approximating the eye movement data.

The heat maps suggest that gaze behaviour differs between the main road and the residential street: the 25% and 50% contours on the main road were approximately circular, whereas on the residential street the 25% and 50% contours were approximately elliptical. Descriptive statistics indicate, that standard deviation and offset to the centre of the lane at the horizon differ on the horizontal dimension, but not on the vertical dimension, which was confirmed by inferential statistics. A post-hoc analysis revealed, that viewing behaviour differed at one subsection of the main road, but was consistent on the other subsections of the main road, as well as on the residential street.

Signal detection theory was used to investigate the optimum field of view shape. For the residential road there is a tendency to look slightly to one side of straight ahead, i. e. towards the near side. SDT suggested the optimum shape to be a 10° / 20° ellipse if the centre of fixation is assumed to be the centre of the lane ahead, or a 10° circle if the centre of fixation is placed slightly to the right in accordance with the recorded data. For design purposes, the former may be the more simple assumption. On the main road the 10° circle was slightly better than the 10° / 20° ellipse. Favouring a common shape for both types of road would ease a potential practical application, however it would have to be assessed whether that lead to additional error.

The tentative field shapes represent the eye movement of the fovea, whereas for the application of the mesopic luminances the peripheral vision is of interest. The method proposed by Uchida et al., 2016 is one approach that might address the issues of peripheral adaptation.

Part IV

SPATIAL SAMPLING OF THE VISUAL FIELD

This part is the accepted version of an article that has been published as:

Winter, J., Fotios, S. & Völker, S. (2017b). The effect of assuming static or dynamic gaze behaviour on the estimated background luminance of drivers. *Lighting Research and Technology*, Epub ahead of print 17 December 2017. doi:10.1177/1477153518757594.

I designed the study, collected, visualised and analysed the data and wrote the manuscript. S. Fotios provided supervision, discussed the interpretation of the results and revised the manuscript. S. Völker gave general advice and helpful comments and proofread the manuscript.

15

INTRODUCTION

The CIE proposed system of mesopic photometry (CIE 191, 2010) is a system for characterising the spectral efficiency of visual performance at low levels of light according to relative contributions of cone (photopic) and rod (scotopic) photoreceptors. This is determined using the S/P ratio of the ambient illumination and the luminance to which the eye is adapted. CIE technical committee JTC-1 has the objective of seeking a method for estimating the state of visual adaptation of road users in order to guide application of the mesopic system; this paper focuses on drivers of motorised vehicles.

Estimation of the state of adaptation of a driver is not a new task in itself, with guidance already available for tunnel lighting (CIE 88, 2004), for assessing the influence of glare via the threshold increment (TI) (CIE 31, 1976; CIE 115, 2010; CIE 140, 2000) and for calculating the visibility level of a small target (ANSI IESNA RP-8-14, 2014). In these, adaptation luminance (L_a) is estimated as the sum of the background luminance (L_b) around a task and the veiling luminance within the scene caused by surrounding sources of high luminance (L_v): $L_a = L_b + L_v$ (Adrian, 1989; Narisada, 1992). This approach takes into account the scattered light due to glare within the visual field (Stiles, 1929b). The aim of estimating adaptation for these purposes is, however, to consider the visibility of a target, foveally fixated and static against its background, typically the road surface. In contrast, determination of mesopic luminance requires an estimate of the adaptation state of the peripheral regions of the retina rather than the fovea.

Adaptation is the process of adjusting to the quantity and quality of light: if the eye is exposed for a sufficient time to a uniform condition every part of retina reaches a steady state and the eye can be said to be adapted to that level of light (Moon & Spencer, 1943). Estimating the state of adaptation within a homogeneous field is relatively straightforward: in typical laboratory trials this is the luminance of the uniform background surrounding a fixation point (Freiding et al., 2007; Walkey et al., 2007; Várady et al., 2007). Estimating the state of adaptation of a driver in the natural setting is not straightforward, however, because the visual scene is likely complex and inhomogeneous. This arises because a single scene is likely to present a range of luminances rather than a uniform luminance, and because the dynamic nature of eye movements and travel along a road mean a number of fields are seen in succession. Different parts of the retina will therefore be differently adapted depending on where, and for how long, gaze is directed (Wördenweber et al., 2007; Boyce, 2014).

For foveal adaptation, one way to estimate the adaptation luminance would be to look at the pattern of fixation points and the time spent at each (Boyce, 2014): Uchida et al., 2016 proposed a method for doing this which took into account eye movement among other parameters. A simpler but possibly less accurate approach would be to use the average luminance of a region of the observed scene in which the majority of fixations were expected to occur. One suggestion is to use a circular field with an angular diameter of 10 to 20 degrees (Narisada, 1992), this being approximately confirmed by eye tracking data (Winter et al., 2017a).

Eye movements comprise two parts, saccades and fixations. Fixations are periods of time, where the gaze rests at a particular position, e. g. when assessing a traffic scene regarding action that needs to be undertaken (we ignore here the miniature movements - tremor, drift, and micro-saccade - that occur during a fixation (Liversedge, Gilchrist & Everling, 2011)). Saccades are the rapid movements of the eye between successive fixations. Eye movements are used in a feedforward role to the motor system, to locate the information needed for the execution of an act (Land, 2006). Note, however, that fixation on an object or area does not imply for certain where the observers attention is focused - gaze location does not uniquely specify the information being extracted (Rothkopf et al., 2007). However, when exposing the retina, or, more precisely, particular parts of it to a light scene, the mechanisms of adaptation are triggered regardless of attention. Of course the longer a gaze rests at a particular part of the road lured by attention, the more likely will the transient re-adaptation process be to converge, i. e. to complete the process as defined by Moon and Spencer, 1943.

The gaze direction of a driver is dynamic, constantly moving to different regions of the visual field, in part determined by experience and distractions (Winter et al., 2017a; Cengiz, Kotkanen et al., 2014; Kountouriotis et al., 2016; Crundall et al., 2003). As a result, different parts of the visual field stimulate different parts of the retina, and this puts the retina into a state of continuous transient adaptation (Adrian, 1987). Transient adaptation is the state of changing adaptation when the visual system is not completely adapted to the prevailing illumination, e. g. when gaze is moving around in a road scene or when looking from the outside to the inside of the vehicle (Boyce, 2014). If these changes of exposure to different luminances are within 2 log units, transition happens very fast (Adrian, 1989). Other findings however indicate that the duration required for the transition depends on whether the change is from low to high or from high to low luminances (Völker, 2006). When driving along a road, the visual field constantly changes, which, therefore, puts the retina into a continuous state of transient adaptation. Although certain areas change

very little, e. g. the road surface, other areas such as shop facades, advertisements etc. present a larger change in luminance.

In one recent study the combined eye-movement and luminance measurements along a road were analysed, with estimates of the visual adaptation calculated as the mean luminances of circular fields of various sizes (1° to 20° in diameter) centred around the fixations of drivers (Cengiz, Kotkanen et al., 2014). A second study examined mean luminances within various elliptical and circular fields of size 1° to 90°, centred 1° below the horizon at the centre of the lane and compared these to the mean luminance on the road surface (Maksimainen et al., 2017). Other studies suggest that only the local luminance (i. e. the luminance at and around a task point) influences visual performance, which is an estimate for adaptation (Moon & Spencer, 1943; Uchida & Ohno, 2014a; Cengiz, Puolakka & Halonen, 2014; Cengiz et al., 2016; Winter et al., 2018). That assumption would make field sizes larger than 2° around an assumed static task point irrelevant.

In summary, while methods for estimating adaption luminance assume a static, uniform and fixed field of view, driving in real situations involves dynamic eye movements across a non-uniform visual field. This paper investigates background luminance, one of the two components of adaptation luminance and suggested by Maksimainen et al., 2017. to be the more significant component for the calculation of mesopic luminances. Specifically, this paper explores the change in background luminance found if the visual field is assumed to be dynamic rather than static. This is examined for both foveal and peripheral visual fields.

16 METHOD

16.1 LUMINANCE DATA

The background luminance component of adaptation was estimated using different approaches using luminance data from three roads and eye tracking data recorded in a natural setting.

Luminance images were gathered from three types of road, these being two real urban traffic scenes (a main road and a residential street as investigated using eye tracking (Winter et al., 2017a)) and one simulated traffic scene (Table 10). The simulated scene is included because it is very likely that application of the mesopic luminances will be within the design process, which is typically done with simulation programs. The simulation was undertaken with a framework based on the software Radiance (Winter, Buschmann & Franke, 2013).

Scene luminances were established at ten regular intervals in each road. The measurement in the two urban traffic scenes was undertaken with a TechnoTeam LMK Color 4 with an 8 mm lens (approximately 63° x 45° field of view) from within a vehicle from behind the driver's seat (see Figures 23 and 24). The simulation resulted in images with the same size and field of view.

Figure 23: Photograph of the interior of the test vehicle to illustrate the location of the fixed image luminance measurement device (mounted behind the driver's seat), which was used to gather a static luminance image series between two luminaires.

The images captured on the main road (OS) contain approaching traffic and a traffic signal close to an intersection. The images taken on the residential street (EA) are free of approaching traffic, as are the images from the simulated road. As the images were captured from within a vehicle from the driver's perspective they included the interior of the vehicle. To make the simulated images comparable

Table 10: Description of the three roads for which the luminance images were gathered.

Type of road*	Road characteristics	Luminaire positioning / spacing	Lighting class**	Road surface characteristics
Main road (OS)	Four lanes, separated carriageways, parked vehicles on right side	Opposite, 32 m	M2	unknown
Residential street (EA)	Two lanes, parked vehicles on both sides	Irregular staggered, 55 m***	M6	unknown
Simulated road (TS)	Two lanes	One-sided, 39 m	M5	R3

*OS, EA and TS are abbreviations of the road names: OS = Otto-Suhr-Allee, EA = Eschenallee, TS = Treskowstraße.
**Lighting class as estimated from CIE 115, 2010, annex E.
***The installation did not follow a regular left-right-left-right staggered pattern. The luminance images were recorded at 10 uniform intervals over a 55 m section which comprised lamp posts on the right, left, left and right.

to the measured images of the real scenes the pixels containing the luminance values of the interior of the vehicle captured on the residential street were copied to the corresponding positions in the simulated luminance image. The headlamps of the vehicle were switched on during field measurement; this was not the case in the simulated images in accordance with current lighting design standards which do not account for headlamps of cars (CIE 140, 2000; ANSI IESNA RP-8-14, 2014).

16.2 ESTIMATION OF FOVEAL L_b BASED ON EYE MOVEMENT

One proposal for estimating the state of adaptation is to consider the pattern of eye movements and the duration spent at each location (Boyce, 2014; Uchida et al., 2016). The background luminance L_b can thus be estimated using the weighted mean luminance of a luminance image L(x,y) of a given road scene, using an eye movement data map EM(x,y) to provide the weighting (Equation (10)).

$$\overline{L}_{b,weighted} = \frac{1}{\sum_{x=1,y=1}^{x=width,y=height} \mathrm{EM(x,y)}} \sum_{x=1,y=1}^{x=width,y=height} \mathrm{EM(x,y)\ L(x,y)} \tag{10}$$

Equation (10) summates for each pixel (at coordinates x,y) the luminance of that pixel (L(x,y)) as weighted by the frequency for which

Figure 24: Images taken from the driver's view point at the ten locations in each of the three roads: residential street (top), main road (middle), simulated road (bottom).

the cumulated eye tracking data (Winter et al., 2017a) suggest that pixel is fixated (EM(x,y)). To estimate the weighted mean luminance of the scene, this summation is divided by the total frequency of these observations.

We use here the eye movement data of car drivers in urban environments at night reported in a previous study (Winter et al., 2017a). These were eye movements of 23 people when driving along two straight roads, a main road and a residential street (Table 10). For the current purpose we are interested in typical gaze behaviour, and for simplicity are considering straight sections of road. It has been shown that different types of road may yield different patterns of gaze behaviour, according to the location of expected hazards, but that different sections of the same type of road tend to yield similar distributions of gaze (Winter et al., 2017a). These roads were a main road (1.46 km) and a residential street (1.14 km). To estimate the proportion of travel time for which the fovea was directed to a particular direction within the scene, the fixations occurring along the whole length of each road were (separately) summated. In other words, the cumulative fixation point data for the whole road were used in the analysis of each of the ten sections of that road.

16.3 ESTIMATION OF PERIPHERAL L_b

Different parts of the retina are exposed to different parts of the scene and thus, for a scene of non-uniform luminance distribution, different parts of the retina will be subject to different states of adaptation. As the application of mesopic luminances is for visual performance in peripheral vision, then what is of interest here is the adaptation state of the peripheral retina. The method described above, i. e. the weighted mean of eye movement data and a luminance image represents a means for estimating the state of foveal adaptation; the estimation of the state of peripheral adaptation needs another approach.

To analyse this issue four factors play a role: the spatial extent of the retina, the spatial distribution of the scene, the movement of the eye and the movement along the road.

16.3.1 *Spatial sampling of the visual field*

Figure 25 shows the sampling fields used to investigate changes in scene luminances. This is a field of diameter 20° centred on the fovea. Within this, luminances are calculated for each of 69 evenly distributed sub-areas, each being a 2° circle, with the central sub-area being superimposed on the fovea. The 20° size was chosen because the experiments contributing to CIE 191, 2010 used a 10° off-axis target which falls at the perimeter of this schematic (Freiding et al., 2007; Walkey et al., 2007; Várady et al., 2007). We first assumed the whole of this field to be relevant, but also investigated the effect of ignoring the upper part of the field assumed to be less critical for drivers.

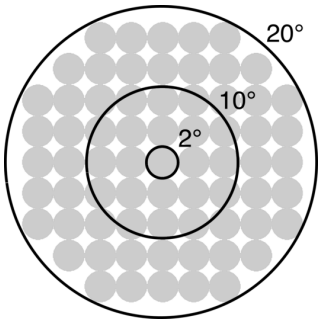

Figure 25: Schematic of the spatial sampling of the visual field, where the central 2° circle represents luminances to which the fovea is exposed, and extending to a diameter of 20°. The 69 sub-areas are each 2° circles, these arbitrarily chosen for analysis of luminance variations across the visual field.

The purpose of adopting these sampling fields is to illustrate the range of luminances to which different parts of the retina might be exposed to in a given situation, as indicated by Wördenweber et al., 2007, p. 271 and based on the method of spatial sampling (Wang, Stein, Gao & Ge, 2012). We recognise that light will also fall into the

spaces between the circular sub-regions, but the additional precision produced by including these data is not required for the current analysis. Note that these circular areas are not intended to represent receptive fields, i. e. the collated activity of a number of photoreceptors, which increase in size with increasing eccentricity and decreasing luminance (Boyce, 2014), nor does this simplified model intend to cope with the curvature or optics of the eye.

16.3.2 *Static assumption*

Consider the sampling fields overlaid on a road scene. It is common in road lighting to assume a static fixation point, such as when assessing glare (CIE 31, 1976) or visibility (Adrian, 1989). Figure 26 reveals the range of luminances the retina can be assumed to be exposed to with static fixation on an example road scene (here the simulated road TS). In this case it is assumed that the field of view was centred at the horizon of the lane, as identified in previous research (Winter et al., 2017a). The luminances in Figure 26 were determined from the simulated road scene, the purpose being to illustrate the change in these mean luminances with the change from static to dynamic assumptions. While we expect that the range of luminances encountered in real scenes would vary and may be higher or lower than these (Völker, 2006) we do not expect that the change between static and dynamic assessments would change. To estimate background luminance for the foveal static field we used the average luminance of pixels in the central 2° field of the sampling pattern.

The peripheral areas of the retina exposed to the road surface are influenced by luminances with an exponent of -1, i. e. in the range 0.99 to 0.10 $\mathrm{cd/m^2}$, the left and right peripheral areas are influenced by the surrounding buildings (simulated five-storey housing with a grey concrete surface) with luminances having an exponent of -2, i. e. in the range 0.099 to 0.01 $\mathrm{cd/m^2}$, and the areas exposed to the sky are influenced by the rather dark luminances with an exponent of -3, i. e. , in the range 0.0099 to 0.001 $\mathrm{cd/m^2}$. Some areas are influenced directly by the light sources, which were as bright as 35 $\mathrm{kcd/m^2}$ in this example of the simulated street (although in Figure 26 the exponent is lower due to reporting the mean luminance within a 2° circular area). In real road scenes the surrounds tend to be brighter (with a luminance of about $10^{-2}\,\mathrm{cd/m^2}$ in the residential street EA and about $10^{-1}\,\mathrm{cd/m^2}$ in the main road OS) and there may be more sources of glare (such as the headlamps of approaching vehicles or the tail-lights or brake-lights of vehicles ahead) which would be additional contributors to the scene as well as the headlamps of one's own vehicle.

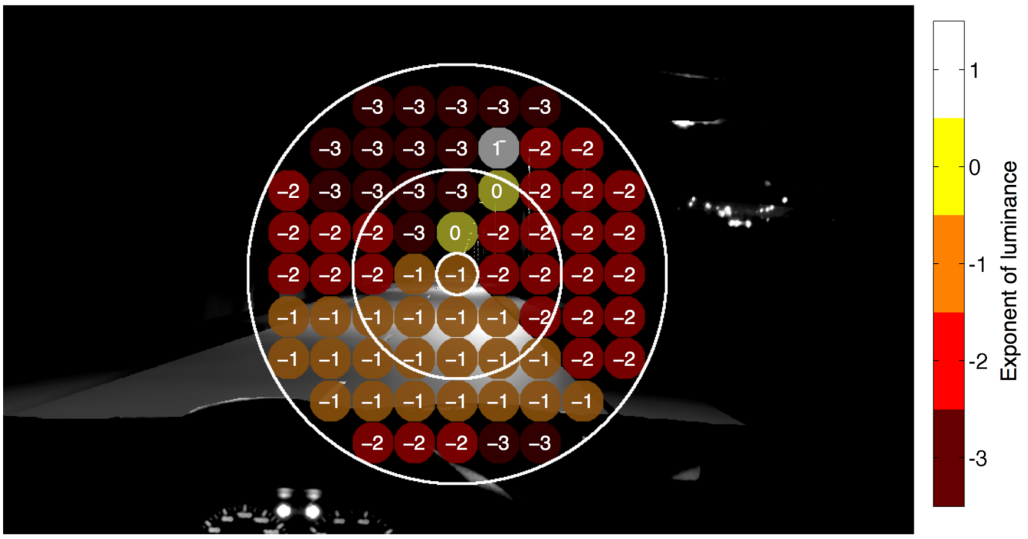

Figure 26: Assuming a static fixation at the centre of lane at the horizon this visualization shows the various mean luminances to which the retina is exposed on the simulated road TS. These numbers are the exponent of the mean luminance within each of the 2° circular patches distributed across the visual field. The white circles indicate visual field sizes of 2°, 10° and 20°. Note that the maximum values within the patches, especially the ones with the very bright pixels of the fixed road lighting can be as high as 35 kcd/m^2.

16.3.3 *Dynamic assumption*

Next, consider how eye movement behaviour effects the estimate of luminance projected to a specific part of the retina. The eye does not look straight ahead but tends to scan the visual field, with a pattern that is different for different observers. To represent this, we used the eye movement data of 23 drivers, as captured using mobile eye tracking in two roads (Winter et al., 2017a). These data are a step towards representing where most of the people tend to look at most of the time, rather than the gaze behaviour of a single observer or an assumed static fixation.

Figure 27 (left) shows a sample scene upon which are mapped the accumulated locations of visual fixations toward that scene as determined using eye tracking (Winter et al., 2017a). The sampling fields were overlaid upon each of these fixations, aligning the region assumed to influence the fovea to the centre of each fixation point (Figure 28). For each fixation the scene luminance was established for each sub-area of the sampling fields (scene luminance here being the mean luminance of pixels contained in each sub-area). The weighted mean luminance of each sub-area of the sampling fields was then determined across all fixations, thus representing what each sub-area of the retina was exposed to, based on the relative proportion of time the fovea, and therefore the whole retina, was exposed to a particu-

lar direction. For each of the roads that process was undertaken for each of the ten locations at regular intervals between two lamp posts for which luminances were determined (Section 16.1). Or, in other words, the method for calculating a weighted luminance as described in Equation (10) was undertaken for each of the 69 sub-regions of the spatial sampling of the visual field. To estimate background luminance for the foveal dynamic field we used the weighted luminance of pixels in the central 2° field of the sampling pattern.

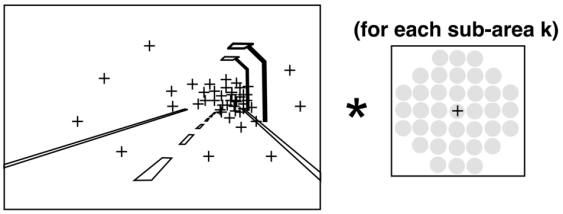

Figure 27: Example of the process for simulating the probable luminance to which a particular sub-area of the sampling fields was exposed to based on eye movement. A weighted mean luminance was calculated for each of the 69 sub-areas (+ represents a fixation within the scene / the fovea within the sampling fields). Note that the graphic of the sampling fields is just a mock-up and does not consist of 69 sub-areas. Figure 28 depicts the procedure more precisely.

Figure 29 reveals the range of weighted mean luminances the various parts of the sampling fields are exposed to on the simulated street (TS). Comparing Figure 29 with Figure 26 it is evident, that due to distribution of eye movements, a larger part of the sampling fields are exposed to the very bright light sources. The areas of the retina exposed to very low luminances in the assumed static fixation are now shown to be influenced by higher luminances. The lower areas of the sampling fields are mostly influenced by the road surface and remain within the same range of the exponent of the luminance.

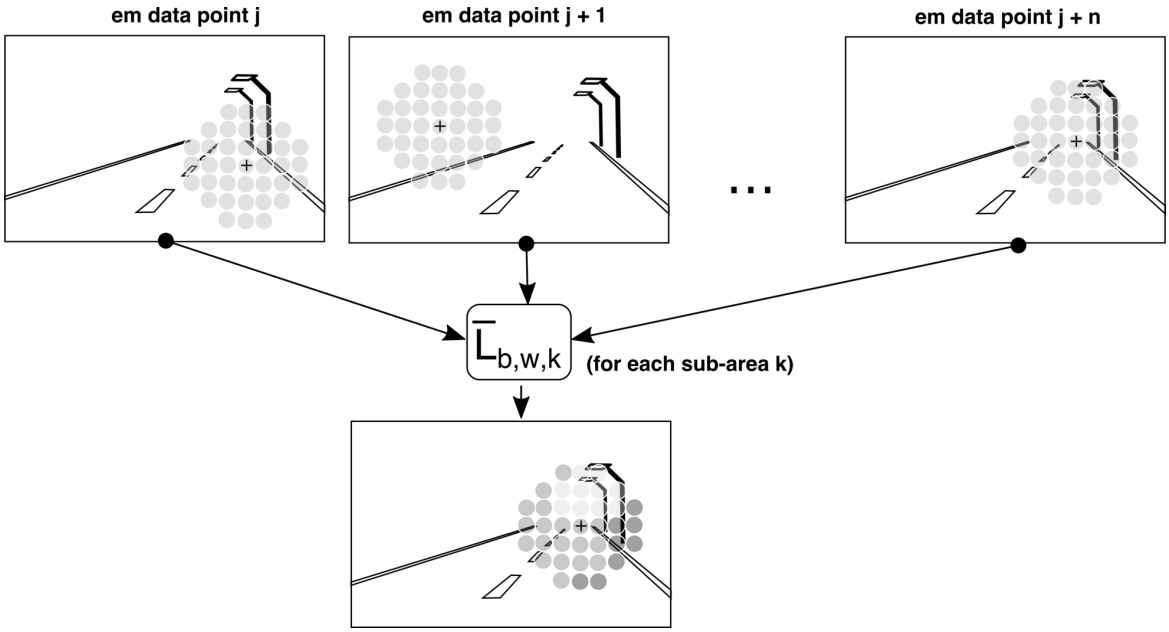

Figure 28: The calculation of the weighted mean luminance for each of the 69 sub-areas was undertaken as follows: for each fixation (+) of the eye movement data the mean luminance of each 2° sub-area of the sampling fields was calculated, summed up and divided by the number of fixations. Note that the change of grey value in the lower part represents the weighted mean luminance of each of the 69 sub-areas.

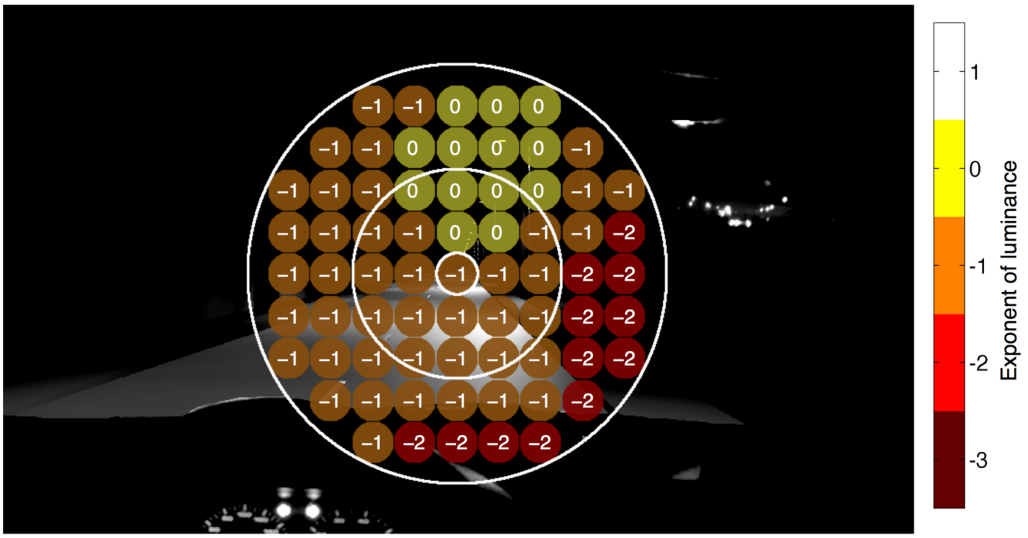

Figure 29: Distribution of weighted mean luminances for the simulated road TS. The numbers are the exponent of the weighted mean luminance within each of the 2° circular patches distributed across the sampling fields, estimated assuming that the gaze is dynamic and each particular sub-area of the assessment pattern has a certain probability to be exposed to a particular part of the scene. Note that compared to Figure 26 each weighted mean luminance within the sampling fields is based on eye movement data and contrary to Figure 26 this visualization does not represent the position of the sampling fields within the scene (which was centred to the horizon at the centre of lane for Figure 26). The white circles indicate the diameter of visual field sizes of 2°, 10° and 20° within the sampling fields.

17

RESULTS

Two methods were used for estimating background luminance within the field of view: a static approach (the fixed field of view) and a dynamic approach which considered the dynamic eye movements of a driver. The dynamic approach is intended to represent typical gaze behaviour, thus to estimate the relative proportion of time for which regions of the retina are exposed to a particular direction within urban street scenes after dark.

Figures 30 to 32 illustrate mean luminances representing the static assumption (on the left) and weighted mean luminances representing the dynamic assumption (on the right) for two of the ten locations along each road, one being a more homogeneous section (top rows of each Figure) and the other a more heterogeneous section (bottom rows).

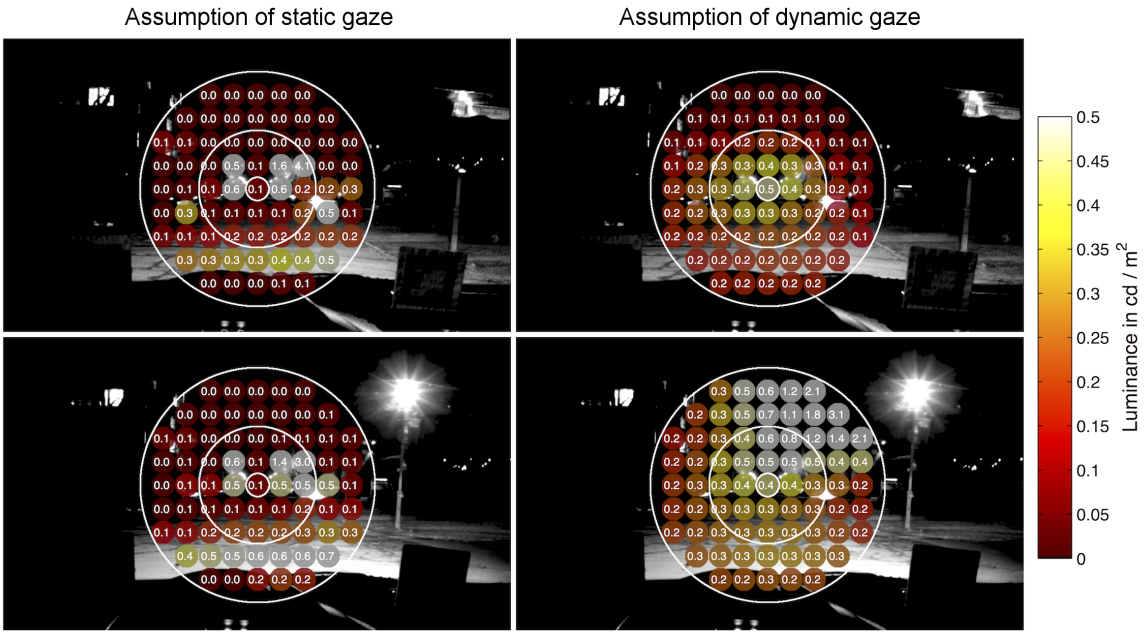

Figure 30: Mean luminances within each of the 69 sub-regions of the simplified visual field for two locations of residential street EA. The top row and bottom row show examples of two locations. The luminances are determined according to the static (left-hand column) and dynamic (right-hand column) assumptions of gaze behaviour. Note that luminances shown as 0.0 indicate < 0.1 rather than zero.

First, note that when the visual scene includes sources of high luminance (such as the headlamps of approaching vehicles or the fixed road lighting installation) the dynamic approach shows that these in-

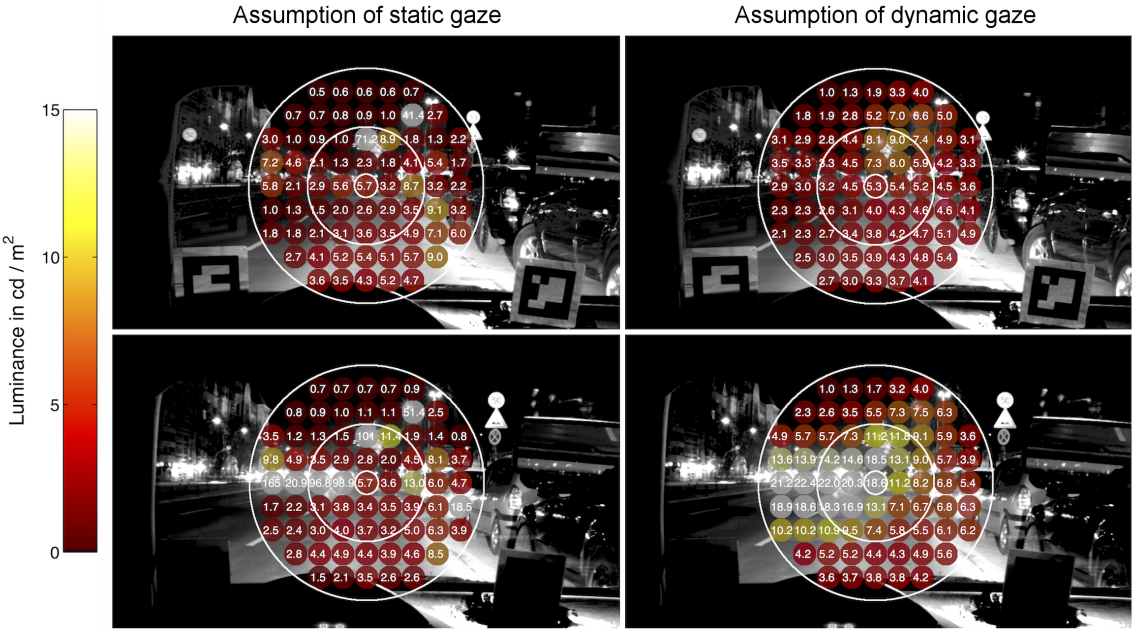

Figure 31: Mean luminances within each of the 69 sub-regions of the simplified visual field for two locations of main road OS. The top row and bottom row show examples of two locations. The luminances are determined according to the static (left-hand column) and dynamic (right-hand column) assumptions of gaze behaviour.

fluence a wider part of the field of view than does the static approach. This can be seen by comparing the left and right hand images of the bottoms rows of Figures 30 to 32.

Statistical analysis was carried out with three independent variables: equivalent retinal location within the sampling fields, road type, and static vs. dynamic assumption. The dependent variable was mean luminance. Factor levels for retinal location were foveal and peripheral, where foveal consisted of the results of the central 2° circle and peripheral the 68 sub-regions surrounding the fovea. Road type consisted of three levels: residential street EA, main road OS and simulated street TS, factor assumption comprised of level static and dynamic. Ten images were captured between two lamp posts along each road, which resulted in ten samples for each of the foveal retinal location factor combinations and 680 samples for each of the peripheral retinal location factor combinations. It was not intended to compare road types with each other as expected luminance differences were present by definition of the road lighting classes of CIE 115, 2010; the roads were chosen to reassemble different classes.

Mean luminances from nine of the twelve factor combinations were not suggested to be normally distributed according to the Shapiro-Wilk test ($p < 0.05$). Foveal dynamic EA and TS and foveal static TS were normally distributed ($p \geq 0.24$). Hence the statistical analyses were carried out using non-parametric tests of difference. The

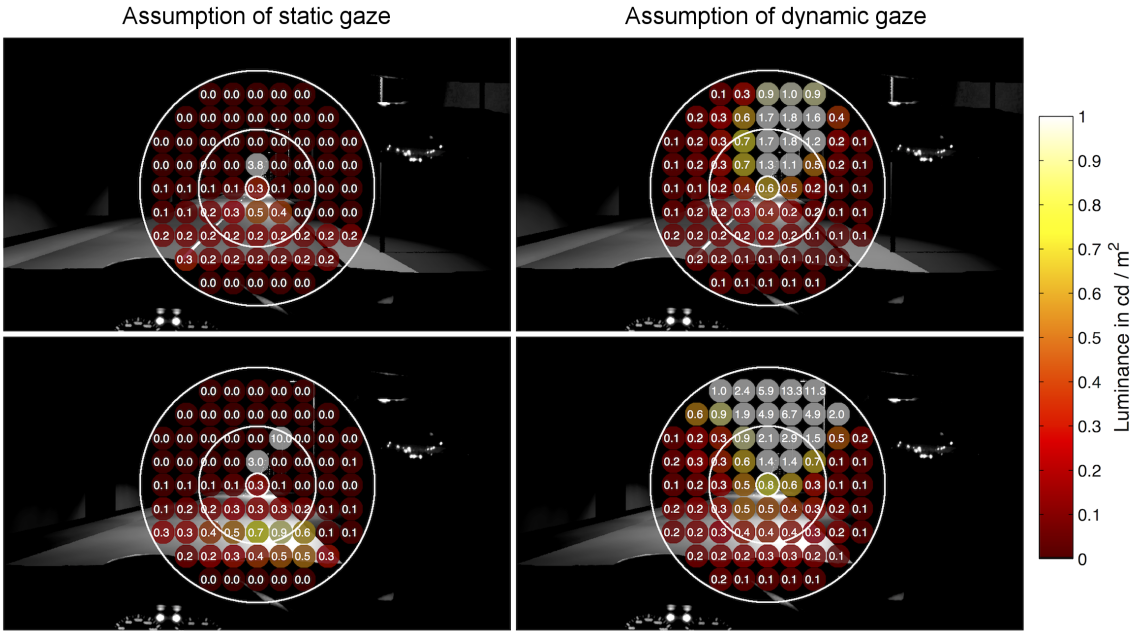

Figure 32: Mean luminances within each of the 69 sub-regions of the simplified visual field for two locations of simulated street TS. The top row and bottom row show examples of two locations. The luminances are determined according to the static (left-hand column) and dynamic (right-hand column) assumptions of gaze behaviour. Note that luminances shown as 0.0 indicate < 0.1 rather than zero.

Wilcoxon paired signed rank test was used for comparing factor assumption (static vs. dynamic). The Wilcoxon rank sum test was used for comparing factor retinal location (foveal vs. peripheral), this alternative test being used because the compared items were of unequal sample sizes ($N = 10$ within foveal observations and $N = 680$ within peripheral observations). Effect sizes were calculated as $r = Z/\sqrt{N_1 + N_2}$ (Rosenthal, 1994; Pallant, 2010) and interpreted according to Cohen, 1992 i. e. absolute value < 0.1 = negligible effect size, ≥ 0.1 to 0.3 = small effect size, > 0.3 to 0.5 = medium effect size, and ≥ 0.5 = large effect size.

17.1 STATIC VERSUS DYNAMIC

Figure 33 compares mean luminances estimated following the static and dynamic assumptions, for the three roads, for the foveal and peripheral fields. The medians of the mean luminances estimated with the static assumption are lower than those estimated using the dynamic assumption in all six comparisons. The Wilcoxon paired signed rank test suggests the difference to be significant in five cases ($p < 0.05$, large effect sizes for foveal comparisons, small effect sizes for peripheral comparisons except TS, which had a medium effect size) but

does not suggest a difference for the foveal field on main road OS ($p = 0.13$, small effect size).

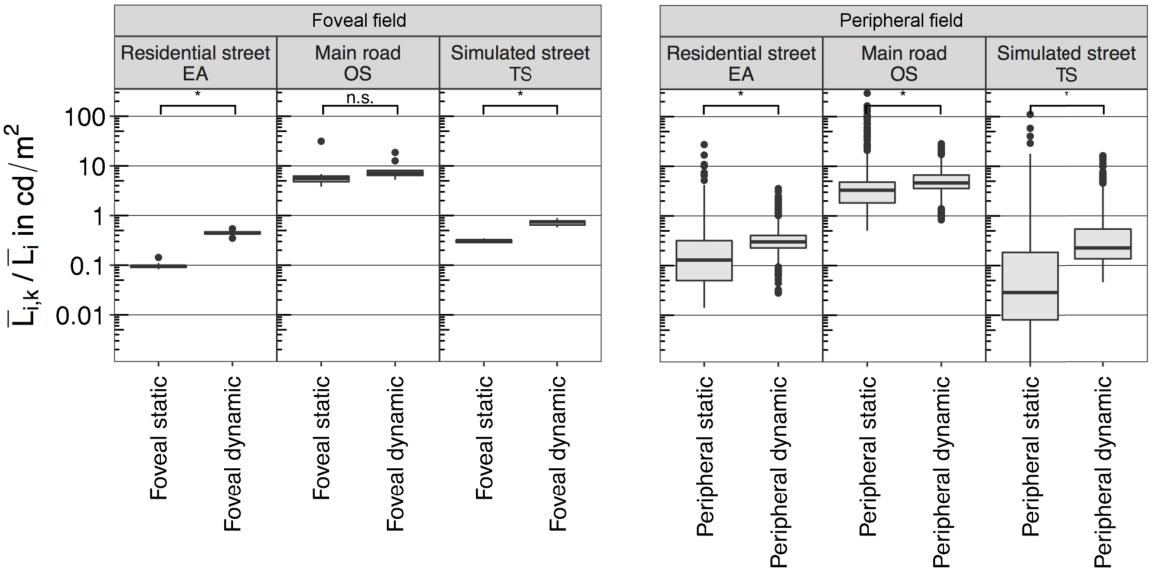

Figure 33: Boxplot comparing the static assumption to the dynamic assumption based on the calculated mean luminances for $i = 10$ images for the foveal retinal location and for $i = 10$ images with $k = 68$ sub-areas each for the peripheral retinal locations (significant differences with $p < 0.05$ are indicated with *, n.s. otherwise). Note that the data of simulated street TS does not contain headlamps of one's own vehicle.

17.2 FOVEAL VERSUS PERIPHERAL

Figure 34 shows the same data as Figure 33 but redrawn to facilitate direct comparison of location in the visual field, i. e. foveal vs. peripheral. In five cases, the median of the mean luminances of the peripheral field locations is lower than that of the foveal field ($p < 0.05$, Wilcoxon rank sum test, small effect sizes). For residential street EA and the static assumption, the difference between foveal and peripheral fields is not suggested to be significant ($p = 0.5$, negligible effect size).

17.3 OMITTING THE UPPER QUADRANT OF THE SPATIAL SAMPLING PATTERN

In this analysis it has been assumed that all 68 sub-regions are equally relevant: this may not be the case. In particular the upper quadrant of a typical road scene is less likely to contain potential hazards (Figure 35). Hence the analysis was repeated but with the visual field reduced to exclude the upper quadrant.

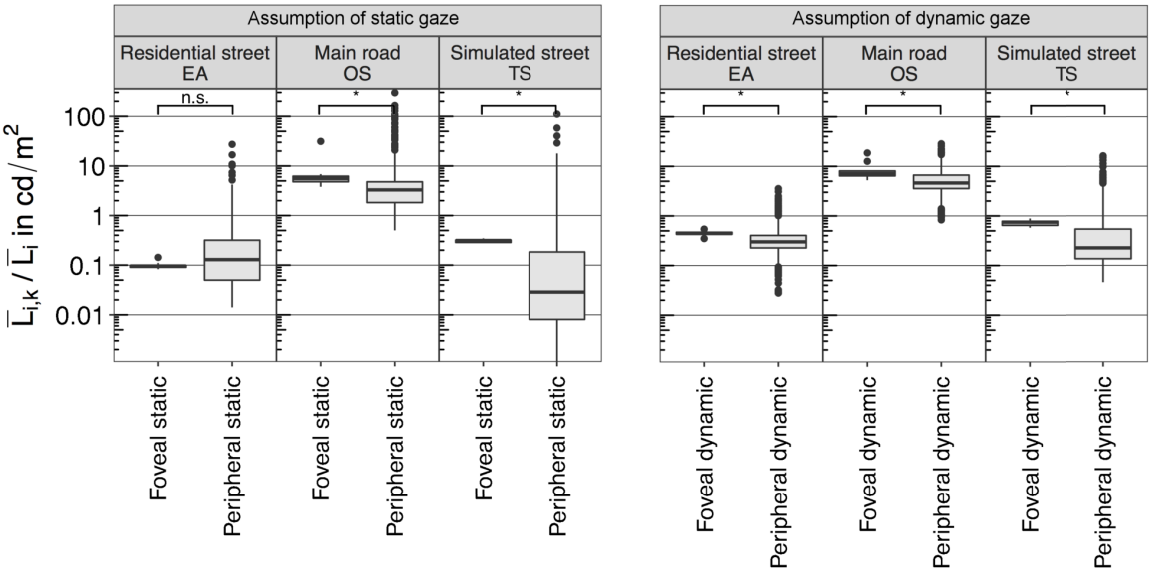

Figure 34: Boxplot comparing foveal retinal location to the peripheral retinal location based on the calculated mean luminances for $i = 10$ images for the foveal retinal location and for $i = 10$ images with $k = 68$ sub-areas each for the peripheral retinal locations (significant differences with $p < 0.05$ are indicated with *, n.s. otherwise). Note that the data of simulated street TS does not contain headlamps of one's own vehicle.

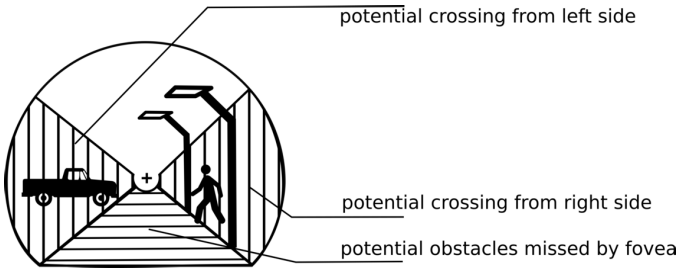

Figure 35: A typical urban road scene when driving along a straight patch of a road.

For the static assumption, the sampling pattern is centred within the scene and therefore the upper quadrant of the visual field of the sampling pattern matches the upper quadrant of the road scene.

For the dynamic assumption, omission of the upper quadrant becomes of particular significance if downward eye movement causes the road ahead (and hence the likely location of hazards) to fall into the upper quadrant. The road ahead begins to fall into the upper quadrant (for these flat roads) when the direction of gaze is 3° or more below the horizon: in the current eye tracking data, gaze direction was above this for 93% of the time.

The analyses of Sections 17.1 and 17.2 were repeated for this reduced field. Consider first the static vs. dynamic comparison (Fig-

ure 36). For the peripheral field, the reduced field led to the same conclusions as did the whole peripheral sampling field (Figure 33).

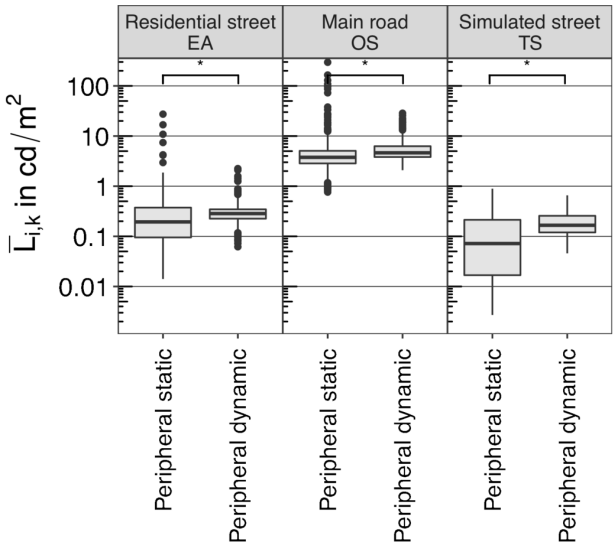

Figure 36: Boxplot showing mean luminances in the peripheral field according to the assumption of static or dynamic visual field. In these data the upper quadrant of the visual field is omitted. These data are for the $i = 10$ images with $k = 48$ sub-areas each for the peripheral retinal locations (significant differences with $p < 0.05$ are indicated with *, n.s. otherwise). Note that the data of simulated street TS does not contain headlamps of one's own vehicle.

Consider next the foveal versus peripheral comparison (Figure 37). Here, there was a change to one conclusion: in residential street EA, the median of the foveal static field is lower than the median of peripheral static ($p < 0.05$, negligible effect size) whereas analysis with the whole field did not suggest a difference. This still contrasts with the five other analyses which suggest that the foveal field has a higher luminance than the peripheral field.

17.4 APPLICATION

For practical application, the interim recommendation of CIE JTC-1 (CIE TN 007, 2017) proposes to use the average luminance of the design area (i. e. the luminance of the road surface as of CIE 140, 2000) as an estimator for the adaptation state. In another study it was identified that a 10° circle centred at the centre of lane at the horizon is a good estimator for that part of the visual field which encapsulates typical eye movements (Winter et al., 2017a), and such a field has been examined in recent studies (Cengiz, Kotkanen et al., 2014; Maksimainen et al., 2017).

Figure 38 compares the mean luminances of the peripheral field, with both static and dynamic assumptions, to the mean luminance on the road and to the mean luminance within a horizon-centred 10°

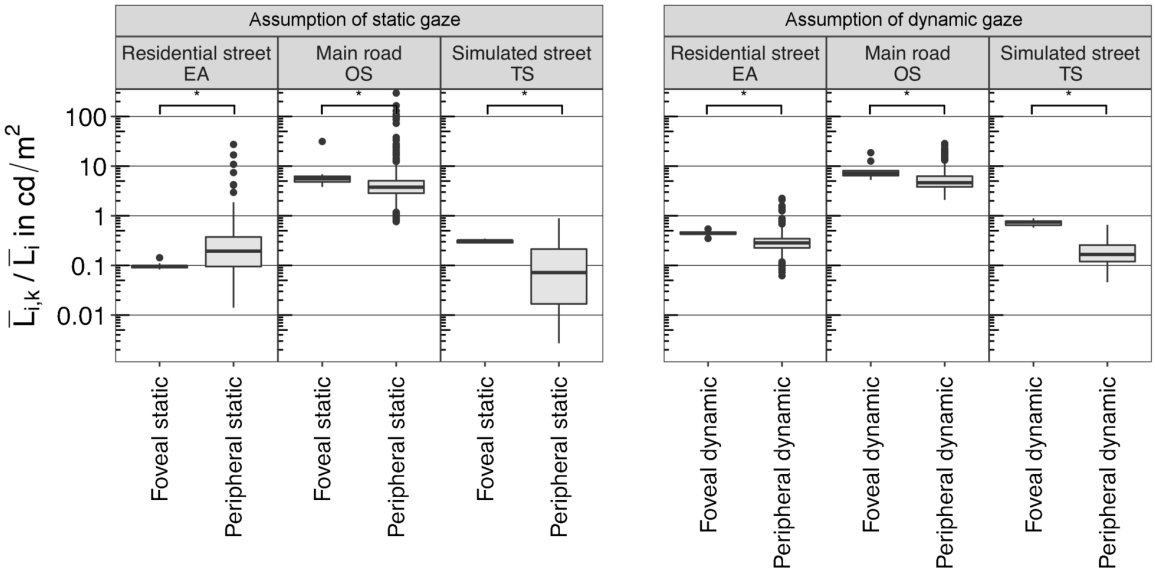

Figure 37: Boxplots comparing foveal retinal location to the peripheral retinal location based on the calculated mean luminances for $i = 10$ images for the foveal retinal location and for $i = 10$ images with $k = 48$ sub-areas each for the peripheral retinal locations, i. e. without the peripheral results of the upper quadrant (significant differences with $p < 0.05$ are indicated with *, n.s. otherwise). Note that the data of simulated street TS does not contain headlamps of one's own vehicle.

circle (for the residential street EA it was centred at the dominant location of gaze, which was 3.8° to the near side). The medians of the mean luminances within the 10° circle are higher than those estimated with the static or dynamic assumption in all six comparisons ($p < 0.05$, Wilcoxon rank sum test, small effect size). Consider next predictions of luminance using mean luminance of the road surface. In five of the six cases the road surface suggests a lower or equal luminance than do the spatial sampling based estimates (peripheral dynamic EA and OS, $p < 0.05$, small / negligible effect size; peripheral static EA, peripheral static OS and peripheral dynamic TS not suggested to be significantly different, $p \geq 0.12$, negligible effect size, Wilcoxon rank sum test). In one case the road luminance leads to a higher predication of background luminance (peripheral static TS, $p < 0.05$, small effect size, Wilcoxon rank sum test).

This analysis suggests that if a horizon-centred 10° circle (dominant location of gaze centred for residential street EA) is used to estimate background luminance, it leads to a slightly high estimate of background luminance; if instead the road surface luminance is used, this tends to lead to a slightly low estimate of background luminance, which agrees with the findings of Uchida et al., 2016.

Next, consider the impact of the visual field assumption for lighting design. This is illustrated here by determination of the mesopic

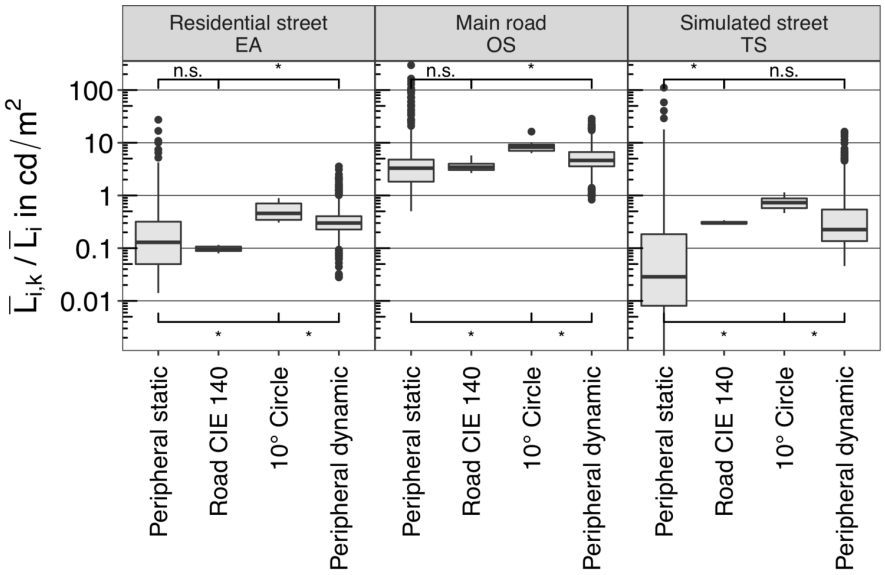

Figure 38: Boxplots comparing peripheral retinal location to the simplified methods (road / 10° circle) based on the calculated mean luminances for $i = 10$ images for the simplified methods and for $i = 10$ images with $k = 68$ sub-areas each for the peripheral retinal locations (significant differences with $p < 0.05$ are indicated with *, n.s. otherwise). Note that the data of simulated street TS does not contain headlamps of one's own vehicle.

enhancement factor (F_{mes}), the ratio of the mesopic luminance to the photopic luminance (CIE TN 007, 2017), for two different spectra (Table 11). Veiling luminance (L_v) was set to zero in the calculation of F_{mes}.

For the residential road, where median luminances lie in the range of 0.1 to 0.5 cd/m^2, then the choice of the estimation method appears to influence F_{mes}. For example, the road surface approach having the lowest median luminance suggests that F_{mes} departs further from unity than do the other approaches. For the main road, however, the choice of method for estimating background luminance has little effect on F_{mes}. This is because the main road, in this example, had a median luminance of > 3 cd/m^2 which is close to the upper limit of the mesopic range (5 cd/m^2). Note however that these are luminances higher than those typically recommended for main roads (CIE 115, 2010).

Table 11: Mesopic enhancement factor (F_{mes}) calculated for the three roads (EA, OS, TS) for four approaches to estimating background luminance, and for lighting of two SPDs (a white LED with S/P ratio = 1.71 and a HS lamp with S/P ratio = 0.60).

Type of road	Method for estimating background luminance	Median luminance (cd/m^2)	Mesopic enhancement factor (F_{mes})	
			S/P=1.71	S/P=0.60
Residential street EA	Road CIE 140	0.10	1.23	0.85
	Peripheral static	0.13	1.20	0.87
	Peripheral dynamic	0.30	1.14	0.91
	10° circle	0.46	1.12	0.93
Main road OS	Road CIE 140	3.43	1.02	0.99
	Peripheral static	3.29	1.02	0.99
	Peripheral dynamic	4.62	1.00	1.00
	10° circle	8.25	1.00	1.00
Simulated road TS	Road CIE 140	0.30	1.14	0.91
	Peripheral static	0.03	1.35	0.76
	Peripheral dynamic	0.23	1.16	0.90
	10° circle	0.73	1.09	0.94

18

SUMMARY

The aim of this paper is to investigate assumptions made when estimating background luminance, a component (alongside veiling luminance due to glare) in estimates of a drivers' state of adaptation. Background luminances were therefore estimated using two approaches, these assuming static and dynamic visual fields. Dynamic eye movement was represented by the eye tracking records of a previous study (Winter et al., 2017a). Scene luminances were represented by images taken at ten locations along each of three roads: a main road, a residential road, and a simulated road. Luminances were determined for a 2° central field, representing the fovea. For the peripheral regions, the 20° circular region surround the fovea was divided into 68 individual 2° regions, and the mean luminance determined for each of these.

While standard approaches assume a static visual field, the driver experiences a dynamic field, due to movements of the vehicle and the driver's head and eyes. Furthermore, the visual scene is complex, meaning it comprises a range of surfaces of different luminances rather than being a simple uniform field. The results (Figure 33) suggest that background luminances estimated assuming a dynamic visual field are higher than those estimated assuming a static visual field, for both the foveal and peripheral regions. This finding did not change when omitting that parts of the visual field (the upper quadrant of the sampling pattern) considered less relevant for driving.

Within the estimated peripheral luminances, the range from minimum to maximum tends to be higher for the static assumption than for the dynamic assumption. Assuming that the duration of a fixation typically lies in the range of 0.35 s to 0.8 s (Chapman & Underwood, 1998; Underwood et al., 2002) and that the range of operation of the fast adaptation mechanisms (within 0.2 s, neural adaptation) seems to cover only 2 log units (Adrian, 1989; Boyce, 2014) this makes the dynamic assumption a more likely outcome when the gaze moves within the scene from fixation to fixation. Another way to see the dynamic approach is by looking at the weighted luminances as a likely outcome when considering the whole group of drivers. While the adaptation of a specific driver might be influenced by particularly different luminances (e. g. if the gaze rests at an extreme location), the adaptation of the majority of drivers, however, can be assumed to be influenced by the weighted mean luminance.

The background luminance projected towards either foveal or peripheral regions may be of interest. It was found that background lu-

minances determined for the foveal region were significantly greater than those determined for the peripheral region, for both the static and dynamic assumptions. That finding changed in one case when omitting the upper quadrant of the sampling pattern. The peripheral luminances were, however, much more heterogeneous.

Compared with the background luminance estimated for a dynamic peripheral field, a horizon-centred 10° circle (dominant location of gaze centred for residential street EA) led to a slightly higher estimate and the road surface luminance to a slightly lower estimate. As to whether this matters, that depends partly on where the background luminance lies within the mesopic range. For lower luminances (the residential road in this study) then the different approaches to estimating background luminance affect the estimate of mesopic enhancement factor (F_{mes}). For higher luminances approaching the upper boundary of the mesopic range (the main road in this case) then there is little effect on F_{mes}. CIE TN 007, 2017 proposes use of the average luminance of the design area (i. e. road surface) to estimate background luminance. The current work suggests this may lead to a lower estimate of background luminance than that determined for a larger peripheral field, and that this may affect consideration of the mesopic effect at low luminances.

Part V

SUMMARY

19 GENERAL DISCUSSION

19.1 CONTRAST DETECTION IN THE CONTEXT OF DRIVING

Publication *I* (Winter et al., 2018, Chapter 7) dealt with the question how visual performance is influenced by scenes containing inhomogeneous areas and glare sources in the field of view. An experiment was carried out to investigate how contrast threshold for target detection is affected by the presence of glare and by extraneous light sources using the method of ascending limits.

The results indicated that the observer's ability to detect contrasts depends on the local luminance around the task point, where glare negatively influences the ability of detecting contrasts as calculated with existing formulas (CIE 31, 1976).

Higher luminances at and around the task point led to improved visual performance as predicted by current models for foveal vision (Adrian, 1989). For peripheral visual performance the prediction did not match very well, which is not surprising as the tested model is applicable for foveal vision only. It confirms, however, the conclusion of others (Moon & Spencer, 1943; Uchida & Ohno, 2014a; Cengiz, Puolakka & Halonen, 2014; Cengiz et al., 2016): adaptation is mainly influenced by the local luminances around the task point. That makes sense from an anatomical point of view, as the retina adapts via neural and photochemical adaptation locally to the various luminances the retina is exposed to in an inhomogeneous visual field. When the gaze moves while driving it can be assumed that the faster mechanism of neural adaptation handles changes from fixation to fixation, whereas the much slower photochemical adaptation handles changes more subtly such as when switching from a brighter illuminated main road to a dark residential street (Section 2.4).

Local adaptation prevails.

Those findings lead to two conclusions:

1.) Adaptation is influenced by the local surrounding, i. e. foveal adaptation is not the same as peripheral adaptation, which means it is necessary to consider particular parts of the retina separately. Meaning there is not a single peripheral adaptation, because in a typical complex traffic scene different parts of the retina are exposed to different parts of the scene and, therefore, will result in different states of adaptation.

Foveal adaptation ≠ peripheral adaptation

2.) Recent studies considered mean luminances within circles / ellipses of various sizes from 1° to 90° as the field influencing peripheral adaptation (Cengiz, Kotkanen et al., 2014; Maksimainen et al., 2017). From the just discussed point of view of local adaptation one

could question that method, as field sizes bigger than 5° seem irrelevant for assessing luminances influencing a particular part of the retina. Probably even 5° is too big, but based on this study that cannot be concluded, as the size of the extraneous light source had that characteristic. Nevertheless it might make sense to assess the luminances influencing foveal adaptation based on the frequency of eye movement (i. e. the dynamic assumption), where a particular simplified geometry might represent typical eye movement behaviour as suggested by Narisada, 1992. Peripheral adaptation would have to be estimated then again within another simplified geometry around the simplified geometry reassembling typical (foveal) eye movement, e. g. by dilating the 10° circle into a 20° circle to incorporate the periphery around a fixation. That, however, makes it impossible to analyse areas influencing particular parts of the retina directly, as the whole scene results in a single mean luminance. But it might be of interest to investigate the extent of inhomogeneity, i. e. the variety of potential states of adaptation within typical scenes.

Global influence in complex scenes?

In the presence of the extraneous light source and glare, the negative influence of glare is overestimated with current models. That disagrees with the local adaptation conclusion and indicates a global influence. A possible explanation for that could be an influence on the size of the pupil diameter, which is a global mechanism reacting to changes of luminance within a scene, probably being decreased in size under the inhomogeneous condition and thus causing less glare induced stray light (Masket, 1992). Crawford, 1936 hypothesised: the pupil size is influenced by the brightness of the general field of view, by its size and by glare sources in it, both in respect of their intensities and their positions relative to the direction of fixation.

Maksimainen et al., 2017 analysed the influence of glare on the calculation of the mesopic adaptation coefficient m and found that it did not matter if the veiling luminance was included into L_a or not. As the finding of this study additionally suggests a reduced influence of glare I decided to omit that factor in the luminance analysis of publication *III* (Winter et al., 2018, Chapter 7) and focused solely on the background luminance, which is one of the two factors determining the adaptation luminance (Equation (4)).

19.2 EYE MOVEMENT WHEN DRIVING AFTER DARK

CIE JTC-1 has requested data regarding the size and shape of the distribution of drivers' eye movement in order to characterise visual adaptation, that representing the dynamic assumption. Whereas other studies reported eye movement per driver over time, i. e. they reported the change in eye movement and thus change in exposure of the retina towards particular parts of the scene of single drivers along a track (Cengiz et al., 2016; Heynderickx et al., 2013). That answering

the question where a particular driver looked at a particular point in time and the resulting changes over time. Narisada, 1992 proposed that it is irrelevant what changes in luminance particular drivers are exposed to as it is unlikely that they are being exposed to those precise order of changes again. Thus I concluded that it should be of interest where the majority of drivers tend to look at most of the time in order to characterise the state of adaptation based on the probability the gaze was directed to within typical scenes. Therefore, another approach was necessary which I implemented by cumulating all available gaze direction data for a longer duration, both fixations and saccades, toward the road ahead, which I reported in publication *II* (Winter et al., 2017a, Part iii). Gaze falling into the interior of the vehicle (e. g. on instruments or navigation) was sacrificed for simplicity of the analysis.

10° circle approximates eye movement.

In the analysis of the cumulated data of 23 subjects it was found for the main road that the distribution of eye movement data points tends to be circular and the focus of attention is the centre of the road ahead at the horizon. A 10° circle centred at said focus of attention approximated the viewing behaviour best based on methods of signal detection theory.

On the residential road there is a tendency to look also at the near side, the location of potential pedestrians and of junctions where priority is given to those entering the road, which resulted in the simplified geometry approximating the viewing behaviour either a 10° / 20° ellipse if centred at the centre of lane at the horizon or a 10° circle if centred at the centre of the cumulated data, that being a horizontal offset of 3.8° from the centre of lane towards the curb.

EM(x,y) required for dynamic assumption.

The cumulated eye movement data EM(x,y) for the main road OS and the residential street is the required data set for being able to undertake follow up research concerned with the dynamic assumption in publication *III* (Winter et al., 2017b, Part iii).

Others analysed the mean luminances within circles / ellipses of various size (Cengiz, Kotkanen et al., 2014; Maksimainen et al., 2017), among which the here reported simplified geometries approximating the viewing behaviour of drivers were. Those simplified geometries (10° circle / 10°/20° ellipse), however, represent foveal eye movement, this representing areas within the visual field influencing foveal adaptation. As discussed in Section 19.1 peripheral adaptation in a complex traffic scene will be most likely different depending on the retinal location and, therefore, needs another approach for estimation, either by simplified geometries with increased size (representing the periphery around typical foveal eye movement) or with increased resolution, i. e. analysing different parts of the peripheral visual field as in the proposed spatial sampling of a driver's visual field in publication *III* (Winter et al., 2017b, Part iii). Another caveat is that these simplified geometires do not represent the actual Gaussian distribution

of the data, because they are flat, equally weighting the area within and thus probably leading to different results when estimating foveal adaptation with the raw eye movement data EM(x,y).

19.3 SPATIAL SAMPLING OF THE VISUAL FIELD

Publication *III* (Winter et al., 2017b, Part iv) addressed the issue of proposing a method for estimating peripheral adaptation at various locations: the spatial sampling of a driver's visual field. With that method 69 2° circular sub-regions within the visual field are assessed. The central 2° circle is assumed to represent luminances influencing the fovea and the other 68 sub-regions are assumed to represent luminances influencing the periphery. That is following the local adaptation hypothesis stating different parts of the retina will be influenced by different parts of the scene, thus leading to different states of adaptation. The method was applied to analyse the static as well as the dynamic assumption.

Static assumption

The static assumption is based on the thought that if changes of exposure to different luminances are within ±2 log units, transition happens very fast (Adrian, 1989). I. e. it is assumed that re-adaptation converges within the duration of a fixation, which would make the mean luminance of a task area a good estimator for the state of adaptation, which for foveal adaptation commonly is the mean luminance of the road surface (CIE 140, 2000; CIE 31, 1976).

Dynamic assumption

The dynamic assumption is intended to represent typical gaze behaviour, thus to estimate the relative proportion of time for which regions of the retina are exposed to a particular direction within urban street scenes after dark. Publication *II* (Winter et al., 2018, Part iii) provided data for following the dynamic assumption, describing typical eye movement behaviour in the context of driving in urban environments at night.

The analysis was undertaken by applying the method of the spatial sampling of a driver's visual field on a luminance image series consisting of 10 measurements between two successive lamp posts on a main road, a residential street and a simulated street. The results of the static and dynamic assumption were compared to the mean luminance within a 10° circle and the mean luminance of the road.

19.3.1 *Peripheral vs foveal*

Peripheral < foveal

The mean luminance within the central 2° circle represented luminances assumed to influence the state of adaptation of the fovea and the other 68 mean luminances the areas influencing the periphery. The foveal median luminance was higher than the peripheral median luminance (both for the static and the dynamic approach), although

the range of peripheral luminances from minimum to maximum was much wider.

As peripheral areas of the scene such as the pave walk tend to be darker and as these results suggest that the periphery of the retina is exposed to lower luminances it is evident that overall peripheral vision performs poorer than the fovea when at a lower state of adaptation, as predicted by the contrast detection formula of Adrian, 1989. When exposing a peripheral part of the retina to the road that difference in adaptation level might not be relevant, as depending on the magnitude of the change neural adaptation will be able to re-adapt quick enough to countervail the difference.

19.3.2 *Static vs dynamic*

Static < dynamic

When comparing the results of the static and dynamic approach- where the visual scene includes sources of high luminance (such as the headlamps of approaching vehicles or the fixed road lighting installation) the dynamic approach shows that these influence a wider part of the field of view than does the static approach (Figures 26 and 29). That is plausible because changes of luminance of that magnitude are unlikely to result in stable states of adaptation between two fixations.

The findings confirmed that observation meaning the median luminance of the static approach is lower than that of dynamic approach leading to an overall lower estimate of adaptation, both for the foveal and peripheral estimates.

That might play a role in the overall state of adaptation of those areas of the retina being exposed to such high luminance sources frequently, which encounter vaster changes in luminance, as the luminances analysed here were the mean luminances within a 2° circle, diminishing the magnitude of the change due to calculating the mean over an area. Receptive fields in the periphery, however, where hundreds to thousands of photoreceptors are interconnected to a single ganglion cell might mitigate that assumption (Boyce, 2014).

19.4 PRACTICAL IMPLICATION

10° circle overestimates.

The results of the spatial sampling of a driver's visual field were compared to recently used methods (mean luminance within a 10° circle (Cengiz, Kotkanen et al., 2014; Maksimainen et al., 2017)) and current standards and recommendations (mean luminance of road surface (CIE 140, 2000; CIE TN 007, 2017)). Compared to the peripheral results the 10° circle led to higher estimates of background luminance than all other methods (static / dynamic, road, as well if omitting the upper quarter). Calculating a single mean luminance within the 10° circle also conceals the true variability within the periphery, which

Road surface has tendency to underestimate.

spans a range from minimum to maximum of several log. The mean luminance of the road surface tended to underestimate when compared to the dynamic assumption and to give a fair estimate when compared to the static assumption.

First, from the findings and underlying research I cannot suggest whether the static approach or the dynamic approach comes closer to the truth representing the states of adaptation of the periphery, as the actual state of adaptation of a human observer in a road scene cannot be measured in vivo, i. e. on the retina. Therefore, it is necessary to build a case around the theory, pick a likely scenario and point out the implication on calculating the adaptation coefficient m and luminance L_{mes} and based on that the implications for the use cases of the mesopic system (Page 5).

In practical application of the mesopic system such as when designing a road lighting installation the only thing known for sure is the mean luminance of the road and the glare caused by the installation, as defined in CIE 140, 2000. CIE TN 007, 2017 proposes the road surface as the task area which is why it is recommended to use the average luminance of the road as estimate for the peripheral state of adaptation. Further peripheral task areas such as pave walks are not defined for the design process, yet, which is why the current interim recommendation of JTC-1 proposes the mean luminance of the road as sole relevant task area for the peripheral state of adaptation.

As a consequence the following question arises: when a particular part of the peripheral retina is exposed to the road surface as a result of a saccade and a fixation, i. e. said particular part was subject to a change in background luminance, can it be assumed that said particular part reaches a steady state of adaptation? If the answer was yes, it could be assumed that the mean luminance of the road surface would be a fair estimate of the current state of adaptation of that particular part of the retina. To answer that question it is necessary to know a possible range of luminances particular parts of the retina might be influenced by before the fixation exposes a part of it to the road. As described earlier in Section 19.1 I focused on one of the parameters of adaptation luminance: L_b, which is why the influence of glare is neglected in the following line of thoughts. The consequences of that decision are discussed in Section 19.5.5.

Will re-adaptation converge within the duration of a fixation?

Figure 39 depicts an ordered version of Figure 7 showing a fixation followed by a saccade followed by a fixation. The theoretical background for the assumed duration of typical saccades, fixations and neural adaptation were presented in Sections 2.4 and 2.5.1. When the gaze moves from fixation $i-1$ via a saccade to fixation i the peripheral results of the dynamic assumption represent the variety of possible starting points of fixation $i-1$ and therefore the possible range of weighted luminances for the 68 sub-regions of the periphery (Figure 40). The saccade puts the retina into a state of transient ad-

From transience to steadiness.

aptation, i. e. adaptation processes are triggered and might result in a steady state during the following fixation. During the saccade and at the beginning of the fixation vision is assumed to be impaired, selectively for detecting motion but less or not for detecting coloured contrasts (Section 2.5.1). If the change of luminances a particular part of the retina undergoes is within 2 log it is assumed that neural adaptation copes with the change and re-adapts that particular part of the peripheral retina now exposed to the road surface to the luminance level of the road surface (Section 2.4) within the duration of the fixation to a steady state.

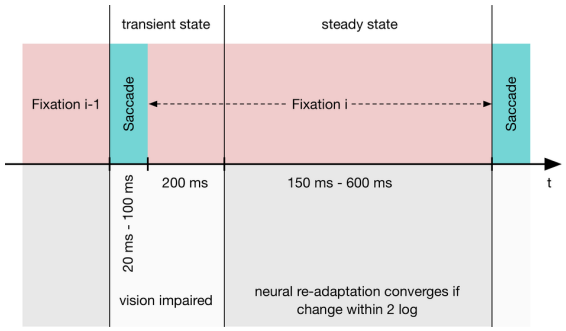

Figure 39: The sequence of saccades and fixations result in continuous processes of re-adaptation during eye movement over time, i. e. a transient state. Depicted are possible durations of saccades, of neural adaptation and of fixations from recent research. See this as an ordered version of Figure 7, where the depicted order would be repeated over and over again. If the duration of the fixation is long enough and the magnitude of change was within 2 log it is assumed, that adaptation reaches a steady state.

Sub-areas of very low luminance or sub-areas containing very bright luminances are probably less likely to converge, i. e. they do not reach a steady state within the duration of a fixation, thus the transient state might be better represented by the dynamic assumption, as this can be seen as an overall non-converged state of adaptation. The continuous exposure of some parts of the periphery of the retina to very bright luminances of the road lighting installation due to eye movement will also influence a wider field in the peripheral retina as represented by the results of the static assumption. Besides the just described deficiencies of the static assumption they might be considered as a starting point for assessing adaptation if the gaze was focused around the centre of lane at the horizon. That is the case in 48 % of the time, i. e. the gaze rests in the area between ± one 2° circle (i. e. within ±3° horizontally / vertically) and 7.5 % of the time within one 2° circle (i. e. within ±1° horizontally / vertically).

Static or dynamic assumption likelier initial position?

The movement of the own vehicle was not considered in that line of thought, yet. Table 12 depicts distances covered within a typical duration of a fixation for various common speed limits on urban roads ranging from 3 m to 11 m. If a particular part of the retina is exposed

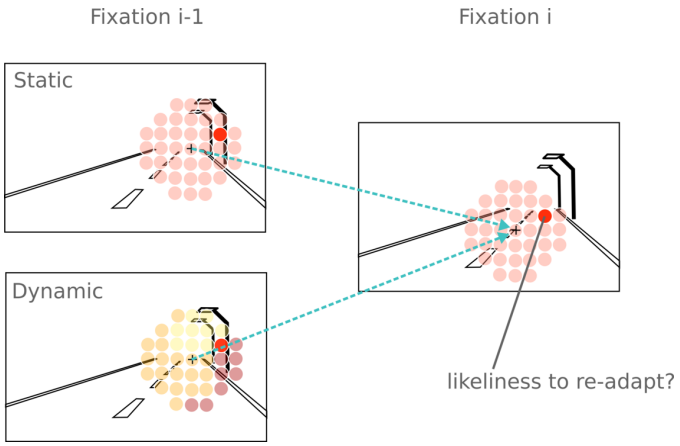

Figure 40: Assume any particular peripheral part of the retina is exposed to the road surface during the current fixation i, here represented by the saturated red circle in the upper right (+ represents the foveal position). Depending on the magnitude of the change of luminance said particular part was exposed to in the previous fixation $i-1$ one can assess whether it is likely or not that neural re-adaptation converges. The previous fixation has two possible initial states: the results of the static assumption represent the case that gaze was centred at the centre of lane at the horizon, the results of the dynamic assumption represent the probable weighted mean luminance based on typical eye movement of drivers.

Table 12: Covered distance within a given duration of a fixation and a given speed of the own vehicle.

Speed	Covered distance in 0.35 s	Covered distance in 0.8 s
30 km h^{-1}	2.9 m	6.7 m
50 km h^{-1}	4.9 m	11 m

to the road within a fixation it can be assumed that the change of luminance along the road due to the movement of the vehicle is quite homogeneous as defined in the requirements of the lighting classes CIE 115, 2010, which is why I conclude that it is not unreasonable to exclude that factor from the following discussion. In areas further away of the road in the periphery of the scene that cannot be assumed. There changes might be much more heterogeneous leaving particular parts of the retina exposed to such areas within the duration of a fixation less likely to reach a steady state. There the results of the dynamic assumption give a better estimate of overall adaptation.

Movement of the driver's vehicle.

Table 13 depicts the range of luminances found for the static and dynamic assumptions based on the findings of Winter et al., 2017b. That table shows the range in log from the minimum / maximum value of the method of the current row in relation to the median of the road surface. E. g. the results in Figure 38 suggests that the me-

Minimum to maximum log range.

Table 13: The log range of luminances from minimum / maximum within the 68 peripheral sub-areas and 10 images to the median of the CIE road 140 method as reference based on the data of Winter, Fotios and Völker, 2017b (see Section 17.4). The quantiles represent the amount of data of the peripheral method that is within the reported range, e. g. in the 99 % quantile the seven results furthest away from the reference median were excluded.

Type of road	Method	Minimum to maximum log range			
		Quantiles			
		50 % ($N = 340$)	95 % ($N = 646$)	99 % ($N = 673$)	100 % ($N = 680$)
Residential street EA	Peripheral static	−0.4 to +0.4	−0.8 to +0.8	−0.8 to +1.6	−0.8 to +2.5
	Peripheral dynamic	−0.5 to +0.5	−0.5 to +1.0	−0.5 to +1.3	−0.5 to +1.6
Main road OS	Peripheral static	−0.2 to +0.2	−0.8 to +0.8	−0.8 to +1.5	−0.8 to +1.9
	Peripheral dynamic	−0.2 to +0.2	−0.5 to +0.5	−0.6 to +0.7	−0.6 to +0.9

Note: the log ranges were calculated with $\log_{10}(\text{median}(\overline{L}_{i,road}) / \min(\overline{L}_{i,k}))$ and $\log_{10}(\max(\overline{L}_{i,k}) / \text{median}(\overline{L}_{i,road}))$ for the $i = 10$ images and $k = 68$ sub-regions.

dian of the mean luminances of peripheral static and the road were similar for the residential street and the main road. The minimum to maximum range in log for the whole dataset (i. e. the 100 % quantile), however, is −0.8 to 2.5 for the residential street, which is above the assumed capability of the fast neural adaptation of 2 log, whereas on the main road the minimum to maximum range is −0.8 to 1.9, which is more likely to result in a steady state of adaptation. As discussed the dynamic assumption is the better initial starting point for estimating peripheral adaptation anyways and for the predicted minimum to maximum range it seems plausible to assume re-adaptation finished. If omitting the most extreme outliers, i. e. by quantifying only the 99 %, 95 % and 50 % quantiles, the assumption of resulting in a steady state becomes likely for both initial starting points. The simulated street is not taken into account further as pointed out in Section 19.5.4.

Steady state of adaptation likely.

That leads to the conclusion that using the mean luminance of the road surface as an estimate for adaptation is not unreasonable, even if the more likely dynamic assumption represents the initial overall state of adaptation of the periphery of the retina, which actually is higher than the mean luminance of the road. As a consequence one can assume that the road as a task area represents a predictor for peripheral visual performance when it comes to detecting objects: al-

though that is more likely to be valid after the first 200 ms of the fixation.

One could question whether the findings of others reported in Section 2.4 imply that the transient state is irrelevant. Vision seems to be impaired during a saccade and the initial duration of a fixation, but whether certain stimuli during the transient state might trigger attention and result in input for the unconscious process of finding the target of the next fixation, as vision seems to be impaired selectively. I. e. impaired for motion detection but not impaired for colour contrast detection. If vision during the saccade mattered the finding of the higher peripheral median of the dynamic assumption would represent the overall initial transient state of adaptation better and, therefore, be a predictor for peripheral visual performance during a saccade and the initial duration of the fixation. E. g. if that was true considering an estimate for the peripheral state of adaptation based on the dynamic assumption would represent peripheral visual performance during eye movements and at the beginning of a fixation.

Is vision impaired during a saccade?

Based on the theoretical ranges of duration for a saccade, fixation and time to re-adapt the ratio between transient and steady state can be assessed. E. g. 200 ms re-adaptation plus 20 ms saccade (= transient state, see Figure 39) and 600 ms fixation (= steady state) results in a 27 % / 73 % transient / steady ratio, 200 ms re-adaptation, 100 ms saccade and 150 ms fixation in a 67 % / 33 % transient / steady ratio. For shorter times of re-adaptation 0 ms the emphasis moves towards the steady state (40 % / 60 % and 3 % / 97 %). As a consequence both states of adaptation are not neglectable.

At this point it is not reasonable to follow one case only, as I cannot suggest an answer to the question whether vision during a saccade does or does not matter, which is why both assumptions (peripheral dynamic representing the state of adaptation and mean luminance of the road representing the state of adaptation) need to be assessed further on. That raises the question what the consequences are when underestimating or overestimating the state of adaptation when calculating the mesopic adaptation coefficient m and luminance L_{mes}, which depends on the use case of application.

19.4.1 *Relevance to the use cases of the mesopic system*

CIE TN 007, 2017 recommends using the average luminance of the design area (i. e. the road surface as of CIE 140, 2000) as the estimated adaptation luminance. As discussed above that seems plausible because when the gaze moves within the scene it is likely that peripheral parts of the retina re-adapt within 0.2 s to the prevailing luminance on the road and reach a steady state of adaptation. For the transient state the overall state of peripheral adaptation is better represented by the median of the dynamic assumption, however, which

is higher, meaning the mean luminance of the road surface tends to underestimate. That only would be relevant in the initial onset of a fixation (where neural adaptation adjusts to the new luminance) or if vision during a saccade would be a source of information or if other task areas than the road were relevant.

I will discuss that on each of the use cases of the recommended system of mesopic photometry. Figures 41 and 42 back my line of thought with data for predicted mesopic enhancement factors of various SPDs and luminous efficacies of various light sources.

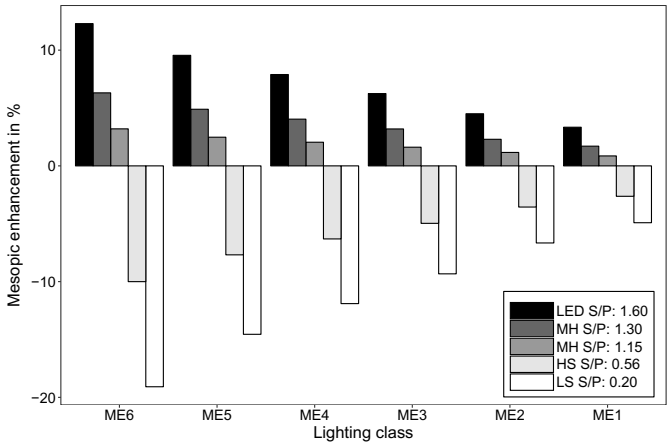

Figure 41: Predicted increase / decrease of peripheral visual performance (i. e. mesopic enhancement factor F_{mes} of CIE TN 007, 2017) compared to when using photopic luminances for exemplary SPDs with various S/P ratios and assumed adaptation luminances as defined in the lighting classes of CIE 115, 2010. Note: HS = high pressure sodium, LS = low pressure sodium, MH = metal halide.

1.) CHOOSE SPD TO ENHANCE PERIPHERAL VISION: based on the SPDs of Figure 41 the answer to the question "which SPD supports peripheral visual performance best?" is always the same: LED best, HS worst, i. e. the order in between the SPDs does not change. Therefore, it does not matter how well the state of adaptation is estimated, neither an underestimation nor an overestimation changes the answer to that question. SPDs that would change the relative order to each other within the range of the various lighting classes would be theoretical monochromatic-like line spectra, i. e. a SPD with a single peak at the wavelength with maximum mesopic efficiency for a given combination of L_a and S/P, if they existed with a relevant change of efficiency at all within the range of $0.3\,\mathrm{cd/m^2}$ to $2.0\,\mathrm{cd/m^2}$. If they existed they most likely would be poor SPDs in other aspects of lighting quality, such as colour rendering. In regard to that matter this is a theoretical decision that can be made without harm to safety.

No precise estimate required.

2.) CHOOSE ENERGY EFFICIENT LIGHT SOURCE: Figure 42 depicts various examples of the change of mesopic efficacy on a $\mathrm{lm\,W^{-1}}$ basis for the lighting classes of CIE 115, 2010. It is obvious that if selecting a particular light source based on mesopic efficacy as criterion the answer will be different depending on the lighting class, i. e. a correct prediction of the state of adaptation is necessary. E. g. if assessed based on the photopic efficacy the $127\,\mathrm{lm\,W^{-1}}$ LS lamp is 41 % more efficient than the $90\,\mathrm{lm\,W^{-1}}$ LED luminaire. That described benefit diminishes completely if assessed with mesopic efficacy at ME6. In this case both underestimation and overestimation might result in false decisions when assessing SPDs based on $\mathrm{lm\,W^{-1}}$, resulting in potentially less savings of energy if the wrong decision is made.

Precise estimate matters.

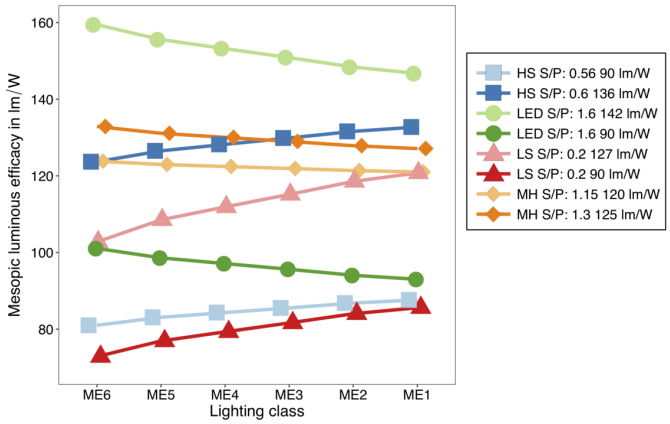

Figure 42: Luminous efficacy multiplied with the mesopic enhancement factor F_{mes} for various light sources and for the lighting classes of CIE 115, 2010. Lamp parameters (S/P ratio and $\mathrm{lm\,W^{-1}}$) are examples from the latest product catalogue of a major manufacturer, the LED was a luminaire. Note: HS = high pressure sodium, LS = low pressure sodium, MH = metal halide.

3.) REDUCE LIGHT LEVEL: there is a different outcome depending on whether a method tends to give a fair estimate or whether it tends to underestimate. As underestimation over-predicts the mesopic enhancement factor F_{mes}, e. g. LED at L_a = ME6 predicts a possible reduction of 12 %, whereas ME3 predicts only 6 % (Figure 41). As a consequence underestimation is a factor decreasing safety, whereas overestimation diminishes possible energy savings. To answer that question one must review the following two cases:

Precise estimate mandatory for maintaining safety.

A.) TRANSIENT STATE OF ADAPTATION: If assuming the results of the dynamic assumption give a fair estimate for the transient state and based on the finding that the median of the road surface tends to be lower: can it be tolerated that peripheral visual performance is diminished due to underestimation during the saccades and the initial fixation? Factors against this case are: vision during the saccade is likely to be suppressed anyways and one can question whether

the median of the results of the dynamic assumption as an estimate of the transient state is of relevance. Because of the heterogeneity of the results the median leads to an overall higher estimate but the total variety within the retina is heterogeneous spanning 1.5 to 2.1 log (Table 13, the total range of the dynamic results), which then represents states of adaptation only of parts of the periphery. Meaning: due to the wide range of potential states of adaptation of the periphery using the median of peripheral dynamic predicts potential light level reduction without harming peripheral visual performance for some areas, whereas the higher adapted areas suffer a decrease of peripheral visual performance. That because their performance is not enhanced (compare the predicted increase of performance of ME6 vs the higher lighting class ME1 in Figure 41).

B.) STEADY STATE OF ADAPTATION: Assuming re-adaptation during a fixation reaches a steady state makes the mean luminance of the road surface a plausible estimate of adaptation for the currently to that part of the scene exposed parts of the retina. In that case decreasing the light level as predicted by F_{mes} keeps peripheral visual performance in the design area at a constant level. Areas outside the design area are likely at other adaptation levels, which is why their visual performance will be affected if at higher adaptation levels.

Both the transient and the steady state of adaptation represent plausible outcomes at different points in time in typical stages of eye movement when estimating adaptation. On top of that adaptation of parts of the retina exposed to the design area, i. e. the road surface, will differ from parts exposed to other areas of the scene ranging from a sixth ($10^{-0.8}$) to 79 times higher ($10^{+1.9}$), which is the minimum to maximum range of the dynamic assumption. That means if the light level will be reduced based on the average luminance of the road the predicted peripheral visual performance will be valid for the design area and the duration of the steady state. For those parts of the retina that are assumed to be at a higher state of adaptation in the transient state or exposed to other parts in the scene the predicted peripheral visual performance will be lower, which means decreasing the light level will reduce peripheral visual performance for those parts of the retina. According to Adrian, 1989 visual performance will be improved with higher states of adaptation, so this might be less relevant if potential objects to be detected have high contrast in states of adaptation further away from the performance decrease knee (physiological change of Weber contrast to Ricco contrast). For the areas with a lower state of adaptation the predicted visual peripheral performance will be increased, but contrast detection in lower states of adaptation is worse, especially below the performance knee. As a result it is safer to overpredict for this use case, e. g. if designing for ME6 using ME5 as the adaptation luminance to predict F_{mes}, that resulting in a lower light level reduction.

19.5 LIMITATIONS

Estimating the state of adaptation is cannot be compared to common photometric metrology that can be measured as precise as e. g. the base units of the International System of Units. The heterogeneity of the scene, continuous eye movement and movement of the vehicle require compromises to be made and likely cases can be suggested based on a hypothetical frame, which unfortunately cannot be verified or falsified by measurements in the retina. That leaves room for speculation and interpretation and certain topics are pointed out below.

19.5.1 *Eye movement data*

The eye movement data was gathered on one straight section of a main road and one straight section of a residential street. From that point it cannot be said whether that represents the viewing behaviour for all possible roads and the population of drivers. The sample size, however, was quite high (23 drivers) and consisted of both experienced and inexperienced individuals. Viewing behaviour was analysed along sub-sections of the road and it was found to be consistent in terms of spatial distribution but not in terms of the centre of gaze. The former is a hint that the distribution on other roads might be consistent but to proof that further research is required.

19.5.2 *Spatial sampling*

The spatial sampling pattern was arbitrarily chosen to match the size of the fovea, i. e. 2°, and the extent of the experiments of CIE 191, 2010, i. e. 10° off-axis. It is of relevance how the chosen size and field influences the outcome of the results. First the 10° circle can be assumed to be a version of the sampling pattern with less accuracy. It is obvious that the variability of the scene when calculating the mean luminance within the 10° circle is masked. In contrast to that how would the findings of a sampling pattern of 1° or 0.1° size differ? Very high and very low luminances would have an increased impact on the calculation of the mean luminance. Most likely the impact will be more distinct on the results of the static assumption and less on the results of the weighted mean luminance of the dynamic assumption, as the latter weights towards the centre of the scene which tends to be less heterogeneous. But whether the outcome of the overall state of adaptation in terms of median of the results will lead to the same findings, e. g. if the very high and very low luminances would lead to outliers equally distributed on both ends of the data (minimum and maximum), or not, cannot be said which is why more research on that topic is necessary.

19.5.3 *Likeliness of steady state*

Longer durations of a typical fixation than considered in the line of thought of Section 19.4 wouldn't change the conclusion, as longer durations give the mechanisms of adaptation more time to reach a steady state. Shorter durations of a typical fixation would increase the probability for the dynamic assumption to be an estimator for peripheral adaptation, as it may be assumed that for short fixations re-adaptation does not converge and remains in a transient state. That would also be the case if durations of typical saccades were longer than discussed here.

19.5.4 *Simulated street*

The mesopic system is likely to be applied in the design phase of a road lighting installation which is why I have included a simulated street besides the measurements undertaken in two real roads. As I was investigating the state of peripheral adaptation and due to the fact that the scene in the design process of road lighting is defined for the road surface only (CIE 140, 2000) one can question the proposed direction of my findings of my proposed method of the spatial sampling of a driver's visual field for the simulated street. I already enhanced the simulated scenes by adding blocks representing houses and including the interior of the vehicle, copied from the measurements of the residential street. The scene is still quite artificial and unlikely to represent a real scene in terms of luminances in the periphery of the road. That can be seen in the lower medians of especially peripheral static but also peripheral dynamic compared to the two measured real scenes. Which is why I excluded the simulated results in the discussion of practical implication of Section 19.4.

If the precise overall peripheral state of adaptation was of interest during the design phase it is necessary to define more detailed urban standard scenes, which need to contain houses with illumination or shops etc. to make the estimation of the periphery more realistic.

19.5.5 *Veiling luminance*

As defined in Equation (4) the adaptation luminance consists of two components: the background luminance L_b around a task point and the veiling luminance L_v caused by very bright light sources within the visual field. Based on the finding of Maksimainen et al., 2017 and my finding in publication *I* (Winter et al., 2018, Chapter 7) I decided to focus on one of the two components. Questioning how the findings would differ if considering both L_b and as well L_v is legitimate. I can only hypothesise what difference it made. The magnitude of L_v depends on the angular distance of a glare source to the particular area

within the retina of interest, where smaller angular values of θ, i. e. the angle between the assumed task point and the glare source, increase L_v by θ^{-2} (CIE 31, 1976) or depending on the method by θ^{-3} (Uchida & Ohno, 2017). That means the overall adaptation levels are increased compared to the reported results and that for all reported methods from CIE road 140 to peripheral static and dynamic. Peripheral static and dynamic, however, might be affected based on the relative position of a particular sub-area within the visual field, where sub-areas more distant to glare sources are less affected than sub-areas closer to a glare source. I cannot say whether that would affect the median of $\overline{L}_{i,k}$ or whether the effects equalised themselves. The range from minimum to maximum might increase, probably affecting the conclusion that neural adaptation can cover the reported range of luminances as discussed above. Hard facts are required to answer that sufficiently, which I leave for others to answer. Regarding the use cases, however, it has no practical implication for case 1 (unless the resulting adaptation luminance would be above $5\,\mathrm{cd/m^2}$, where SPD has no further influence on peripheral visual performance, which is likely the case for the main road OS).

The second use case will be affected in terms of potential loss of energy savings.

Use case 3 would be affected as it is better for safety to overestimate than to underestimate. As more research needs to point out the overall direction of the effect it cannot be said what the precise implications are, but glare will affect vision twofold: 1.) the veiling luminance will increase the state of adaptation, therefore, less reduction possible and 2.) reduced visual performance as described in Equation (6). Both factors have a negative impact on safety which is why if the third use case would be applied L_v definitively must be considered.

20 CONCLUSIONS

For the application of the recommended system of mesopic photometry in road lighting it is necessary to estimate the peripheral state of adaptation of a driver in an urban environment after dark. Estimating the state of adaptation is not a trivial task due to the extent of the retina and as road scenes after dark are complex, containing inhomogeneous areas such as shops, advertisements and glare sources. On top of that, adaptation is in a continuous transient state due to the movement of the eye and the movement of the vehicle within the scene. JTC-1 of the CIE has requested proposals for how to overcome these problems and recently published an interim recommendation, which was scrutinized. As a reminder the outline of the research addressing those issues in context of this thesis was depicted in Figure 4.

It was found that visual performance, an assumed proxy representing the state of adaptation, is mostly affected by the local luminances around a task point, which is in common with the findings of others. The negative influence of glare, however, was diminished if the visual field contained inhomogeneities, indicating a global influence of the visual field probably on the pupil diameter, which with decreased size leads to less straylight within the eye. Based on that finding and the finding of others I decided to focus on one of the two parameters characterising the state of adaptation: the background luminance and omitted the veiling luminance.

Whereas in current application of estimating the state of adaptation in road lighting a static observer geometry is assumed, another line of thought was examined: the dynamic assumption which is based on the assumption that a fair estimate of a driver's state of adaptation is based on where and for how long gaze was directed to. To follow up with that thought it was necessary to gather eye movement data representing where most of the drivers tend to look at most of the time rather than following an individual driver's change along a track. I quantified the distribution of the data and identified the most suitable simplified geometry approximating the eye movement behaviour, which was a 10° circle centred at the centre of lane at the horizon for a main road and a 10° circle 3.8° towards the near side for a residential street.

The cumulated eye movement data and approximation by the 10° circle represents the areas the fovea is exposed to. CIE JTC-1's task, however, is to identify the state of adaptation of the periphery of the retina. Therefore, I proposed a new method: the spatial sampling of a driver's visual field by analysing 68 sub-regions representing

the periphery of the retina instead of simplified geometries representing the eye movement of the fovea. With the spatial sampling I could show that the periphery of the retina is much more heterogeneous than assumed with simplified geometries in previous research or with complex methods incorporating more factors (e. g. veiling luminance), which mask the influence of particular parts of the visual field. I also identified that the periphery is exposed to lower luminances than the fovea and that the dynamic assumption lead to higher estimates of the state of adaptation than the static assumption. I cannot suggest, however, which method gives a more precise representation, as a reference adaptation cannot be measured within the retina. Theory based on research can back up likely scenarios to build a case which method might be more plausible. The influence of glare in terms of veiling luminance was omitted, which is why it is likely that the overall state of adaptation in reality is higher than reported. Whether the various methods in relation to each other remain constant needs to be answered in future research.

JTC-1 published an interim recommendation for the application of the system of mesopic photometry where it was suggested to use the mean luminance of the road surface (i. e. the design area) as an estimate for the state of adaptation. The mean luminance of the road surface represented the results of the static assumption very well, but compared to the dynamic assumption it tended to underestimate. Although the road surface was representing the median of the static assumption well, the total range of luminances in the periphery was still quite wide. As discussed I cannot suggest whether the static or the dynamic assumption represents a more precise state of adaptation, but I made a hypothetical case analysing the practical implication if a.) the overall state of adaptation of the periphery is higher (dynamic assumption $>$ road) and b.) how likely it is that transient adaptation reaches a steady state during a fixation when a particular part of the retina is exposed to the design area. I found that b.) is a plausible scenario based on theory of previous research, a.) required a per use case analysis.

For the three use cases of the mesopic system it was concluded that when assessing an SPD for best peripheral visual performance (use case 1) the accuracy of the estimation of the state of adaptation is irrelevant, because common SPDs in the range of the lighting classes do not change their relation to each other. Meaning: a SPD that was superior to another SPD in lighting class ME1 will be superior as well in lighting class ME6.

For use case 2 (best luminous efficacy) an accurate estimate helps identifying the most efficient light source. Under- or overestimation would be an issue of potential waste of energy, but not a concern to safety.

Use case 3 (light level reduction): the accuracy of estimation is a concern to safety as a method tending to underestimate over-predicts the possible light level reduction. To be on the safe side I suggest to use the predicted light level reduction of the next higher lighting class, i. e. if designing for ME6 to use the predicted reduction of ME5.

20.1 FUTURE RESEARCH

Some questions remain unsolved and new questions arose.

In publication *I* (Winter et al., 2018, Chapter 7) I identified a positive influence of extraneous light sources within the visual field on the negative impact of glare, which might be an influence on the pupil size. An inhomogeneous background might lead to a smaller pupil size diameter which results in less veiling of a glare source. That, however, is only a hypothesis but would be worth following.

The raw eye movement data analysed in publication *II* (Winter et al., 2017a, Part iii) may contain more insights and answer further questions. E. g. the assumptions I made are based on the duration of fixations while driving were experiments from the laboratory (Chapman & Underwood, 1998; Underwood et al., 2002). It would be of interest to either confirm those findings or report more precise values for the duration of fixations and saccades in real world driving.

Publication *III* (Winter et al., 2017b, Part iv) focused on one of two parameters of adaptation: the background luminance. The proposed method of the spatial sampling of a driver's visual field needs to be enhanced to incorporate veiling luminance as well in order to provide further details regarding the conclusions made within this thesis. Other studies assumed a static fixation point for the evaluation of glare (Maksimainen et al., 2017). However, it might be of interest to consider the glare evaluation based on eye movement, as Carraro, 1985 pointed out the resulting negative influence of glare when the gaze moves around might be based on the closest position a particular part of the retina was exposed to a glare source (without covering it) which might result in higher estimates of L_v.

In Section 2.5.1 it was described that vision during a saccade and at the beginning of a fixation is selectively suppressed for the magnocellular pathway, whereas the parvocellular pathway seems to be unaffected. Whether that is relevant to the task of driving needs to be researched, e. g. whether chromatic contrasts during a saccade contribute to attention and, potentially, a following fixation. That would help to decide whether the described transient state of adaptation is of relevance to driving or not (Figure 39).

REFERENCES

Adrian, W. (1987). Adaptation luminance when approaching a tunnel in daytime. *Lighting Research and Technology*, *19*(3), 73–79.

Adrian, W. (1989). Visibility of targets: Model for calculation. *Lighting Research and Technology*, *21*(4), 181–188.

Adrian, W. (1993). Visibility levels in street lighting: An analysis of different experiments. *Journal of the Illuminating Engineering Society*, *22*(2), 49–52.

Akashi, Y., Rea, M. & Bullough, J. (2007). Driver decision making in response to peripheral moving targets under mesopic light levels. *Lighting Research and Technology*, *39*(1), 53–67.

Bacelar, A., Cariou, J. & Hamard, M. (1999). Calculational visibility model for road lighting installations. *Lighting Research & Technology*, *31*(4), 177–180.

Bakeman, R. (2005). Recommended effect size statistics for repeated measures designs. *Behaviour Research Methods*, *37*(3), 379–384.

Böhm, M. (2013). *Abschlussbericht zum Projekt Nr. FF-FP0328 Erkennbarkeit von Warnkleidung*. FG Lichttechnik, Technische Universität Berlin.

Boomsma, C. & Steg, L. (2012). Feeling safe in the dark. *Environment and Behavior*, *46*(2), 193–212.

Bourdy, C., Chiron, A., Cottin, C. & Monot, A. (1987). Visibility at a tunnel entrance: Effect of temporal adaptation. *Lighting Research and Technology*, *19*(2), 35–44.

Boyce, P. R., Fotios, S. & Richards, M. (2009). Road lighting and energy saving. *Lighting Research and Technology*, *41*(3), 245–260.

Boyce, P. R. (2014). *Human factors in lighting* (3rd ed.). Boca Raton, FL: CRC Press.

Boynton, R. M. & Miller, N. D. (1963). Visual performance under conditions of transient adaptation. *Illuminating Engineering*, *58*, 541–550.

Carraro, U. (1985). *Die Adaptationsleuchtdichte bei inhomogenen Leuchtdichtefeldern unter besonderer Berücksichtigung einer dynamischen Sehaufgabe*. Hochschule für Verkehrswesen. Dresden.

Cengiz, C., Kotkanen, H., Puolakka, M., Lappi, O., Lehtonen, E., Halonen, L. & Summala, H. (2014). Combined eye-tracking and luminance measurements when driving on a rural road: Towards determining of mesopic adaptation luminance. *Lighting Research and Technology*, *46*(6), 676–694.

Cengiz, C., Maksimainen, M., Puolakka, M. & Halonen, L. (2016). Contrast threshold measurements of peripheral targets in night-

time driving images. *Lighting Research and Technology*, *48*(4), 491–501.

Cengiz, C., Puolakka, M. & Halonen, L. (2014). Reaction time measurements under mesopic light levels: Towards estimation of the visual adaptation field. *Lighting Research and Technology*, *47*(7), 828–844.

Chapman, P. R. & Underwood, G. (1998). Visual search of driving situations: Danger and experience. *Perception*, *27*(8), 951–964.

Cohen, J. (1992). A power primer. *Psychological Bulletin*, *112*(1), 155–159.

Collie, A., Maruff, P., Darby, D. G. & McStephen, M. (2003). The effects of practice on the cognitive test performance of neurologically normal individuals assessed at brief test–retest intervals. *Journal of the International Neuropsychological Society*, *9*(03), 419–428.

Commission Internationale de l'Eclairage, CIE Publication 115. (2010). Recommendations for the lighting of roads for motor and pedestrian traffic.

Commission Internationale de l'Eclairage, CIE Publication 140. (2000). Road lighting calculations.

Commission Internationale de l'Eclairage, CIE Publication 146. (2002). Cie collection on glare.

Commission Internationale de l'Eclairage, CIE Publication 191. (2010). Recommended system for mesopic photometry based on visual performance.

Commission Internationale de l'Eclairage, CIE Publication 31. (1976). Glare and uniformity in road lighting installations.

Commission Internationale de l'Eclairage, CIE Publication 88. (2004). Guide for the lighting of road tunnels and underpasses.

Commission Internationale de l'Eclairage, CIE S 017. (2011). International lighting vocabulary.

Commission Internationale de l'Eclairage, TN 007. (2017). Interim recommendation for practical application of the CIE system for mesopic photometry in outdoor lighting.

Crawford, B. H. (1936). The dependence of pupil size upon external light stimulus under static and variable conditions. In *Proceedings of the royal society of London b: Biological sciences* (Vol. 121, *823*, pp. 376–395).

Crundall, D., Chapman, P., Phelps, N. & Underwood, G. (2003). Eye movements and hazard perception in police pursuit and emergency response driving. *Journal of Experimental Psychology: Applied*, *9*(3), 163–174.

Falkmer, T. & Gregersen, N. P. (2005). A comparison of eye movement behavior of inexperienced and experienced drivers in real traffic environments. *Optometry and vision science*, *82*(8), 732–739.

Fawcett, T. (2006). An introduction to roc analysis. *Pattern Recognition Letters*, *27*(8), 861–874.

Findlay, J. M. & Walker, R. (2012). Human saccadic eye movements. *Scholarpedia*, *7*(7), 5095.

Fotios, S. (2013). Lrt digest 1 maintaining brightness while saving energy in residential roads. *Lighting Research and Technology*, *45*(1), 7–21.

Fotios, S. & Gibbons, R. (2018). Road lighting research for drivers and pedestrians: The basis of luminance and illuminance recommendations. *Lighting Research and Technology*, *50*(1), 154–186.

Fotios, S. & Goodman, T. (2012). Proposed uk guidance for lighting in residential roads. *Lighting Research and Technology*, *44*(1), 69–83.

Fotios, S. & Cheal, C. (2011). Predicting lamp spectrum effects at mesopic levels. part 1: Spatial brightness. *Lighting Research and Technology*, *43*(2), 143–157.

Fotios, S., Atli, D., Cheal, C., Houser, K. & Logadóttir, Á. (2015). Lamp spectrum and spatial brightness at photopic levels: A basis for developing a metric. *Lighting Research and Technology*, *47*(1), 80–102.

Foulsham, T., Walker, E. & Kingstone, A. (2011). The where, what and when of gaze allocation in the lab and the natural environment. *Vision Research*, *51*(17), 1920–1931.

Freiding, A., Eloholma, M., Ketomaki, J., Halonen, L., Walkey, H., Goodman, T., ... Bodrogi, P. (2007). Mesopic visual efficiency i: Detection threshold measurements. *Lighting Research and Technology*, *39*(4), 319–334.

Gescheider, G. A. (1985). *Psychophysics method, theory and application* (2nd ed.). London: Lawrence Erlbaum Associates.

Gouras, P. (1967). The effects of light-adaptation on road and cone receptive field organization of monkey ganglion cells. *The Journal of Physiology*, *192*(3), 747–760.

Gouras, P. & Link, K. (1966). Rod and cone interaction in dark-adapted monkey ganglion cells. *The Journal of Physiology*, *184*(2), 499–510.

Harwell, M. R., Rubinstein, E. N., Hayes, W. S. & Olds, C. C. (1992). Summarizing monte carlo results in methodological research: The one- and two-factor fixed effects anova cases. *Journal of Educational and Behavioral Statistics*, *17*(4), 315–339.

Heynderickx, I., Ciociou, J. & Zhu, X. (2013). Estimating eye adaptation for typical luminance values in the field of view while driving in urban streets. In *Towards a new century of light* (pp. 41–47). Paris, France: Commission Internationale de l'Eclairage.

Hofer, H. & Williams, D. R. (2002). The eye's mechanisms for autocalibration. *Optics and Photonics News*, *13*(1), 34–39.

Holladay, L. L. (1926). The fundamentals of glare and visibility. *Journal of the Optical Society of America*, *12*(4), 271–319.

Holmqvist, K., Nyström, M., Andersson, R., Dewhurst, R., Halszka, J. & van de Weijer, J. (2011). *Eye tracking: A comprehensive guide to methods and measures*. Oxford: Oxford University Press.

Hripcsak, G. & Rothschild, A. S. (2005). Agreement, the f-measure, and reliability in information retrieval. *Journal of the American Medical Informatics Association*, *12*(3), 296–298.

Illuminating Engineering Society of North America, RP-8-14. (2014). Roadway lighting.

Judge, S. J., Wurtz, R. H. & Rochmond, B. J. (1980). Vision during saccadic eye movements. i. visual interactions in striate cortex. *Journal of Neurophysiology*, *43*(4), 133–1155.

Kato, H. & Billinghurst, M. (1999). *Marker tracking and hmd calibration for a video-based augmented reality conferencing system*. Human Interface Technology Laboratory, University of Washington.

Kent, M., Altomonte, S., Tregenza, P. & Wilson, R. (2014). Discomfort glare and time of day. *Lighting Research and Technology*, *47*(6), 641–657.

Kountouriotis, G. K., Spyridakos, P., Carsten, O. M. & Merat, N. (2016). Identifying cognitive distraction using steering wheel reversal rates. *Accident Analysis and Prevention*, *96*, 39–45.

Land, M. F. (2006). Eye movements and the control of actions in everyday life. *Progress in Retinal and Eye Research*, *3*(25), 296–324.

Land, M. F. & Lee, D. N. (1994). Where we look when we steer. *Nature*, *369*(6483), 742–744.

Lin, Y. & Fotios, S. (2015). Investigating methods for measuring facial recognition under lamps of different spectral power distribution. *Lighting Research and Technology*, *47*(2), 221–235.

Liversedge, S., Gilchrist, I. & Everling, S. (2011). *The oxford handbook of eye movements*. EBSCO ebook academic collection. Oxford: Oxford University Press.

Logadóttir, Á., Christoffersen, J. & Fotios, S. (2011). Investigating the use of an adjustment task to set the preferred illuminance in a workplace environment. *Lighting Research and Technology*, *43*(4), 403–422.

Logadóttir, Á., Fotios, S. A., Christoffersen, J., Hansen, S. S., Corell, D. D. & Dam-Hansen, C. (2013). Investigating the use of an adjustment task to set preferred colour of ambient illumination. *Colour Research & Application*, *38*(1), 46–57.

Maksimainen, M., Puolakka, M., Tetri, E. & Halonen, L. (2017). Veiling luminance and visual adaptation field in mesopic photometry. *Lighting Research and Technology*, *49*(6), 743–762.

Maltz, M. & Shinar, D. (1999). Eye movements of younger and older drivers. *Human Factors: The Journal of the Human Factors and Ergonomics Society*, *41*(1), 15–25.

Martinez-Conde, S., Macknik, S. L. & Hubel, D. H. (2004). The role of fixational eye movements in visual perception. *Nature Reviews Neuroscience*, *5*(3), 229.

Masket, S. (1992). Relationship between postoperative pupil size and disability glare. *Journal of Cataract & Refractive Surgery*, *18*(5), 506–507.

McNicol, D. (1972). *A primer of signal detection theory*. London: Allen & Unwin.

Minutes of the 4th Meeting of CIE JTC-1: Implementation of CIE 191 Mesopic Photometry in Outdoor Lighting. (Tuesday, 17 December 2013. 2.00–4.00 p.m. CET). Webex-meeting.

Moon, P. & Spencer, D. E. (1943). The specification of foveal adaptation. *Journal of the Optical Society of America*, *33*(8), 444–456.

Mourant, R. R. & Rockwell, T. H. (1970). Mapping eye-movement patterns to the visual scene in driving: An exploratory study. *Human Factors: The Journal of the Human Factors and Ergonomics Society*, *12*(1), 81–87.

Mourant, R. R. & Rockwell, T. H. (1972). Strategies of visual search by novice and experienced drivers. *Human Factors: The Journal of the Human Factors and Ergonomics Society*, *14*(4), 325–335.

Narisada, K. (1992). Visual perception in non-uniform fields. *Journal of Light and Visual Environment*, *16*(2), 81–88.

Owsley, C. (2011). Aging and vision. *Vision Research*, *51*(13), 1610–1622.

Pachamanov, A. & Pachamanova, D. (2008). Optimization of the light distribution of luminaries for tunnel and street optimization of the light distribution of luminaries for tunnel and street optimization of the ight distribution of luminaries for tunnel and street lighting. *Engineering Optimization*, *40*(1), 47–65.

Pallant, J. (2010). *Spss survival manual: A step by step guide to data analysis using spss* (3rd ed.). Sydney: Allen & Unwin.

Perneger, T. V. (1998). What's wrong with bonferroni adjustments. *British Medical Journal*, *316*(7139), 1236–1238.

Pinker, S. (1984). Visual cognition: An introduction. *Cognition*, *18*(1-3), 1–63.

Plainis, S., Murray, I. J. & Charman, W. N. (2005). The role of retinal adaptation in night driving. *Optometry and vision science*, *82*(8), 682–688.

Poulton, E. C. (1989). *Bias in quantifying judgements*. London: Lawrence Erlbaum Associates.

Puolakka, M., Cengiz, C., Luo, W. & Halonen, L. (2012). Implementation of CIE 191 mesopic photometry - ongoing and future actions. In *Proceedings of CIE 2012 lighting quality & energy efficiency* (pp. 64–70). Hangzhou, China: Commission Internationale de l'Eclairage.

Neuroscience. (2001). In D. Purves, G. J. Augustine, D. Fitzpatrick, L. C. Katz, A.-S. LaMantia, J. O. McNamara & S. M. Williams (Eds.), (2nd ed., Chap. Types of Eye Movements and Their Functions.). Sunderland: Sinauer Associates.

Quaia, C., Lefèvre, P. & Optican, L. M. (1999). Model of the control of saccades by superior colliculus and cerebellum. *Journal of Neurophysiology*, *82*(2), 999–1018.

Rayner, K. & Castelhano, M. (2007). Eye movements. *Scholarpedia*, *2*(10), 3649.

Rea, M., Bullough, J. & Zhou, Y. (2010). A method for assessing the visibility benefits of roadway lighting. *Lighting Research and Technology*, *42*(2), 215.

Reece, J., Urry, L., Cain, M., Wasserman, S., Minorsky, P. & Jackson, R. B. (2011). *Campbell biology* (9th ed.). San Francisco: Pearson.

Rinalducci, E. J. & Beare, A. N. (1975). *Visibility losses caused by transient adaptation at low luminance levels* (tech. rep. No. HS-017 803). Transportation Research Board.

Rinalducci, E. J., Lassiter, D. L. & Mitchell, L. (1990). The effects of transient adaptation on cockpit operations. In *Proceedings of the human factors society 34th annual meeting* (pp. 1562–1566). Los Angeles, USA: SAGE Publications.

Rosenthal, R. (1994). The handbook of research synthesis. In H. Cooper & L. V. Hedges (Eds.), (Chap. Parametric measures of effect size, pp. 231–244). New York: Russell Sage Foundation.

Ross, J., Burr, D. & Morrone, C. (1996). Suppression of the magnocellular pathway during saccades. *Behavioural Brain Research*, *80*(1-2), 1–8.

Rothkopf, C. A., Ballard, D. H. & Hayhoe, M. M. (2007). Task and context determine where you look. *Journal of Vision*, *7*(14), 1–20.

Rothman, K. J. (1990). No adjustments are needed for multiple comparisons. *Epidemiology*, *1*(1), 43–46.

Schreuder, D. A. (1975). Fundamental visual problems in tunnels. *Lighting Research and Technology*, *7*(2), 85–87.

Schütz, A. C., Braun, D. I. & Gegenfurtner, K. R. (2009). Object recognition during foveating eye movements. *Vision Research*, *49*(18), 2241–2253.

Stahl, F. (2004). *Kongruenz des Blickverlaufs bei virtuellen und realen Autofahrten - Validierung eines Nachtfahrsimulators* (Diplomarbeit, L-LAB / TU Ilmenau).

Stiles, W. S. (1929a). The effect of glare on the brightness difference threshold. In *Proceedings of the royal society of London. series b, containing papers of a biological character* (Vol. 104, *731*, pp. 322–351).

Stiles, W. S. (1929b). The scattering theory of the effect of glare on the brightness difference threshold. In *Proceedings of the royal society of London. series b, containing papers of a biological character* (Vol. 105, *735*, pp. 131–146).

Stiles, W. S. & Crawford, B. H. (1937). The effect of a glaring light source on extrafoveal vision. In *Proceedings of the royal society of London. series b, biological sciences* (Vol. 122, *827*, pp. 255–280).

Stockman, A. & Sharpe, L. T. (2006). Into the twilight zone: The complexities of mesopic vision and luminous efficiency. *Ophthalmic and physiological optics*, *26*(3), 225–239.

Sullivan, G. M. & Feinn, R. (2012). Using effect size or why the p value is not enough. *Journal of Graduate Medical Education*, *4*(3), 279–282.

Summala, H., Nieminen, T. & Punto, M. (1996). Maintaining lane position with peripheral vision during in-vehicle tasks. *Human Factors: The Journal of the Human Factors and Ergonomics Society*, *38*(3), 442–451.

The European Parliament and the Council of the European Union. (2012). Directive 2012/27/eu of the european parliament and of the council of 25 october 2012 on energy efficiency, amending directives 2009/125/ec and 2010/30/eu and repealing directives 2004/8/ec and 2006/32/ec. *Official Journal of the European Union*, *55*, 1–56.

Theeuwes, J., Alferdinck, J. & Perel, M. (2002). Relation between glare and driving performance. *Human Factors: The Journal of the Human Factors and Ergonomics Society*, *44*(1), 95–107.

Uchida, T. (2015). Adaptation luminance simulation for cie mesopic photometry system implementation. In *Cie session 2015 manchester* (pp. 307–316). CIE.

Uchida, T., Ayama, M., Akashi, Y., Hara, N., Kitano, T., Kodaira, Y. & Sakai, K. (2016). Adaptation luminance simulation for cie mesopic photometry system implementation. *Lighting Research and Technology*, *48*(1), 14–25.

Uchida, T. & Ohno, Y. (2014a). Defining the visual adaptation field for mesopic photometry: Does surrounding luminance affect peripheral adaptation? *Lighting Research and Technology*, *46*(5), 520–533.

Uchida, T. & Ohno, Y. (2014b). Defining the visual adaptation field for mesopic photometry: How does a high-luminance source affect peripheral adaptation? *Lighting Research and Technology*, *47*(7), 845–858.

Uchida, T. & Ohno, Y. (2017). Defining the visual adaptation field for mesopic photometry: Effect of surrounding source position on peripheral adaptation. *Lighting Research and Technology*, *49*(6), 763–773.

Uchikawa, K. & Sato, M. (1995). Saccadic suppression of achromatic and chromatic responses measured by increment-threshold spectral sensitivity. *Journal of the Optical Society of America A*, *12*(4), 661–666.

Underwood, G., Chapman, P., Bowden, K. & Crundall, D. (2002). Visual search while driving: Skill and awareness during inspection of the scene. *Transportation Research Part F: Traffic Psychology and Behaviour*, *5*(2), 87–97.

van Rijsbergen, C. J. (1979). *Information retrieval*. London: Butterworth and Co.

Várady, G., Freiding, A., Eloholma, M., Halonen, L., Walkey, H., Goodman, T. & Alferdinck, J. (2007). Mesopic visual efficiency iii: Discrimination threshold measurements. *Lighting Research and Technology*, *39*(4), 355–364.

Vidovszky-Németh, A. & Schanda, J. (2012). White light brightness-luminance relationship. *Lighting Research and Technology*, *44*(1), 55–68.

Viikari, M., Puolakka, M., Halonen, L. & Rantakallio, A. (2012). Road lighting in change: User advice for designers. *Lighting Research and Technology*, *44*(2), 171–185.

Völker, S. (2006). *Hell- und Kontrastempfindung - ein Beitrag zur Entwicklung von Zielfunktionen für die Auslegung von Kraftfahrzeug-Scheinwerfern* (Habilitation, Universität Paderborn).

Volkmann, F. C. (1962). Vision during voluntary saccadic eye movements. *Journal of the Optical Society of America*, *82*(5), 571–578.

Walkey, H., Orrevetelainen, P., Barbur, J., Halonen, L., Goodman, T., Alferdinck, J., ... Szalmas, A. (2007). Mesopic visual efficiency ii: Reaction time experiments. *Lighting Research and Technology*, *39*(4), 335–354.

Wandell, B. A. (1995). *Foundations of vision*. Sunderland: Sinauer Associates.

Wang, J.-F., Stein, A., Gao, B.-B. & Ge, Y. (2012). A review of spatial sampling. *Spatial Statistics*, *2*, 1–14.

Winn, B., Whitaker, D., Elliott, D. B. & Phillips, N. J. (1994). Factors affecting light-adapted pupil size in normal human subjects. *Investigative Ophthalmology & Visual Science*, *35*(3), 1132–1137.

Winter, J., Buschmann, S. & Franke, R. (2013). Roadrad: A radiance road lighting simulation framework. Retrieved from https://github.com/fglichttechnik/Radiance-RoadLighting-Simulation-Framework

Winter, J., Buschmann, S., Franke, R. & Völker, S. (2013). Influence of inhomogeneous adaptation fields and glare sources on visual performance. In *Proceedings of the 11th lux junior* (pp. 112–113). Dörnfeld, Germany.

Winter, J., Fotios, S. & Völker, S. (2016). Gaze behaviour when driving after dark on main and residential roads. In *CIE 2016 conference: Lighting quality and energy efficiency* (pp. 395–401). Melbourne, Australia.

Winter, J., Fotios, S. & Völker, S. (2017a). Gaze direction when driving after dark on main and residential roads: Where is the dominant location? *Lighting Research and Technology*, *49*(5), 574–585. doi:10.1177/1477153516632867

Winter, J., Fotios, S. & Völker, S. (2017b). The effect of assuming static or dynamic gaze behaviour on the estimated background lumin-

ance of drivers. *Lighting Research and Technology*, Epub ahead of print 17 December 2017. doi:10.1177/1477153518757594

Winter, J., Fotios, S. & Völker, S. (2018). The effects of glare and inhomogeneous visual fields on contrast detection in the context of driving. *Lighting Research and Technology*, *50*(4), 537–551. doi:10.1177/1477153516672719

Winter, J. & Völker, S. (2013). Typical eye fixation areas of car drivers in inner-city environments at night. In *Proceedings of the 12th lux europa* (pp. 317–322). Krakow, Poland.

Wördenweber, B., Wallaschek, J., Boyce, P. R. & Hoffman, D. (2007). *Automotive lighting and human vision*. Berlin: Springer.

Ylinen, A.-M., Tähkämö, L., Puolakka, M. & Halonen, L. (2011). Road lighting quality, energy efficiency, and mesopic design – led street lighting case study. *Journal of the Illuminating Engineering Society*, *8*(1), 9–24.

CONTRIBUTION TO PUBLICATIONS

I Winter, J., Fotios, S. & Völker, S. (2018). The effects of glare and inhomogeneous visual fields on contrast detection in the context of driving. *Lighting Research and Technology*, *50*(4), 537–551. doi:10.1177/1477153516672719

I designed the study, oversaw the data collection, visualised and analysed the data and wrote the manuscript. S. Fotios provided supervision, discussed the interpretation of the results and revised the manuscript. S. Völker gave general advice and helpful comments and proofread the manuscript.

II Winter, J., Fotios, S. & Völker, S. (2017a). Gaze direction when driving after dark on main and residential roads: Where is the dominant location? *Lighting Research and Technology*, *49*(5), 574–585. doi:10.1177/1477153516632867

I designed the study, oversaw the data curation, visualised and analysed the data and wrote the manuscript. S. Fotios provided supervision, discussed the interpretation of the results and revised the manuscript. S. Völker gave general advice and helpful comments and proofread the manuscript.

III Winter, J., Fotios, S. & Völker, S. (2017b). The effect of assuming static or dynamic gaze behaviour on the estimated background luminance of drivers. *Lighting Research and Technology*, Epub ahead of print 17 December 2017. doi:10.1177/1477153518757594

I designed the study, collected, visualised and analysed the data and wrote the manuscript. S. Fotios provided supervision, discussed the interpretation of the results and revised the manuscript. S. Völker gave general advice and helpful comments and proofread the manuscript.

IV Winter, J., Fotios, S. & Völker, S. (2016). Gaze behaviour when driving after dark on main and residential roads. In *CIE 2016 conference: Lighting quality and energy efficiency* (pp. 395–401). Melbourne, Australia

I designed the study, oversaw the data curation, visualised and analysed the data and wrote the manuscript. S. Fotios provided supervision, discussed the interpretation of the results and revised the manuscript. S. Völker gave general advice and helpful comments and proofread the manuscript.

V Winter, J., Buschmann, S., Franke, R. & Völker, S. (2013). Influence of inhomogeneous adaptation fields and glare sources on visual performance. In *Proceedings of the 11th lux junior* (pp. 112–113). Dörnfeld, Germany

I designed the study, oversaw the data collection, visualised and analysed the data and wrote the manuscript. S. Buschmann and R. Franke collected the data under my guidance. S. Völker gave general advice and helpful comments and proofread the manuscript.

VI Winter, J. & Völker, S. (2013). Typical eye fixation areas of car drivers in inner-city environments at night. In *Proceedings of the 12th lux europa* (pp. 317–322). Krakow, Poland

I designed the study, oversaw the data curation, visualised and analysed the data and wrote the manuscript. S. Völker gave general advice and helpful comments and proofread the manuscript.

This document was typeset using the typographical look-and-feel `classicthesis` developed by André Miede. The style was inspired by Robert Bringhurst's seminal book on typography "*The Elements of Typographic Style*". `classicthesis` is available for both LaTeX and LyX:

https://bitbucket.org/amiede/classicthesis/

Final Version as of 16th February 2018 (`classicthesis` version 4.5).